The functional forebrain circuitry of fear-cue inhibited feeding in food-deprived rats: Evidence from complementary pathway tracing and Fos induction maps studies

Author: Christina Jean Reppucci

Boston College

The Graduate School of Arts and Sciences

Department of Psychology

THE FUNCTIONAL FOREBRAIN CIRCUITRY OF FEAR-CUE INHIBITED FEEDING IN FOOD-DEPRIVED RATS: EVIDENCE FROM COMPLEMENTARY PATHWAY TRACING AND FOS INDUCTION MAPS STUDIES

a dissertation

by

CHRISTINA J. REPPUCCI

submitted in partial fulfillment of the requirements

for the degree of

Doctor of Philosophy

August 2015

Title: The functional forebrain circuitry of fear-cue inhibited feeding in food-deprived rats: Evidence from complementary pathway tracing and Fos induction maps studies

By: Christina J. Reppucci

Advisor: Gorica D. Petrovich

Abstract:

The drive to eat, like most motivated behaviors, is controlled by both intrinsic signals from the body as well as extrinsic signals from the environment. Although these factors often act in concert, in some instances environmental cues can override the body's homeostatic signals. Prior work investigating the ability of learned cues to promote overeating in the absence of hunger identified a critical forebrain network composed of the amygdala, medial prefrontal cortex (mPFC), and lateral hypothalamus (LHA). We hypothesized that a similar forebrain network may also be critical when learned fear-cues inhibit eating despite hunger. The amygdala, mPFC and LHA are each anatomically and functionally positioned to influence feeding, and evidence suggests they could work together to support the fear-cue's ability to inhibit feeding by overriding homeostatic hunger signals triggered by food-deprivation. Prior anatomical work identified direct pathways between these three large, heterogeneous regions; however, less is known about the organization of the underlying circuitries, especially between distinct nuclei and/or subdivisions that comprise these structures. Study 1 used a dual retrograde tract tracing design to map the topographical organization of the connections between the amygdala, mPFC, and LHA in detail, and to determine whether amygdalar pathways to the mPFC and to LHA originated from the same or different neurons. We found evidence for

multiple, topographically organized, direct pathways from the amygdala to the LHA, and separate pathways from the amygdala to areas of the mPFC that send direct projections to the LHA. Importantly, nearly all amygdalar projections to the mPFC and to the LHA originated from different neurons, suggesting that amygdala and amygdala-mPFC processing influence the LHA independently. Study 2 used immediate early gene induction to map the patterns of functional activation within this amygdala-prefrontal-lateral hypothalamic network during the expression of fear-cue inhibited feeding behavior, and to assess whether these patterns were similar in males and females. We found differential activation across the network, and activation patterns related to the presentation of fear-cues, the presence of food-related cues, and the amount of food consumed were associated within distinct cell groups in the amygdala, mPFC, and LHA. Together, the studies presented in this dissertation provide anatomical and functional maps for future interrogation of the circuitry underlying fear-cue inhibited feeding.

Keywords: amygdala, prefrontal cortex, lateral hypothalamus, learning, fear, anorexia

Table of Contents

[1] Study 1 has been accepted for publication in Brain Structure and Function under the title: "Organization of connections between the amygdala, medial prefrontal cortex, and lateral hypothalamus: a single and double retrograde tracing study in rats", by C. J. Reppucci & G. D. Petrovich. The final publication is available at Springer via http://dx.doi.org/10.1007/s00429-015-1081-0.

Acknowledgements

I would like to thank my dissertation committee members: my advisor, Dr. Gorica Petrovich, as well as Drs. Alexa Veenema, Elizabeth Kensinger, and Tricia Burdo, my preliminary advisory committee member, Dr. Michael Numan, and my teaching mentor, Dr. Jeffrey Lamoureux for their time, mentorship, and feedback. Many thanks as well, to all past and present members of the Neurobiology of Feeding Behavior Lab. In particular, I would like to acknowledge the technical assistance of Meghana Kuthyar and Heather Mayer in both Studies 1 and 2. Additionally, Liz Choi, Megan Ebner, Michael Hobin, Josh Hwang, Jordan Newmark, Daniel Powell, Grant Schum, Anna Whitham, and Jack Young provided valuable assistance in Study 2. I am grateful to Lauren Anderson, Dr. Sindy Cole, and Sara Keefer for their friendship and comradery. Lastly, I would like to thank my family and loved ones for their encouragement and support throughout this graduate school experience.

This dissertation was supported in part by National Institute of Health grant DK085721 to G.D.P., and various Boston College funding sources, including a Graduate School of Arts & Sciences Dissertation Fellowship to C.J.R.

List of Tables

List of Figures

I. General Introduction

The drive to eat, like most motivated behaviors, is controlled by both intrinsic signals from the body as well as extrinsic signals from the environment. Although these factors often act in concert, in some instances environmental cues can override the body's homeostatic signals. It has been demonstrated that learned cues from the environment can promote feeding in the absence of hunger, or suppress feeding in spite of hunger. More specifically, cues that predict food can induce food intake despite satiation ("cue potentiated feeding") (Grant & Milgram, 1973; Holland, Petrovich, & Gallagher, 2002; Petrovich, Ross, Gallagher, & Holland, 2007; Reppucci & Petrovich, 2012; Weingarten, 1983, 1984), and cues that signal danger can inhibit food intake despite food deprivation ("fear-cue inhibited feeding") (Petrovich & Lougee, 2011; Petrovich, Ross, Mody, Holland, & Gallagher, 2009; Reppucci, Kuthyar, & Petrovich, 2013).This ability of learned environmental cues to control food intake could be adaptive, especially for animals in the wild including ancestral humans (e.g., consuming extra food in times of plenty in anticipation of future shortages, or ceasing to eat in order to flee an imminent threat). However, for modern day humans, especially those living in the developed world and who have easy access to food, the influence of constant, pervasive environmental cues could contribute to onset or maintenance of disease states (e.g., obesity, anorexia).

Substantial progress has been made in identifying the functional forebrain circuitry underlying cue potentiated feeding, while there has been less progress in mapping the circuitry underlying fear-cue inhibited feeding (reviewed in: Petrovich, 2013). The goal of this dissertation was to identify the functional forebrain circuitry

underlying fear-cue inhibited feeding. Importantly, this inhibition of feeding has been well-characterized, and is a general effect of fear that does not depend on the type of stimulus with which an aversive event is associated. Our group has established that both simple, discrete cues (Petrovich & Lougee, 2011; Petrovich et al., 2009) as well as complex, contextual stimuli (Reppucci et al., 2013) previously associated with aversive events will later inhibit feeding in food-deprived male and female rats. However, very little is known about the brain substrates that mediate this behavior.

The focus of this dissertation was to identify the critical circuitry: how it is organized (anatomically) and how it is recruited (functionally) during the expression of fear-cue inhibited feeding. Specifically, our focus was on three forebrain regions: the amygdala, the medial prefrontal cortex (mPFC), and the lateral hypothalamus (LHA). Each of these structures is anatomically (e.g., Hahn & Swanson, 2010, 2012, 2015; Kita & Oomura, 1982; Ono, Luiten, Nishijo, Fukuda, & Nishino, 1985; Swanson, 2000, 2005; Yoshida, McCormack, Espana, Crocker, & Scammell, 2006) and functionally (see: Berthoud & Münzberg, 2011; Petrovich, 2013) positioned to influence feeding, and there is evidence to suggest they could work together to support the fear-cue's ability to inhibit feeding by overriding homeostatic hunger signals triggered by food-deprivation (e.g., Cai, Haubensak, Anthony, & Anderson, 2014; Herry et al., 2008; Land et al., 2014; Laviolette, Lipski, & Grace, 2005; Mena, Selleck, & Baldo, 2013; Namburi et al., 2015; Sotres-Bayon, Sierra-Mercado, Pardilla-Delgado, & Quirk, 2012). Prior studies have shown that the amygdala (Holland et al., 2002) and its functional connections with the mPFC (Petrovich, Holland, & Gallagher, 2005; Petrovich, Ross, Holland, & Gallagher,

2007) and LHA (Petrovich et al., 2005; Petrovich, Setlow, Holland, & Gallagher, 2002) are critical for cue potentiated feeding. Thus, we hypothesized that a similar forebrain network composed of the amygdala, mPFC, and LHA may also be critical for fear-cue inhibited feeding.

Past anatomical work identified direct pathways between the amygdala, mPFC, and LHA. However, these are large regions that are structurally and functionally heterogeneous, and less is known about the organization of the underlying circuitries, especially at the level of the nuclei and/or subdivisions that comprise these structures. To better characterize the amygdala-prefrontal-lateral hypothalamic network the first study in this dissertation mapped the direct connections between these three regions, with particular focus on amygdalar pathways to the LHA directly, and via the mPFC.

Study 1 had two goals; the first was to map in detail the topographical organization of connections between the amygdala, mPFC, and LHA, and the second was to determine whether the pathways from the amygdala to the mPFC and to the LHA originate in the same or different groups of neurons. The approach involved use of the neuronal retrograde tract tracing method. This method is used to identify inputs to the specific region where the retrograde tracer was injected. Retrograde tracers are picked up by the terminal ends of neurons at the injection site, and transported up the axon where they accumulate in the cell body of neurons and can be visualized with immunohistochemical methods. Thus, combining these methods allows mapping of the exact location of neurons that project to the injection site, which cannot be accomplished with the anterograde tracing method (Lanciego & Wouterlood, 2011; Oztas, 2003). In

Study 1 each subject received injections of two different retrograde tracers: one into the mPFC and one into the LHA. With this approach we were able to simultaneously visualize the location of both tracers in the same brain tissue and determine whether the same or different amygdalar neurons project to both structures. If the same neurons were labeled then this would allow for simultaneous amygdalar influence of the mPFC and LHA, while if different neurons were labeled then the amygdala influences the mPFC and LHA by parallel pathways. The results from these experiments produced a detailed map of topographically organized amygdala-prefrontal-lateral hypothalamic pathways, and also served as the framework for the investigation into the functional activation of this network under Study 2.

Only one prior study has examined the neural substrates of fear-cue inhibited feeding, and identified that the amygdala, specifically the central nucleus but not the basolateral area, was critical for the expression of this behavior (Petrovich et al., 2009). That study used neurotoxic lesions that ablated the entire central nucleus or basolateral area (Petrovich et al., 2009). Since these are large and heterogeneous areas it remains unknown which particular division of the central nucleus is critical, or whether any of the cell groups that comprise the basolateral area could also important, albeit not critical, for the expression of this behavior especially given their roles in conditioned fear (see: Ehrlich et al., 2009; Pare & Duvarci, 2012; Pare, Quirk, & Ledoux, 2004). To address this, the second study in this dissertation determined activation patterns within these amygdalar regions, as well as within the mPFC and LHA during fear-cue inhibited feeding.

Study 2 had two goals; the first was to confirm prior behavioral findings that fear-cues can override hunger signals triggered by food-deprivation to inhibit feeding in both male and female rats, and the second was to map the patterns of activation within the amygdala-prefrontal-lateral hypothalamic network during the expression of this behavior, and assess whether these patterns were similar in males and females. Few studies compare behavior and brain activation patterns of males and females (Cahill, 2006; Zucker & Beery, 2010), even though it is a necessary step in characterizing differences between the sexes (McCarthy, Arnold, Ball, Blaustein, & De Vries, 2012). Examining both sexes is especially relevant within this behavioral paradigm given that women have higher reported rates of anxiety and eating disorders (Becker et al., 2007; McCarthy et al., 2012; McLean & Anderson, 2009). Study 2 used a recently established model of fear-cue inhibited feeding (Petrovich & Lougee, 2011; Petrovich et al., 2009). In this paradigm, a cue (in this case a tone) comes to signal a fearful event through associative learning during training. Later, this conditioned stimulus can inhibit eating in subjects even if they are hungry during testing. Patterns of brain activation during the inhibition of the feeding were measured through induction of the immediate early gene *c-fos'* protein product (Fos), which was identified and visualized with immunohistochemical detection techniques. Fos is a commonly used marker of functional activation (an indirect marker of recent neuronal activity) (Chaudhuri, 1997; Curran & Morgan, 1995; Morgan & Curran, 1991). The results from this study identified distinct cell groups within the amygdala-prefrontal-lateral hypothalamic network that were differentially activated, and

as such provided functional maps for future interrogation of the circuitry underlying fear-cue inhibited feeding.

Understanding how environmental cues can override the body's homeostatic signals to alter food intake is important for increasing our knowledge about why we eat when we do. The results presented in this dissertation will enhance our understanding of how the amygdala-prefrontal-lateral hypothalamic network is anatomically organized (Study 1) and how it is functionally recruited during fear-cue inhibited feeding (Study 2). The brain substrates identified in this dissertation give us insight regarding how learned cues from the environment can lead to the inhibition of food intake despite food deprivation, and as such this research may have important clinical implications for anxiety and eating disorders.

II. Study 1: Pathway Tracing

Introduction

The amygdala and medial prefrontal cortex (mPFC) are highly interconnected telencephalic areas critical for cognitive processes, including associative learning and decision-making (e.g., Cassell & Wright, 1986; Euston, Gruber, & McNaughton, 2012; Krettek & Price, 1977; McDonald, 1998; Seymour & Dolan, 2008). Each structure strongly innervates the lateral hypothalamus (LHA) (e.g., Hurley, Herbert, Moga, & Saper, 1991; Kita & Oomura, 1982; Petrovich, Canteras, & Swanson, 2001; Yoshida et al., 2006), which is an important component of the networks underlying the control of feeding and other motivated behaviors (Elmquist, Elias, & Saper, 1999; Swanson, 2005). The amygdala-prefrontal-lateral hypothalamic system is therefore well positioned to exert

cognitive control over behavior, and recent studies on feeding behavior support this notion. Intact amygdala, mPFC, and their connections with the LHA are required for the control of food intake by learned environmental cues, independent of physiological state (Holland et al., 2002; Petrovich et al., 2005; Petrovich, Ross, Gallagher, et al., 2007; Petrovich, Ross, Holland, et al., 2007; Petrovich et al., 2009). Additionally, stimulation of the mPFC μ-opiod (Mena, Sadeghian, & Baldo, 2011) or dopamine (Land et al., 2014) systems elicits robust feeding in sated animals, and these effects depend on activation of the LHA (Mena et al., 2013) and amygdala (Land et al., 2014), respectively.

The connectional organization of this functional amygdala-prefrontal-lateral hypothalamic system is not well-defined. In particular, the topography of specific subsystems between these three large forebrain regions is unknown. This is especially critical given that the amygdala, mPFC and LHA are complex heterogeneous regions comprised of distinct cell groups that mediate different functions (e.g., Ashwell & Ito, 2014; Burgos-Robles, Bravo-Rivera, & Quirk, 2013; Cole, Powell, & Petrovich, 2013; Heidbreder & Groenewegen, 2003; Knapska et al., 2012; Maeng & Shors, 2013; Martinez et al., 2013; Mendoza, Sanio, & Chaudhri, 2014; Senn et al., 2014; Swanson & Petrovich, 1998). Prior work, with anterograde or retrograde tracing methods, has identified direct pathways from the amygdala to the mPFC and to the LHA, as well as direct pathways from the mPFC to the LHA (e.g., Hoover & Vertes, 2007; Hurley et al., 1991; Kita & Oomura, 1982; Krettek & Price, 1977; Krettek & Price, 1978a; Ono et al., 1985; Sesack, Deutch, Roth, & Bunney, 1989). This pattern of connections suggests that in addition to direct pathways, the amygdala could also influence the LHA indirectly

through the mPFC, following mPFC processing (Gabbott et al., 2012). Nevertheless, a comprehensive analysis of the entire system has not been conducted. Additionally, no study to date has examined whether amygdalar pathways to the mPFC and to the LHA originate in common or distinct cell groups, and characterizing how these connections are organized is important for determining whether the amygdala influences the mPFC and LHA simultaneously or independently.

The present study had two aims. The first aim was to map the organization of connections between the amygdala, mPFC, and LHA, in detail. The second aim was to determine whether the pathways from the amygdala to the mPFC and LHA originate in the same or different groups of neurons. We employed a dual retrograde tract tracing design, which involved placements of different retrograde tracers into the mPFC and LHA. To accomplish the first aim, we analyzed single tracer distribution within the amygdala after retrograde transport from the mPFC and LHA, and distribution within the mPFC after retrograde transport from the LHA. To accomplish the second aim, we analyzed the distribution of both tracers simultaneously within the amygdala. Within the amygdala, we analyzed two large areas, critical for associative learning and subsequent control of behavior (including the control of feeding by learned cues (Holland et al., 2002; Petrovich et al., 2009) and fear conditioning (e.g., Anglada-Figueroa & Quirk, 2005; Goosens & Maren, 2001; Ledoux, 2012; Maren, Aharonov, & Fanselow, 1996)): the basolateral area (consisting of the basolateral (BLA), basomedial (BMA), and lateral nuclei (LA)), and the central nucleus (CEA). These two areas are structurally distinct, and based on developmental, cytoarchitectonic, and connectional features are considered

highly differentiated parts of the cortex (basolateral area) or striatum (CEA) (McDonald 2003; Swanson & Petrovich, 1998). Within the mPFC, we focused on four regions defined based on their distinct cytoarchitecture and connections (Heidbreder & Groenewegen, 2003; Swanson, 2004): the anterior cingulate area (ACAd), the prelimbic area (PL), the infralimbic area (ILA), and a rostromedial orbital region (comprised of the medial (ORBm) and ventrolateral (ORBvl) parts of the orbital area). Finally, because of our interest in feeding behavior, two LHA parts were targeted: the dorsal, which contains orexigenic peptides (Broberger, De Lecea, Sutcliffe, & Hokfelt, 1998; Hahn, 2010; Swanson, Sanchez-Watts, & Watts, 2005), and the ventral which lacks these peptides.

Materials & Methods

Subjects. Forty experimentally naïve, male Long–Evans rats approximately 2 months of age (Charles River Laboratories, Portage, MI) were individually housed, maintained on a 12 h light/dark cycle, and had access to food and water *ad libitum*. Upon arrival, subjects were allowed one week to acclimate to the colony room, during which time they were handled daily. All housing and experimental procedures were in compliance with the National Institutes of Health *Guidelines for Care and Use of Laboratory Animals*, and approved by the Boston College Institutional Animal Care and Use Committee.

Surgical procedure. Animals were briefly anesthetized with isoflurane (5%; Baxter Healthcare Corporation, Deerfield, IL), then deeply anesthetized with an intramuscular injection of a mixture (1 ml/kg body weight) of ketamine (50 mg/ml; Fort Dodge Animal Health, Fort Dodge, Iowa) and xylazine (10 mg/mL; LLOYD

Laboratories, Shenandoah, Iowa). While under anesthesia, animals received two stereotaxically placed iontophoretic injections of retrograde tracers in the right hemisphere: one into the mPFC and the other into the LHA. Injection placements of 3% Fluoro-Gold (FG; Fluorochorome, LLC, Denver, CO) dissolved in 0.9% saline, and 2% Cholera Toxin B Subunit (CTB; 104; List Biological Laboratories, Inc., Campbell, CA) dissolved in deionized water were counterbalanced for location across subjects. Each tracer was delivered through a glass micropipette (~50 μm tip diameter) by applying a positive current (5 μA, 5 second on/off intervals) for 10 minutes. This method allows for precise placement of the tracers with little damage to surrounding tissue and minimal risk of uptake from fibers of passage (Lanciego & Wouterlood, 2011).

Histological procedures. Twelve to fifteen days following surgery, rats were briefly anesthetized with isoflurane, and then deeply anesthetized with an intraperitoneal injection of tribromoethanol (375 mg/kg; Sigma-Aldrich, St. Louis, MO). Rats were then transcardially perfused with 0.9% saline followed by 4% paraformaldehyde in 0.1M borate buffer. Brains were extracted and post-fixed overnight in the same fixative containing 12% sucrose, and then rapidly frozen in hexanes cooled in dry ice and stored at -80°C. Brains were sliced in 30μm coronal sections using a sliding microtome and were collected into four adjacent series. Three tissue series were collected into a 0.02M potassium phosphate buffered saline (KPBS) solution. One was mounted on gelatin-coated slides and Nissl stained with thionin for identification of cytoarchitectonic borders (Simmons & Swanson, 1993), and the other two series were processed immediately for immunohistochemical detection of each retrograde tracer (single-label). The fourth tissue

series was collected into a tray containing a cryoprotectant solution (0.025M sodium phosphate buffer with 30% ethylene glycol and 20% glycerol), and stored at -20^{o}C for later processing of combined detection of both tracers (double-label).

Single-label immunohistochemistry. One series of tissue was stained for detection of FG. Free-floating sections were incubated in a blocking solution for 1 hour at room temperature to minimize nonspecific antibody binding. The blocking solution contained KPBS, 0.3% Triton X-100 (Sigma-Aldrich, St. Louis, MO), 2% normal goat serum (S-1000; Vector Laboratories, Burlingame, CA), and 10% non-fat milk (M-0841; LabScientific, Livingston, New Jersey). After blocking, the tissue was incubated with the primary antibody, anti-FG raised in rabbit (1:20,000; AB153; Millipore, Billerica, MA) in the blocking solution for 72 hours at 4°C. The tissue was rinsed with KPBS and then incubated with the secondary antibody, biotinylated goat anti-rabbit IgG (1:500; BA-1000; Vector Laboratories, Burlingame, CA) in the blocking solution for 45 minutes. Subsequently, the tissue was rinsed with KPBS and then reacted with avidin-biotin complex (PK-6100; Vector Laboratories, Burlingame, CA) for 45 minutes. After rinsing with KPBS, the tissue was incubated in a diaminobenzidine solution (SK-4100; Vector Laboratories, Burlingame, CA) for one minute with constant manual agitation to produce a color reaction.

A second series of tissue was stained for detection of CTB. The processing procedure was identical to that described above, except for the following differences. The

normal serum used was from horse (S-2000; BA-9500; Vector Laboratories, Burlingame, CA), the primary antibody was anti-CTB raised in goat (1:5,000; 703; List Biological Laboratories, Inc., Campbell, CA), and the secondary antibody was biotinylated horse anti-goat IgG (BA-9500; Vector Laboratories, Burlingame, CA).

After processing, tissue sections were mounted onto SuperFrost Plus slides (Fisher Scientific, Pittsburgh, PA), dried overnight at 45^{o}C, dehydrated through alcohols, cleared in xylenes, and coverslipped with DPX (13512; Electron Microscopy Sciences, Hatfield, PA).

Double-label immunohistochemistry. For simultaneous visualization of both tracers, one series of brain tissue (n=4) underwent fluorescent double-label immunohistochemical processing. Tissue was rinsed from the cryoprotectant storage solution with several washes in KPBS, and then incubated for 72 hours at 4°C in a blocking solution (KPBS containing 0.3% Triton X-100, 2% normal donkey serum (017-000-001; Jackson ImmunoResearch, West Grove, PA)), with both primary antibodies: anti-FG (1:10,000) and anti-CTB (1:5,000). After rinses in KPBS, tissue was incubated for one hour in the dark in the blocking solution containing the secondary antibodies: Alexa 488 anti-rabbit (1:200; A21206; Invitrogen, Carlsbad, CA) and Alexa 546 anti-goat (1:200; A11056; Invitrogen, Carlsbad, CA), both raised in donkey. Following rinses in KPBS, tissue was mounted in semi-darkness onto slides (SuperFrost Plus), dried, coverslipped with Vectashield HardSet Mounting Medium with DAPI (H-1500; Vector Labs, Burlingame, CA), and stored at 4^{o}C until analysis.

Image Acquisition & Analysis.

Single-label detection. The analysis was conducted with an Olympus BX51 light microscope with attached Olympus DP72 camera, using DP2-BSW software (Olympus America Inc, Center Valley, PA). Images of the areas with tracer deposits and the adjacent Nissl-stained tissue were acquired at 4X. To determine the location and extent of the tracer deposits, neuroanatomical borders were drawn onto the Nissl-stained image and then transposed to the adjacent immunohistochemically-stained image using ImageJ software (NIH). These injection sites were then drawn on computerized versions of the standard rat brain atlas drawings (Swanson, 2004) using illustration software (Adobe Illustrator CS5.5). Based on this analysis, well-defined and localized injections were identified and retrogradely labeled neurons were analyzed in those brains. Retrograde labeling was analyzed within the amygdala regions of interest (basolateral area and CEA) for all injection sites in the mPFC and LHA. Additionally, retrograde labeling was analyzed within the mPFC for each LHA injection site. The LHA was examined for retrograde labeling following mPFC injections, but only very sparse labeling was observed, consistent with prior reports (Allen & Cechetto, 1993; Goto, Canteras, Burns, & Swanson, 2005; Hahn & Swanson, 2012, 2015; Hoover & Vertes, 2007; Saper, 1985; Villalobos & Ferssiwi, 1987), and thus this pathway was not systematically analyzed. Tracer-labeled neuron mapping was conducted from images acquired at 10X using ImageJ, confirming labeling at 20X and cytoarchitectonic borders (Nissl) at 4X, as needed. The locations of labeled neurons were plotted directly onto computerized versions of the standard drawings of the rat brain (Swanson, 2004) using illustration

software (Adobe Illustrator CS5.5). Retrograde labeling was not illustrated if fewer than 5 labeled neurons were observed. The pattern of retrograde labeling was not dependent on the specific retrograde tracer used; FG and CTB injections in similar regions produced indistinguishable patterns. The brains with less localized injection sites were also systematically examined; patterns of labeling were compared to the plots from the ideal injections to verify topographical patterns of labeling, and these brains were also inspected as potential candidates for double-label analysis (see below).

The parcellation and nomenclature of the rat brain followed Swanson (2004), except for the following differences. The term "basolateral area of the amygdala" refers to the area comprised of the BLA (anterior and posterior parts; BLAa, BLAp), BMA (anterior and posterior parts; BMAa, BMAp), and LA. Rostromedial ORB refers to the combined area of the ORBm and ORBvl as defined in the Swanson atlas (+5.20 to +4.20 from bregma). LHA injections were grouped by their placement within dorsal or ventral LHA, which we defined here as the parts above (dorsal LHA) or below (ventral LHA) a horizontal line through mid fornix.

To better characterize the topography of amygdalar projections to the mPFC, the distribution of retrogradely labeled neurons in the amygdala was quantified in regard to cell group and rostrocaudal location for the plotted cases of ACAd, PL, and ILA injections (which varied in dorsoventral placement, but were located in a similar rostrocaudal location within the mPFC). Rostromedial ORB was not included in this analysis because injections were considerably more rostral than injections into the ACAd, PL, and ILA, and thus it would not be possible to determine if differences in the

distribution of amygdalar inputs were due to its ventral location (compared to ACAd, PL) or rostral location (compared to ACAd, PL, ILA). For each case, representative images (tracer, Nissl) of the cell groups within the basolateral area of the amygdala were acquired at 10X for each level of the Swanson atlas (2004). Using ImageJ, regions of interest (ROIs) were created for each cell group (BLAa, BLAp, BMAp, and LA; there was no labeling in BMAa) on the Nissl-stained tissue images, and transposed to the images of the adjacent tracer-stained tissue. The number of retrogradely labeled neurons within each ROI was quantified using the ImageJ cell counter by a trained observer unaware of the injection site location. For each brain, the percent of labeled neurons located in each cell group was calculated (e.g., # of labeled neurons in BLAa/total # of labeled neurons in the entire basolateral area), as well as the percent of all labeled neurons in the rostral (atlas levels 26-28), mid (atlas levels 29-31), and caudal (atlas levels 32-34) basolateral area collapsed across cell groups (e.g., # of labeled neurons in rostral/total # of labeled neurons in the entire basolateral area).

Double-label detection. The analysis was conducted with a Zeiss Axioplan II fluorescence microscope (Carl Zeiss Microscopy GmbH, Jena, Germany) and attached Hamamatsu camera (Bridgewater, NJ). Based on the findings from the single-label analysis, only the posterior basolateral amygdalar nuclei (BLAp, BMAp) contained retrograde labeling following both LHA and mPFC injections. Thus, to examine whether any neurons in the BLAp/BMAp region project to both the mPFC and LHA, four cases where inspection of both series of single-label tracer-stained tissue revealed labeling in this potential region of overlap were chosen for double-label processing and analysis. To

examine potential double labeling, consecutive images were taken throughout atlas levels 30-34 (Swanson, 2004).

Images were pseudocolored with red for CTB, green for FG, and blue for DAPI (nuclear counterstain); contrast was enhanced, and images were triple stacked using Improvision OpenLab (PerkinElmer, Waltham, MA) imaging software. All analysis was conducted from the triple-merged images, however, single images were consulted as needed to confirm the cell and stain type. Neurons were deemed tracer-positive if they had robust cytoplasmic staining and a clearly visible DAPI-stained nucleus. For each image the number of FG-positive, CTB-positive, and FG+CTB double-labeled neurons (visualized as yellow) were counted and summed across all images for each brain. The percent of all labeled neurons for each brain that was positive for both FG and CTB was then calculated (#double-labeled/[#FG + #CTB + #double-labeled]).

Results

Projections from the amygdala to the medial prefrontal cortex. The patterns of retrograde labeling in the amygdala were analyzed following injections into four discrete mPFC regions: ACAd, PL, ILA, and rostromedial ORB. Detailed descriptions of labeling patterns, and plots from representative injections are illustrated below. The densest labeling was observed after injections into the PL and ILA, while injections into rostromedial ORB resulted in the sparsest labeling. In all cases, retrograde labeling was restricted to the basolateral area of the amygdala (Fig. 2.1). There was no labeling in the CEA. Most of the labeling was concentrated within BLAa and BLAp and adjacent ventral LA, while the ventral mPFC injections also produced substantial labeling in BMAp.

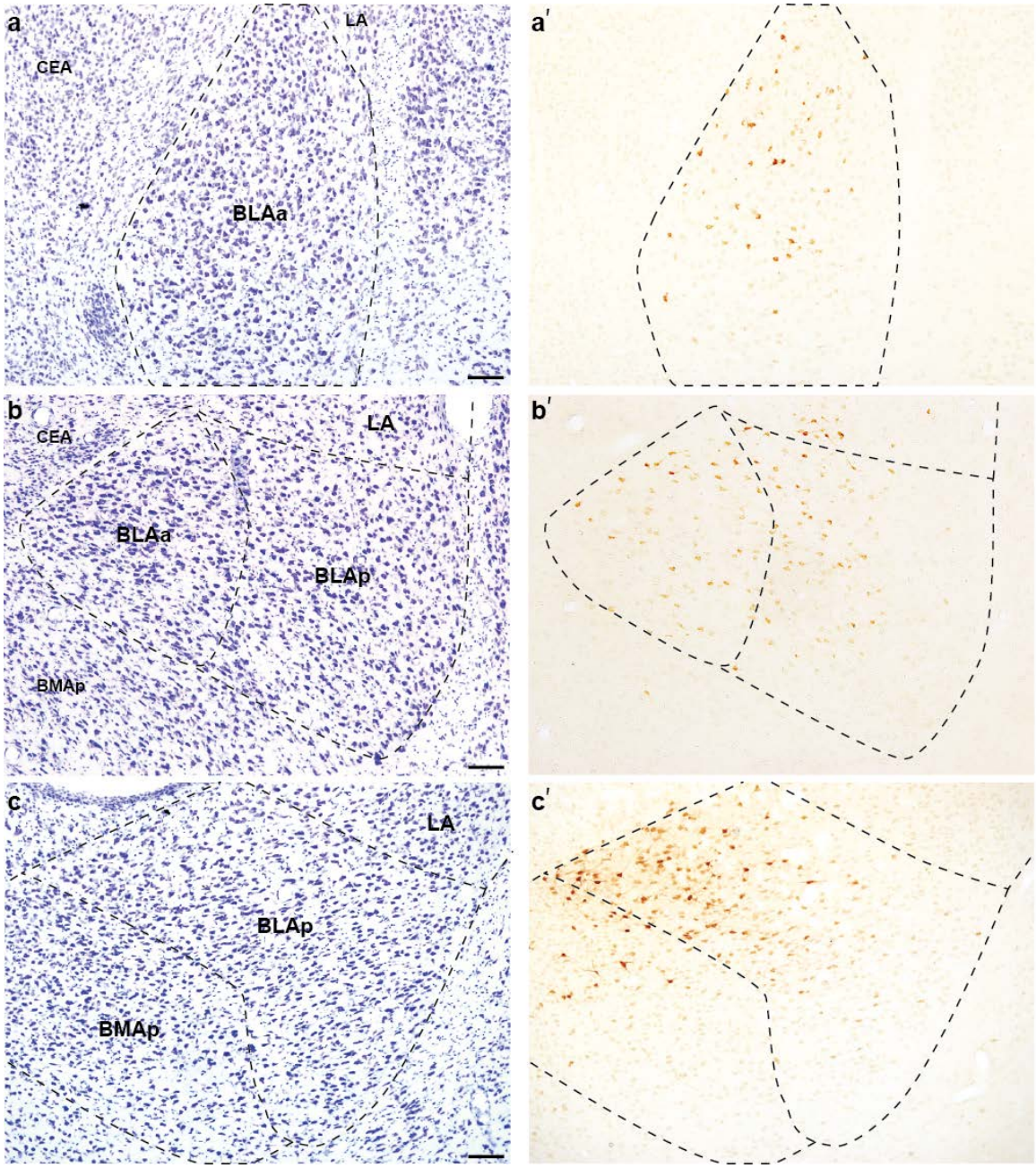

Fig. 2.1 Representative images of retrograde tracer labeling in the basolateral area of the amygdala after tracer placement in the ACAd (**a'**; #32), PL (**b'**; #25), and ILA (**c'**; #35). **a**, **b**, **c** Adjacent Nissl-stained tissue. Scale bars = 100μm.

Projections to the anterior cingulate area. In two cases, the retrograde tracer injection was contained within the ACAd. The retrograde labeling pattern for one of these, #32 (Fig. 2.2a, c), is shown in detail. The pattern of labeling for another injection that was centered more caudally but still contained within ACAd (#52, Fig. 2.2b), was identical but less dense than #32.

The majority of labeled neurons following injections into the ACAd was contained within the BLAa (Fig. 2.1a) and BLAp. There were also some labeled neurons in the ventral portion of the LA, which formed a dorsal extension of the labeling in the BLA. Labeling was densest in the caudal third of the BLAa (atlas levels 28-29), an area that corresponds to the intermediate division of the basal nucleus (Savander, Go, LeDoux, & Pitkänen, 1995), before quickly tapering off caudally. There were no retrogradely labeled neurons within the BMAa or BMAp.

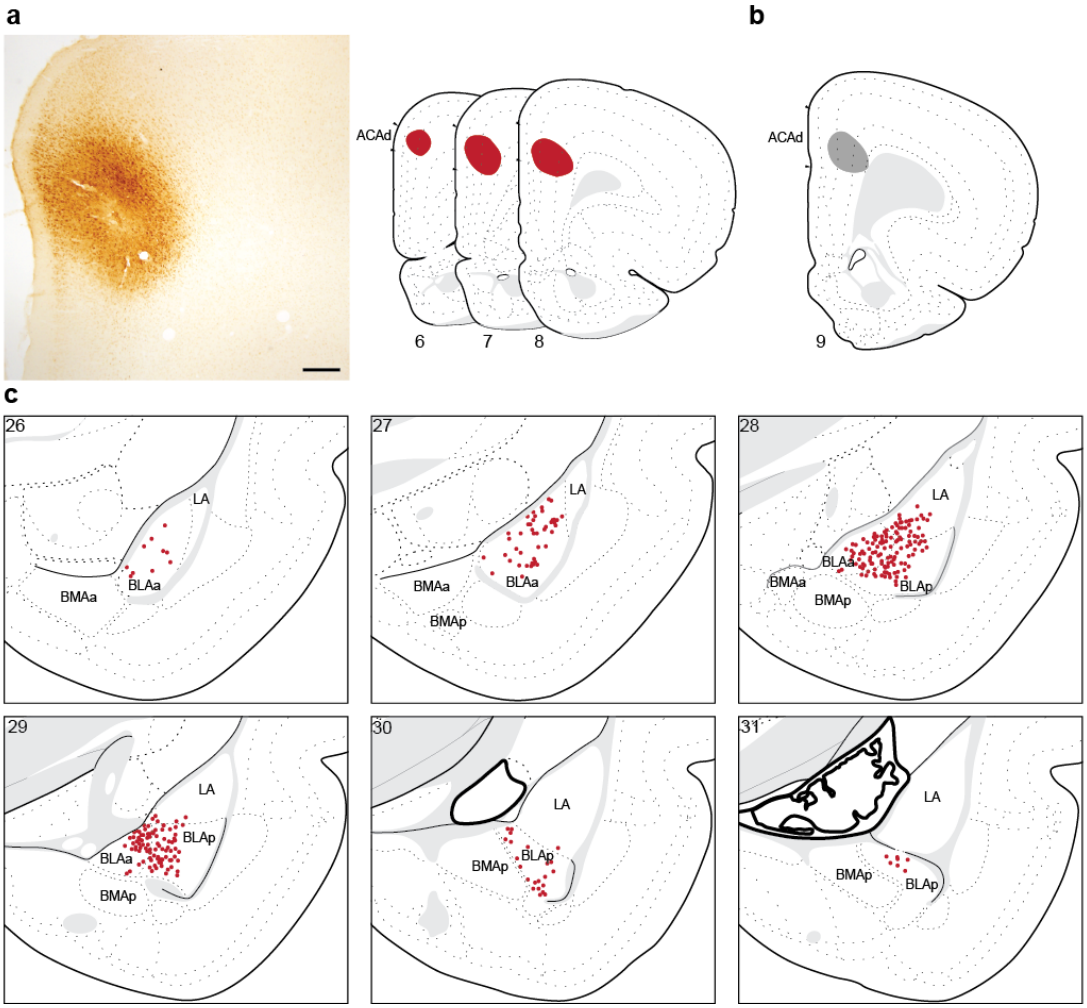

Fig. 2.2 The distribution of labeling within the amygdala following retrograde tracer injection into the ACAd. **a** Photomicrograph of the injection center, and illustration of the rostrocaudal extent of the injection spread for case #32. **b** Illustration of injection center for a comparison injection into ACAd (#52). **c** Labeled neurons (red dots) were plotted onto rat brain templates derived from Swanson (2004), arranged from rostral to caudal. Numbers denote atlas levels, scale bar = 200 µm.

Projections to the prelimbic area. In six cases, the retrograde tracer injection was predominately contained within the PL. The retrograde labeling pattern for one of these, #25 (Fig. 2.3a, c), is shown in detail because the tracer most completely filled the PL and its pattern of retrograde labeling was representative of other cases with injections into the PL (Fig. 2.3b). Five injections were used as comparisons; one was slightly smaller than the plotted example (#46), two were centered more rostrally and dorsally within the PL (#21 and #22), and two had dorsal spread into the ACAd (#20 and #33).

Injections into the PL produced the largest rostrocaudal spread of labeling in the amygdala of any mPFC injection. Similar to ACAd injections, the majority of labeled neurons were within the BLAa and BLAp (Fig. 2.1b), but there were more labeled neurons across the rostrocaudal extent of LA. The densest labeling was in the caudal BLAa (atlas levels 29-30). There were no retrogradely labeled neurons within the BMAa, while there were some in the caudal half of BMAp, typically at the border with BLAp. We found a similar pattern for all the comparison injections. The pattern was nearly identical for #46. For the two cases that included dorsal spread into ACAd (#20 and #33), the density of labeling was similar to the plotted example, but the location was shifted slightly rostromedially such that the pattern of labeling was an intermediate to the plotted ACAd and PL injections. Back-labeling following the two most rostral PL injections (#21 and #22) was overall much less dense, and did not produce labeling in the most caudal third of the basolateral area (i.e., caudal LA, BLAp, BMAp).

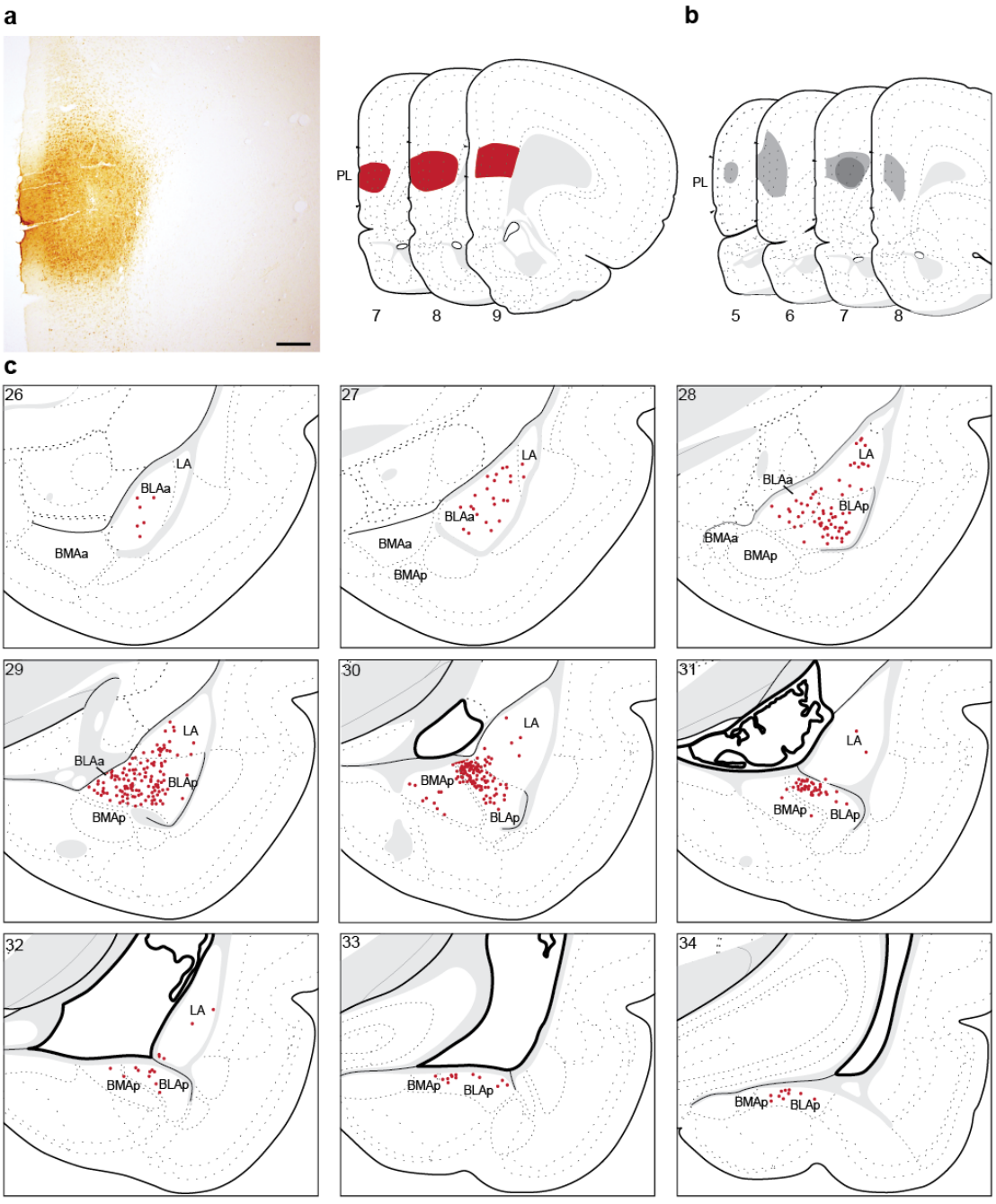

Fig. 2.3 The distribution of labeling within the amygdala following retrograde tracer injection into PL. **a** Photomicrograph of the injection center, and illustration of the rostrocaudal extent of the injection spread for case #25. **b** Illustration of the injection centers for comparison injections into PL (#20-22, #33, #46). **c** Labeled neurons (red dots) were plotted onto rat brain templates derived from Swanson (2004), arranged from rostral to caudal. Numbers denote atlas levels, scale bar = 200 µm.

Projections to the infralimbic area. In four cases, the retrograde tracer injection was contained within the ILA. The retrograde labeling pattern for one of these, #35 (Fig. 2.4a, c), is shown in detail because the injection site for this case most completely filled the entire ILA. Of the additional cases that were used for comparison analysis (Fig. 2.4b), two were smaller than the plotted case and did not include the most ventral third (#27) or half (#45) of ILA, while the third included the dorsoventral extent of ILA but was restricted to layers 5 and 6 (#36).

The majority of retrogradely labeled neurons after ILA injections were contained within the caudal basolateral area, specifically within the BLAp (Fig. 2.1c), where the densest labeling was medially within its rostral half. Labeling within the BLAa was restricted to its caudal half. There were no retrogradely labeled neurons within the BMAa, while there was moderate labeling within the BMAp, concentrated adjacent to the BLAp forming a continuum of labeled neurons across the BLAp/BMAp border. There were also scattered neurons throughout the rostrocaudal extent of the LA. The overall pattern was similar in the comparison injections. In cases where the injections were centered slightly more dorsal than the plotted example (#27 and #45), there was additional BLAa labeling, similar in location to that following injections into PL. The smallest ILA injection (#36), produced the same pattern of labeling, but less dense than the plotted example.

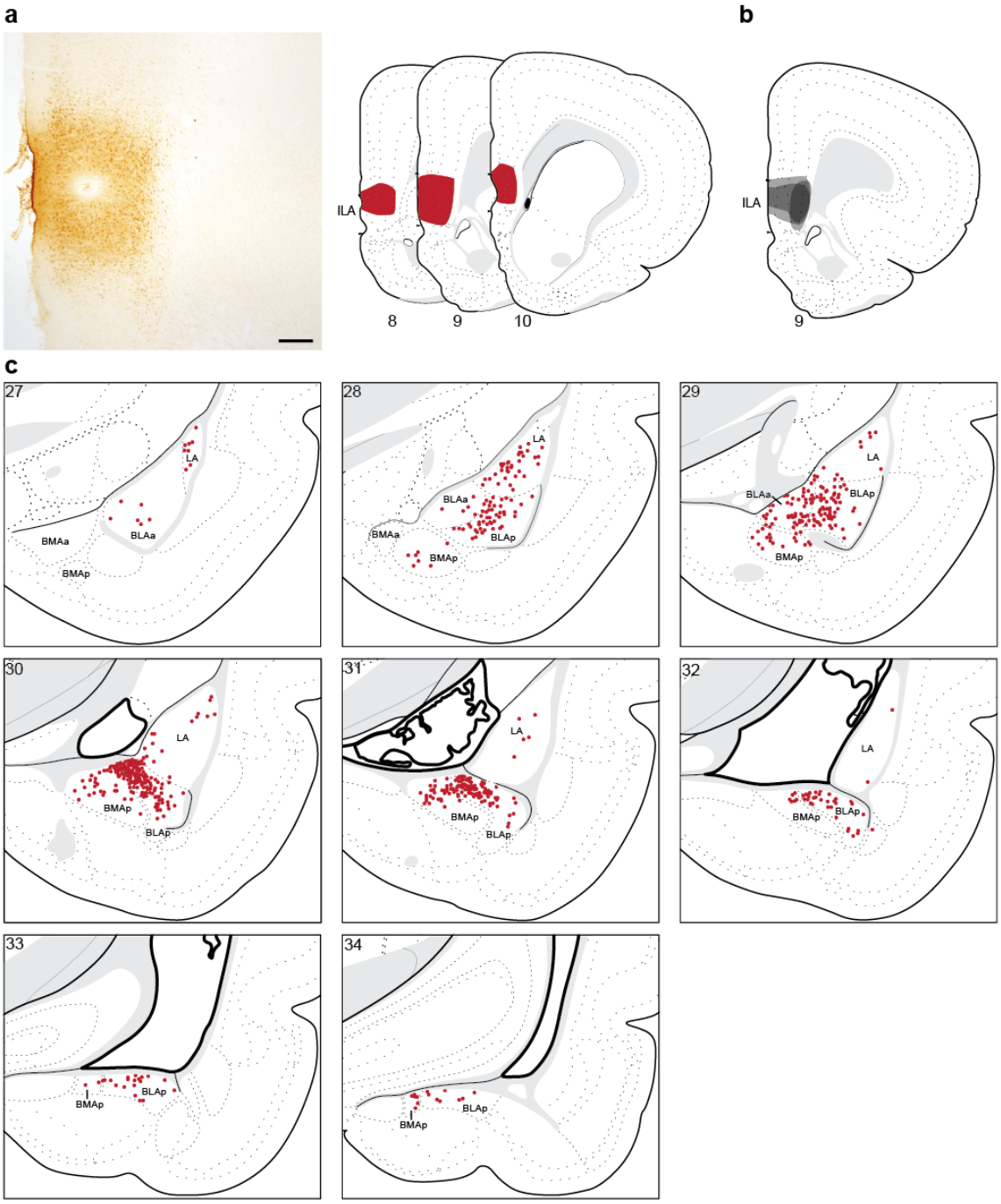

Fig. 2.4 The distribution of labeling within the amygdala following retrograde tracer injection into ILA. a Photomicrograph of the injection center, and illustration of the rostrocaudal extent of the injection spread for case #35. b Illustration of the injection centers for comparison injections into ILA (#27, #36, #45). c Labeled neurons (red dots) were plotted onto rat brain templates derived from Swanson (2004), arranged from rostral to caudal. Numbers denote atlas levels, scale bar = 200 μm.

Projections to the rostromedial orbital area. In six cases, the retrograde tracer injection was concentrated within very rostral and ventral mPFC. The retrograde labeling analysis for one of these, #40 (Fig. 2.5a, c), is shown in detail because its injection site was nearly completely contained within the rostromedial ORB (ORBm and ORBvl), and its pattern of retrograde labeling was representative of patterns from other injections into this region (Fig. 2.5b). Of the additional five cases, one was similarly contained within the ORBm and ORBvl but was smaller in size (#51), and one was contained exclusively within the ORBvl (#43). Injections in the remaining three cases spread dorsally into rostral PL (#48, #50, #49).

Injections into the rostromedial ORB resulted in the sparsest amygdalar labeling of any mPFC area. The majority of retrogradely labeled neurons were located within the BLAa and adjacent rostral part of the BLAp, while very few labeled neurons were found in LA. This pattern was consistent for all the comparison injections, except for the largest (#48) where labeling was more robust and continued further caudally, compared to the plotted case (#40).

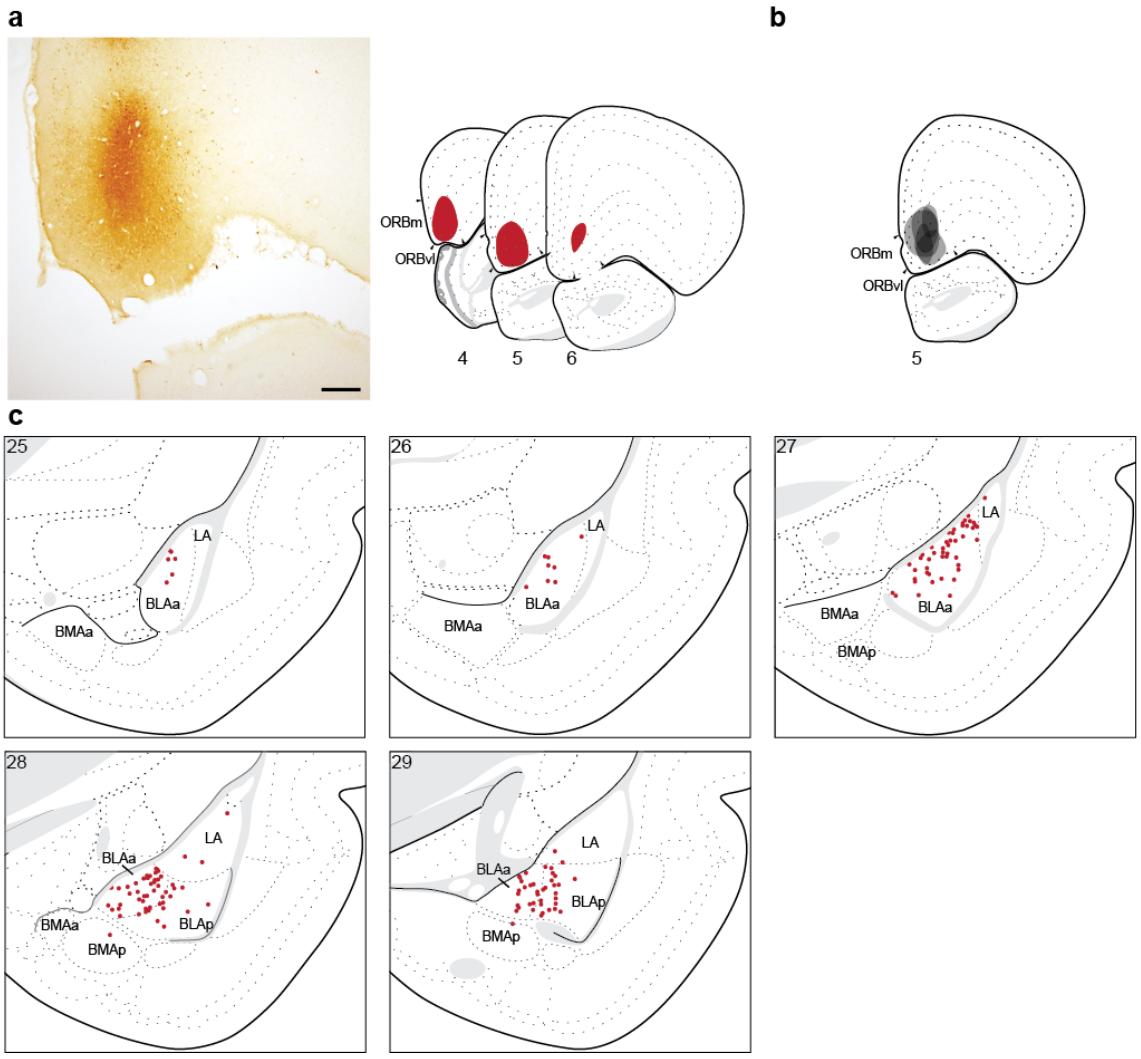

Fig. 2.5 The distribution of labeling within the amygdala following retrograde tracer injection into rostromedial ORB (ORBm, vl). **a** Photomicrograph of the injection center, and illustration of the rostrocaudal extent of the injection spread for case #40. **b** Illustration of the injection centers for comparison injections into very rostral mPFC (#43, #48-51). **c** Labeled neurons (red dots) were plotted onto rat brain templates derived from Swanson (2004), arranged from rostral to caudal. Numbers denote atlas levels, scale bar = 200 µm.

Topography of amygdala projections to the medial prefrontal cortex. We observed no labeling within the CEA following tracer injections into any region of the mPFC. This finding demonstrates that the CEA does not send any direct projections to the mPFC. In contrast, we found substantial labeling within the basolateral area of the amygdala following retrograde tracer injections in the mPFC, and these connections were topographically organized. Specifically, the most dorsal mPFC tracer injection placement (ACAd) more heavily labeled rostral regions (BLAa), while the most ventral mPFC tracer injection placement (ILA) more heavily labeled caudal regions (BLAp and BMAp), and mid dorsoventral placed mPFC injections (PL) produced an intermediate pattern of labeling (Fig. 2.6). A quantitative analysis of the distribution of labeling confirmed this pattern (Table 2.1). Thus, we found a rostrocaudal to dorsoventral topography in amygdala projections to the mPFC.

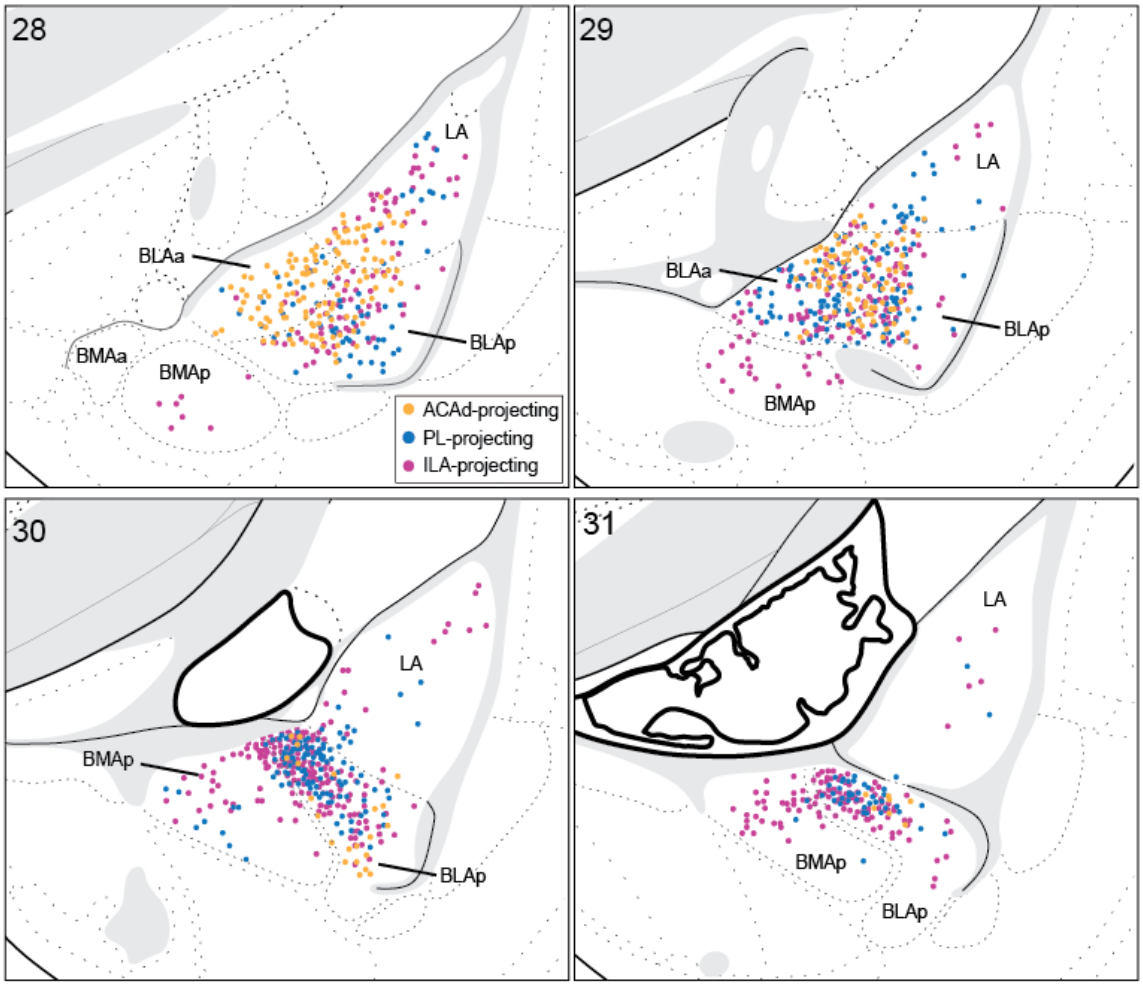

Fig. 2.6 Topographical distribution of basolateral area projections to the mPFC. Combined labeling plots in the amygdala following ACAd (orange; from Fig. 2.2c), PL (blue; from Fig. 2.3c), and ILA (pink; from Fig. 2.4c) injections. Labeled neurons were plotted onto rat brain templates derived from Swanson (2004), arranged from rostral to caudal. Numbers denote atlas levels.

Table 2.1 Quantitative distribution of retrogradely labeled neurons within the amygdala following mPFC injections into the ACAd (#32), PL (#25), and ILA (#35). For each mPFC target, shown are the percent of labeled neurons located within each cell group (there was no labeling in BMAa), and the percent of labeled neurons located within the rostral (atlas levels 26-28), mid (atlas level 29-31), and caudal (atlas levels 32-34) basolateral area (collapsed across cell groups).

	% by cell group				% by rostrocaudal location		
	BLAa	**BLAp**	**BMAp**	**LA**	**Rostral**	**Mid**	**Caudal**
ACAd	48.47	35.11	0.00	15.65	57.69	42.31	0.00
PL	19.21	60.84	7.39	12.56	20.69	69.46	9.85
ILA	8.72	59.93	18.00	13.36	18.18	66.79	15.03

Projections from the amygdala and medial prefrontal cortex to the lateral hypothalamus. Retrograde tracer injections into the dorsal LHA produced strikingly different patterns of labeling in the amygdala and mPFC compared to injections into the ventral LHA. Injections into dorsal LHA primarily labeled the CEA (Fig. 2.7a) and the entire dorsoventral and rostrocaudal extent of the mPFC (Fig. 2.8a). In contrast, injections into ventral LHA primarily labeled regions of the basolateral area of the amygdala (Fig. 2.7d), and a select ventrocaudal portion of the mPFC (Fig. 2.8b).

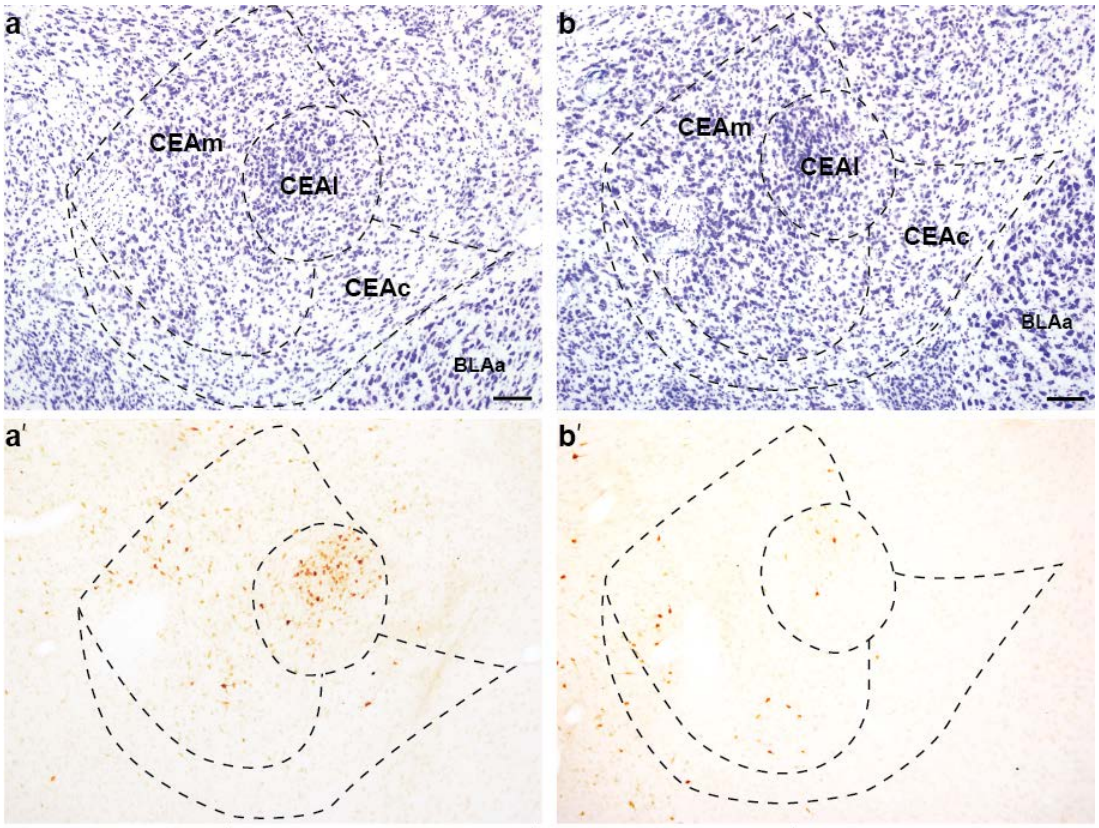

Fig. 2.7 Representative images of retrograde tracer labeling in the amygdala; the CEA after tracer placement into dorsal (**a'**; #23) and ventral (**b'**; #21) LHA, and the basolateral area of the amygdala after tracer placement into dorsal (**c'**; #23) and ventral (**d'**; #21) LHA. **a, b** Adjacent Nissl-stained tissue. Scale bars = 100μm. (continued on next page)

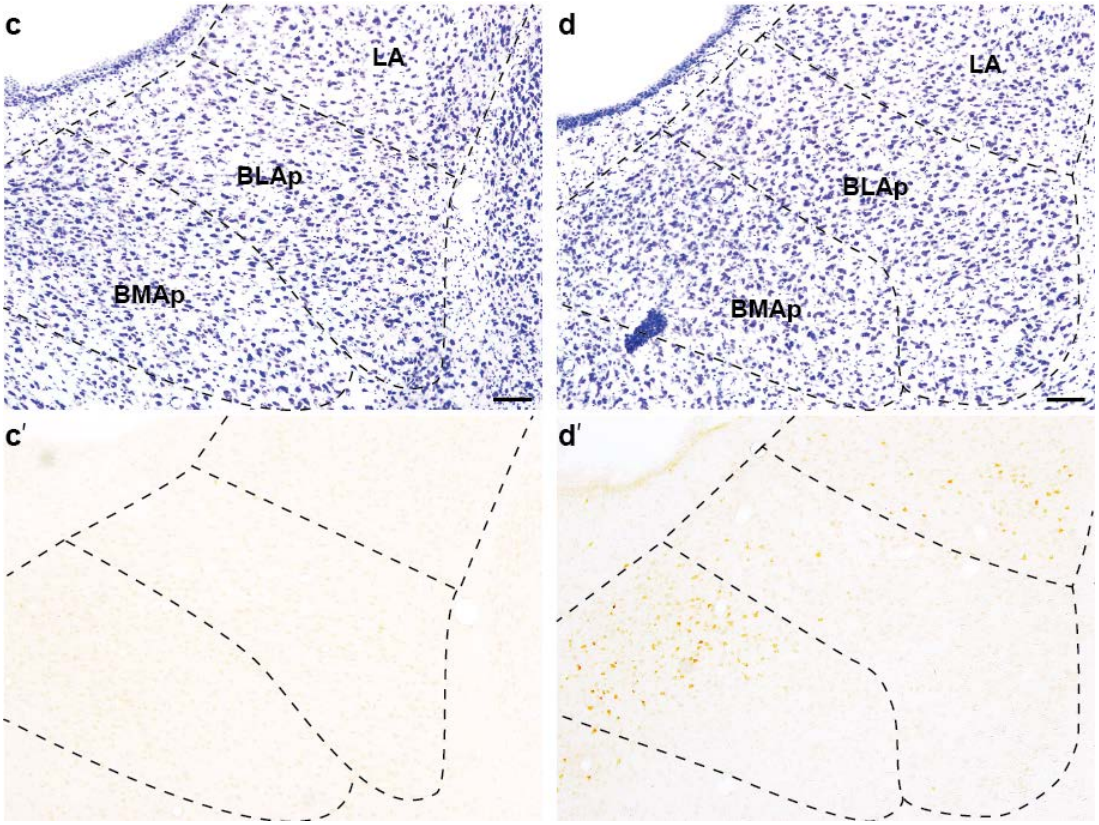

Fig. 2.7, continued

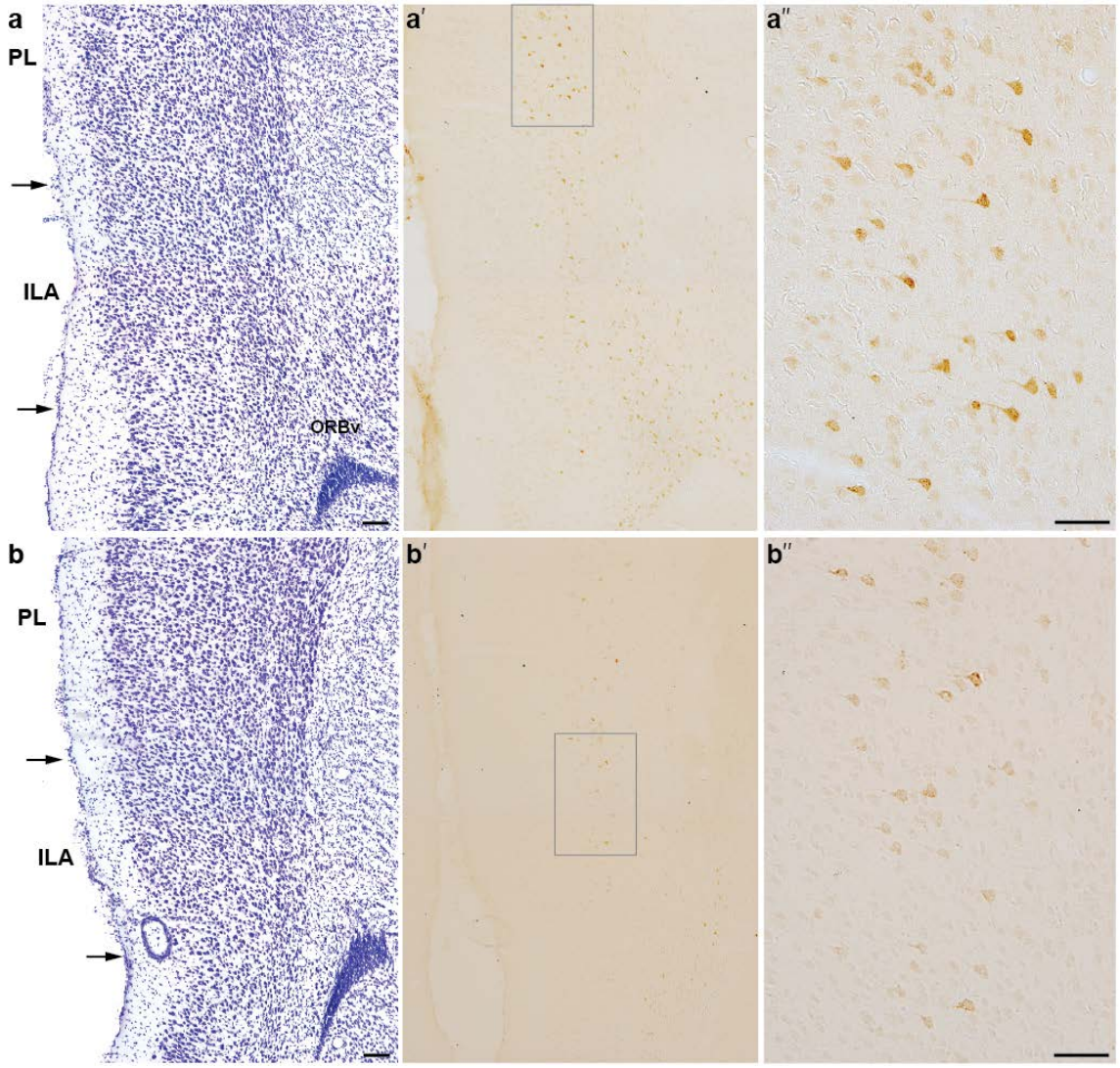

Fig. 2.8 Photomicrographs show retrograde tracer labeling in the mPFC after tracer placement into dorsal (**a'**; #23) and ventral (**b'**; #24) LHA, and adjacent Nissl-stained tissue (**a**, **b**); scale bars = 100µm. Labeling within layer 5 after dorsal (**a'')** and ventral (**b'')** LHA, as indicated by gray boxes on **a'** and **b'**; scale bars = 50µm.

Projections to the dorsal LHA. In seven cases, the retrograde tracer injection was predominately located within the dorsal LHA. The retrograde labeling pattern for one of these, #23 (Fig. 2.9a, c, d), is shown in detail because the injection was centered above fornix, it most completely included the entire dorsal portion of the LHA, and the pattern of labeling was representative of other injections into this region (Fig. 2.9b). Other injections were centered more dorsally with some spread into the zona incerta (#37 and #55), or were placed medial to fornix (#26, #28, #40 and #41).

Within the amygdala, the majority of labeled neurons following injections into the dorsal LHA was concentrated within the CEA. Sparser labeling was present in the BMAa and the most rostral portion of the BMAp (Fig. 2.9c). In contrast, there was no significant labeling in the LA, BLAa, or BLAp following dorsal LHA injections (Fig. 2.7c). Within the CEA there were labeled neurons in all three subdivisions (lateral part (CEAl), medial part (CEAm), and capsular part (CEAc)); the division with the overall greatest number of labeled neurons was the CEAm, though the single densest group of labeled neurons was within CEAl (Fig. 2.7a, 2.8c). This dense group of labeled neurons was completely contained within the CEAl rostrally (atlas level 26), and formed a continuum with CEAm caudally. This distinct labeling was also present in other cases with dorsal LHA injections (#26, #28, #40 and #41), except for the two most dorsal cases (#37 and #55), suggesting that the CEA most strongly projects to areas bordering fornix.

Retrograde tracer injections into the dorsal LHA also resulted in extensive labeling of the mPFC (Fig. 2.8a, 2.9d), throughout its entire rostocaudal extent. This labeling was almost entirely contained within layer 5, although there was some labeling

in layer 6 caudally. Most of the labeling was concentrated within the PL and ILA, but extended dorsally through the ACAd. Rostrally, labeling extended laterally from ORBm, across the ORBvl and the lateral part of the orbital area (ORBl). Caudally, there were labeled neurons in layer 6 of the ventral part of the orbital area (ORBv). The labeling pattern was similar in the comparison injections, with minor variations in density. There was less labeling in rostral mPFC (atlas levels 4-6) for most of the cases, while in two cases (#37 and #55) there was more labeling in caudal ILA (atlas level 11).

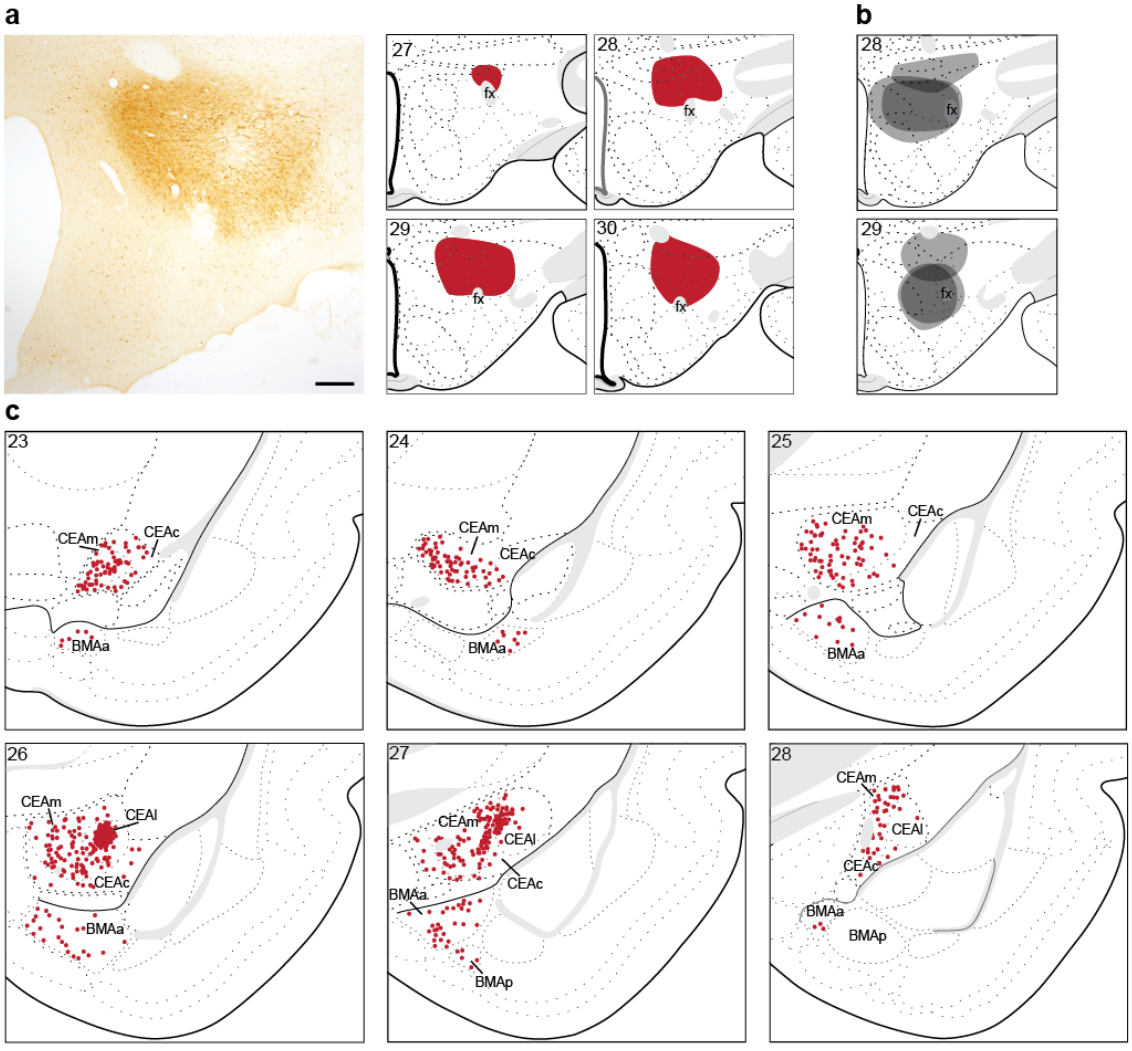

Fig. 2.9 The distribution of labeling within the amygdala (**c**) and mPFC (**d**) following retrograde tracer injection into dorsal LHA. **a** Photomicrograph of the injection center, and illustration of the rostrocaudal extent of the injection spread for case #23. **b** Illustration of the centers of other injections into dorsal LHA (#26, #28, #37, #40, #41, #55). **c-d** Labeled neurons (red dots) were plotted onto rat brain templates derived from Swanson (2004), arranged from rostral to caudal. Numbers denote atlas levels, scale bar = 200 µm. (continued on next page)

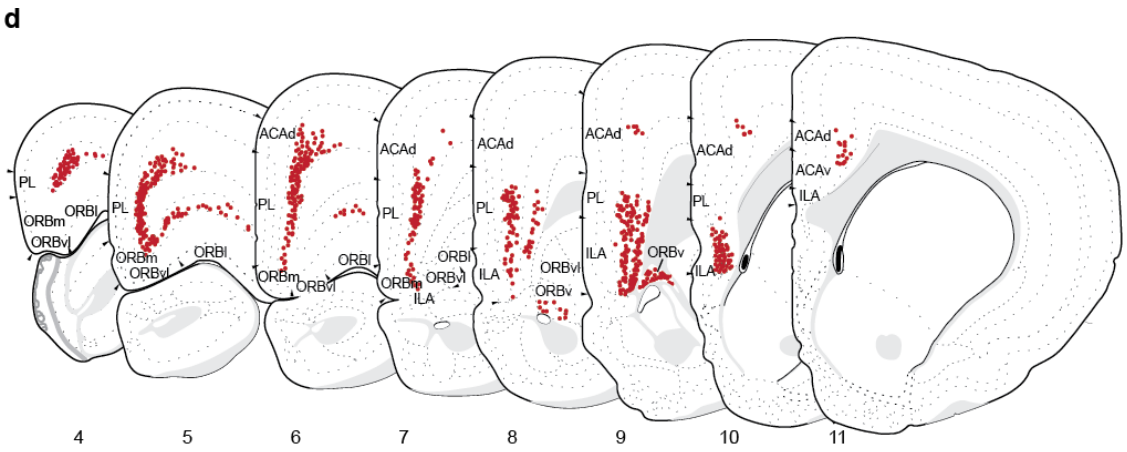

Fig. 2.9, continued

Projections to the ventral LHA. In six cases, the retrograde tracer injection was contained within ventral LHA. The retrograde labeling pattern for one of these, #21 (Fig. 2.10a, c, d), is shown in detail because the tracer injection most completely filled the entire ventral LHA, and its pattern of labeling was representative of other cases following injections into this region (Fig. 2.10b). Among comparison injections, one (#24) was very similar in size and placement to the represented case, two were located ventrolaterally and mostly within the tuberal nucleus (TU; #51 and #53), and two were smaller, located medially, and primarily contained within the ventral zone of the juxtaventromedial region of the LHA (LHAjvv; # 29 and #52).

Following retrograde tracer injection into the ventral LHA, the majority of labeled neurons in the amygdala were within three distinct groups within the basolateral area: the medial half of the BMAa, the dorsal half of the BMAp, and a small ventrolateral group in the LA (Fig. 2.7d, 2.10c). The dense labeling within the BMAa was located medially and extended across its rostrocaudal extent. The labeling in the BMAp was concentrated dorsally, and tapered off laterally in the BLAp. Caudally, labeled neurons in the BMAp and BLAp, together with posterior amygdalar nucleus (labeling not shown), formed a continuous group below and parallel to the stria terminalis. The third group was in the caudal third of the LA, specifically within its ventrolateral corner. There was no labeling in the BLAa. Sparser labeling was observed throughout the CEA, mostly in CEAc but also in CEAl and CEAm (Fig. 2.7b). Overall labeling in the CEA was light to moderate in the plotted example, but was much lighter in the comparison injections which did not

include the region bordering fornix (#29, #51, #52, #53), suggesting that the perifornical region of the LHA is preferentially the target of CEA inputs.

This pattern of labeling was replicated in the case where the injection was nearly identical (#24), except for slightly more labeling in the CEA, which may be attributed to injection's spread dorsally and medially around fornix. In the comparison injections labeling in the BMAa was lighter than the plotted example, however labeling in other basolateral area regions depended on injection placement. In the cases where the injection was located more medially (#29 and #52) the pattern of labeling in BMAp, BLAp, and LA was similar to the plotted example. The two cases restricted to the most ventrolateral edge of the ventral LHA (#51 and #53) had more restricted BMAp labeling (only labeling caudally, adjacent to posterior amygdalar nucleus) and there was no labeling in LA.

In contrast to dorsal LHA injections that produced extensive mPFC labeling, ventral LHA injections produced very restricted labeling within the ventrocaudal region, specifically in the ventral PL, ILA and ORBv (Fig. 2.8b, 2.10d). Similar to the pattern after dorsal LHA injections, labeling was mainly contained within layer 5, but included some labeling in layer 6. All comparison cases had a similar pattern of mPFC labeling, with minor variations in density.

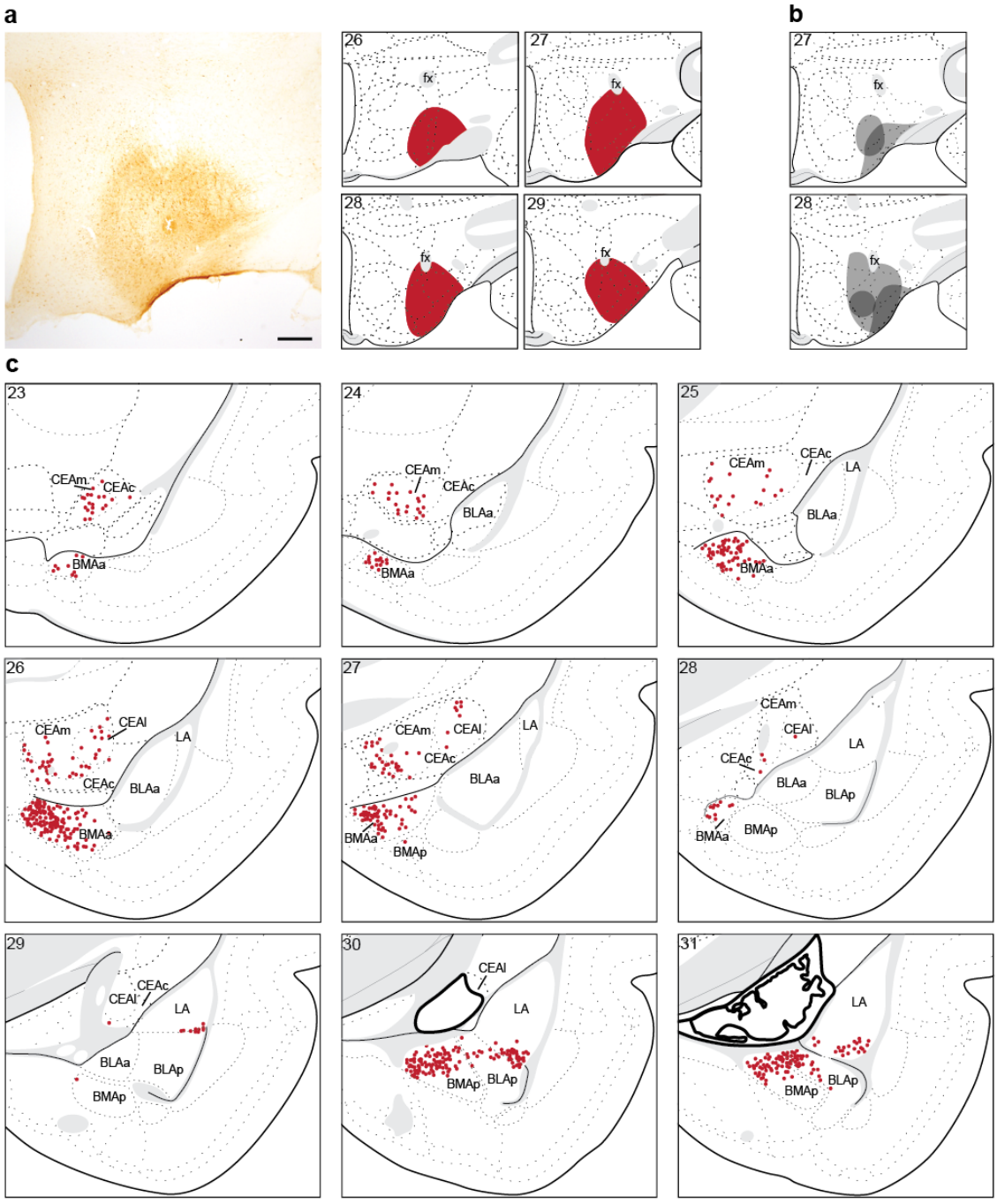

Fig. 2.10 The distribution of labeling within the amygdala (**c**) and mPFC (**d**) following retrograde tracer injection into ventral LHA. **a** Photomicrograph of the injection center, and illustration of the rostrocaudal extent of the injection spread for case #21. **b** Illustration of the centers of other injections into ventral LHA (#24, #29, #51-53). **c-d** Labeled neurons (red dots) were plotted onto rat brain templates derived from Swanson (2004), arranged from rostral to caudal. Numbers denote atlas levels, scale bar = 200 µm. (continued on next page)

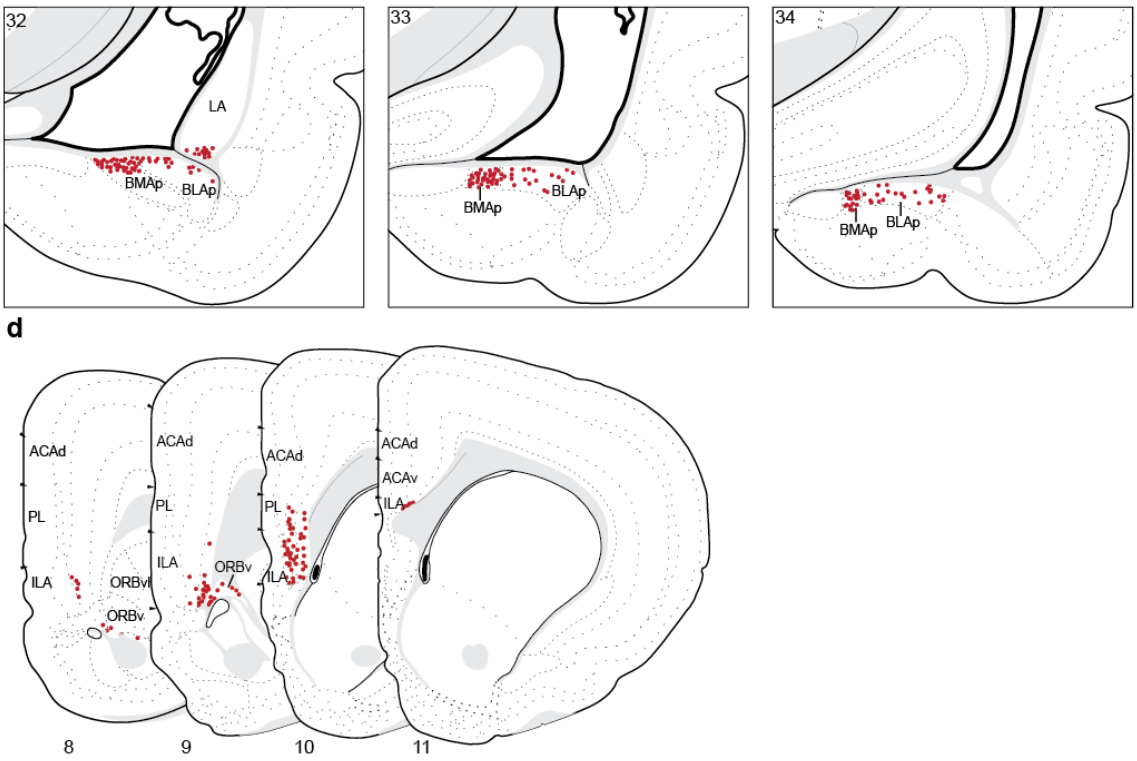

Fig. 2.10, continued

Parallel amygdala pathways to the medial prefrontal cortex and lateral hypothalamus. The single-label analysis of retrograde labeling patterns, described above, revealed that amygdalar projections to the mPFC and LHA arise primarily in separate nuclei. Specifically, the BLA most strongly innervates the mPFC, while the BMA and CEA most strongly innervate the LHA. Rostrally, there was no potential for overlap as the populations of neurons projecting to the mPFC and LHA were topographically distinct (i.e., BLAa to mPFC; BMAa and CEA to LHA). Caudally, however, labeling from injections into the mPFC and LHA was present in adjacent nuclei, BLAp and BMAp, particularly across their border region (Fig. 2.11a).

Examination of the double-labeled tissue confirmed that separate populations of neurons within the basolateral area of the amygdala innervate the mPFC and LHA. There was very little overlap between the two populations of neurons rostrally, as expected from the analysis of single-labeled tissue. Even caudally, where the two populations of retrograde tracer-labeled neurons were intermixed, the occurrence of double-labeled neurons was very seldom (Fig. 2.11b). Indeed, only 1.31 ± 0.29% (mean ± SEM, n=4) of all tracer-labeled neurons were double-labeled, indicating they projected to both targets. Thus, more than 98% of all labeled neurons projected to only one target, thereby confirming that amygdala pathways to the mPFC and LHA arise primarily in separate populations of neurons.

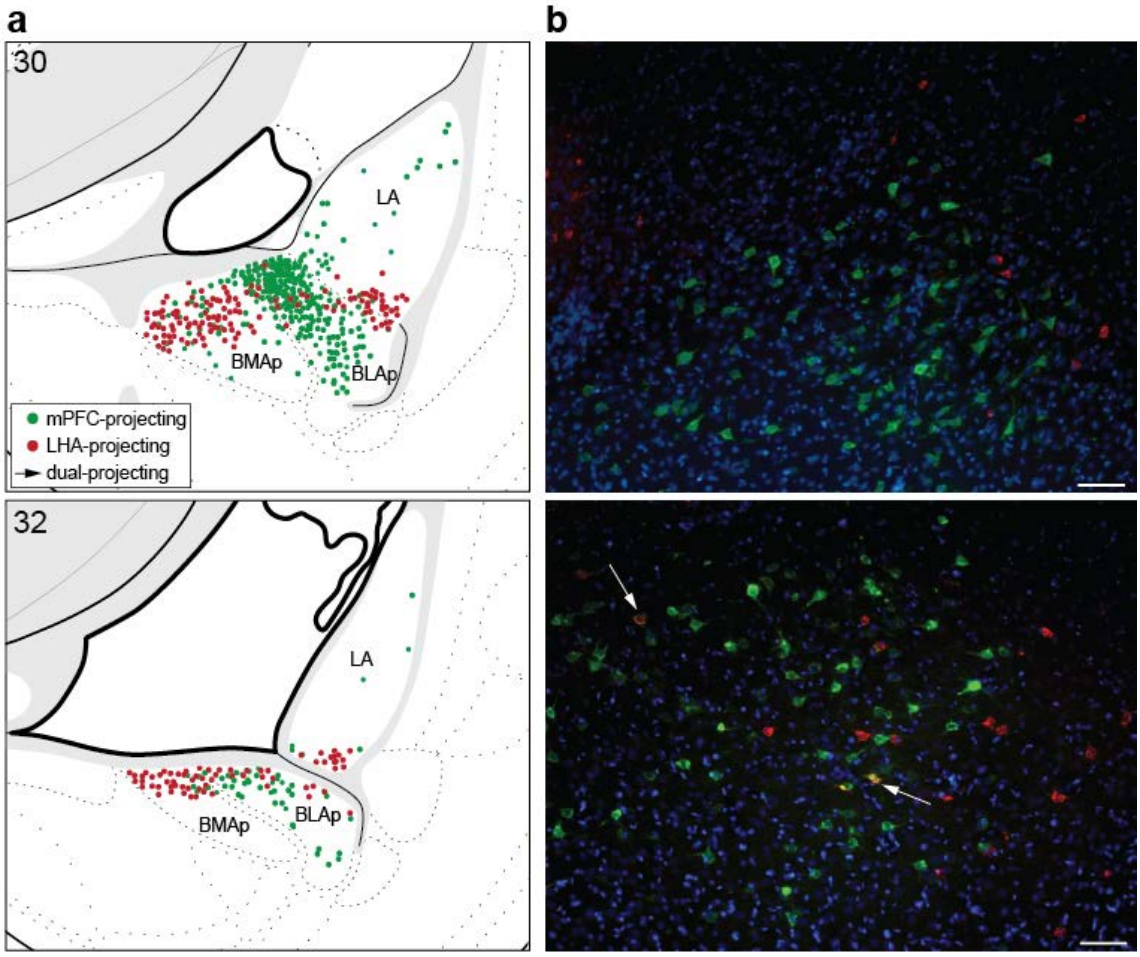

Fig. 2.11 Distribution of mPFC-projecting (green) and LHA-projecting (red) neurons in the caudal basolateral area of the amygdala. **a** Illustration of total amygdala projections to all mPFC areas and both LHA regions **(**combined labeling plots from single-label analyses shown in Figs. 2.2c, 2.3c, 2.4c, 2.5c, 2.9c, and 2.10c). Labeled neurons were plotted onto rat brain templates derived from Swanson (2004); numbers denote atlas levels. **b** Representative images from a single brain used in the double-label analysis for simultaneous visualization of both tracers (case #20, injection in PL and a large injection in LHA). Arrows indicate double-labeled neurons which project to both the mPFC and LHA (yellow); scale bars = 100µm.

Discussion

This study examined the organization of connections between the amygdala, mPFC, and LHA with dual retrograde tract tracing and immunohistochemical techniques. Within the amygdala, we analyzed the topography of pathways from the CEA and basolateral area to the mPFC and LHA in detail. These areas are cytoarchitectonically heterogeneous, and we characterized distinct pathways from their different nuclei that form multiple subsystems within the amygdala-prefrontal-lateral hypothalamic network. We found that both the CEA and the basolateral area send direct projections to the LHA, while only the basolateral area also sends direct projections to the mPFC. Within the LHA, the CEA and basolateral area innervate different regions, the dorsal and ventral LHA, respectively. Additionally, the strongest pathways from the basolateral area to the mPFC and LHA were from different nuclei, the BLA and BMA, respectively, and nearly all (>98%) of these projections originated from different neurons. To our knowledge, this was the first study to directly examine whether the same or different amygdalar neurons project to the mPFC and LHA. Thus, we found evidence for multiple, direct pathways from the CEA and basolateral area to the LHA, and separate pathways from the BLA to areas of the mPFC that send direct projections to the LHA (Fig. 2.12).

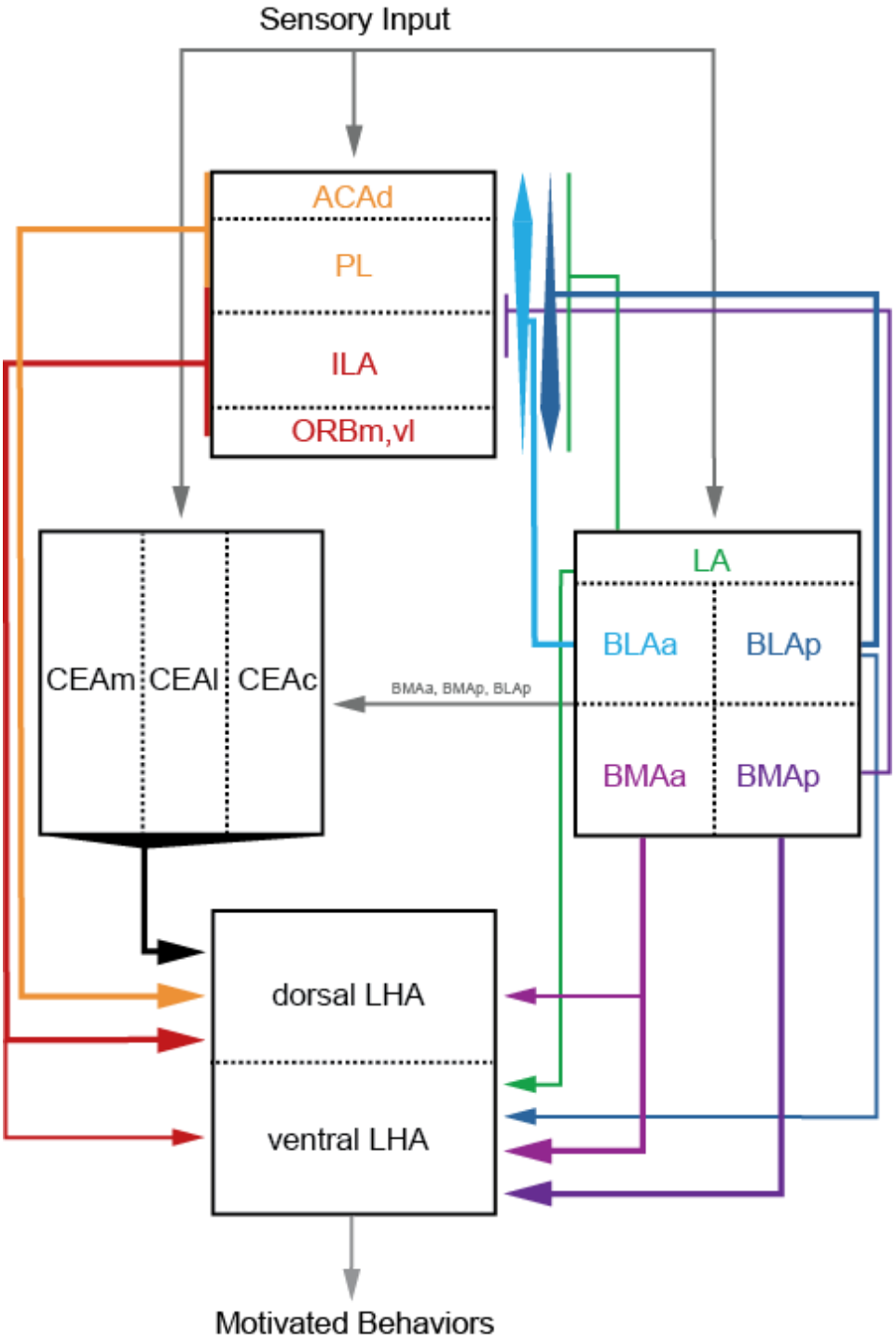

Fig. 2.12 Summary of projections characterized in the present study. Selected other known projections are shown in gray.

Comparisons with prior studies.

Amygdalar projections to the mPFC. The current study found extensive direct projections to the mPFC from the basolateral area of the amygdala, but not from the CEA, in accordance with prior observations (Hoover & Vertes, 2007; McDonald, 1991; Swanson & Petrovich, 1998). The primary sources of the afferents to the mPFC were the BLAa and BLAp, and adjacent regions, dorsally the LA and ventromedially the BMAp (Fig. 2.1). These pathways are topographically organized (Fig. 2.6, Table 2.1); the BLAa more heavily projects to the dorsal mPFC (e.g., ACAd, dorsal PL) compared to the caudal nuclei, the BLAp and BMAp, which more heavily project to the ventral mPFC (e.g., ventral PL, ILA). This detailed topography adds to prior retrograde tracing work which had shown a topographical organization of projections from the basolateral area of the amygdala to the entire prefrontal cortex (McDonald, 1987). The rostocaudal to dorsoventral topography of amygdala to mPFC projections had been observed in prior work, however that study more strongly emphasized a rostrocaudal to rostrocaudal topography, especially for ILA inputs (Hoover & Vertes, 2007). In the present study, we also observed a similar topography for amygdalar inputs to the PL, in that our more rostrally placed injections into PL (Fig. 2.3b) only produced labeling in the most rostral basolateral area (BLAa and very rostral BLAp), and injections into very rostral mPFC, the rostromedial orbital area, resulted in labeling restricted mainly to the BLAa (Fig. 2.5).

We found the most substantial retrograde labeling within the amygdala after injections into either the PL or ILA. The largest rostrocaudal extent of labeling was observed following injections into PL, which is in agreement with prior work (Hoover &

Vertes, 2007). Although the rostrocaudal spread of amygdalar retrograde labeling was greater following PL injections, the overall amount of labeling was similarly strong following injections into the PL and ILA, which was consistent with prior reports (Hoover & Vertes, 2007). In comparison, the amount of retrograde labeling after ACAd injection was much less, which was also previously reported (Hoover & Vertes, 2007).

Our findings are in general agreement with prior anterograde tracing work that found extensive innervation of the mPFC by the amygdala. In early studies injections were large and therefore preclude direct comparisons with specific nuclei in the current study. Injections that encompassed the LA, BLAa, and BLAp produced dense labeling within the PL and ILA, and the highest density within layer 5 (Krettek & Price, 1977). That study reported denser projections to the mPFC from BLAp compared to the BLAa, however, the reduced amount of labeling after BLAa injections may be explained by considerable spread into the CEA (Krettek & Price, 1977). A later study (Kita & Kitai, 1990) with a more sensitive tracer (Lanciego & Wouterlood, 2011) also reported strong innervation of the mPFC (with particularly dense terminations in layer 5) after caudal (i.e., BLAp, BMAp, and caudal LA) but not after rostral (i.e., BLAa, rostral LA) injections into the basolateral area. In contrast, we found that the BLAa and BLAp projected equally strongly to the mPFC, albeit to different regions (i.e., dorsal and ventral mPFC, respectively; Table 2.1). In agreement with the rostrocaudal amygdala to dorsoventral mPFC topography we observed, a previous study found that the BMAp moderately innervated layer 5 of the ventral mPFC (e.g., ILA, ventral PL), but did not innervate the dorsal mPFC (e.g., dorsal PL, ACAd) (Petrovich, Risold, & Swanson,

1996). In the present study, we did not observe any labeled neurons in the BMAa after retrograde tracer placement into any mPFC location, in agreement with very sparse innervation restricted to the superficial layers of the ILA from the BMAa (Petrovich et al., 1996).

Amygdalar projections to the LHA. Connections from the amygdala to the hypothalamus are well known (Petrovich et al., 2001), and prior anterograde studies determined that the most substantial input to the LHA is from the CEA, while the basolateral area more strongly innervates the medial zone nuclei (Petrovich et al., 2001). Similarly, a retrograde tracing study found that the greatest contribution to the LHA was the CEA, but also noted labeling in the BMA, LA, and BLA (Ono et al., 1985). Extending prior work, here we found that the CEA and basolateral area nuclei most strongly projected to different parts of the LHA, the dorsal and ventral LHA, respectively (Fig 2.7). Specifically, all subdivisions of the CEA were labeled after retrograde injections into the dorsal LHA with the greatest contribution from CEAm and CEAl, while the medial half of the BMAa, the dorsal half of the BMAp and laterally adjacent BLAp, and a small ventrolateral group in the LA were labeled after injections into the ventral LHA.

Based on prior anterograde work, the amygdala densely innervates three distinct fields across rostrocaudal LHA (Petrovich et al., 2001), which may explain why some previous studies with single retrograde tracer deposits in LHA did not produce labeling in the CEA (Cassell, Gray, & Kiss, 1986; Kita & Oomura, 1982). The first field spans the dorsal LHA and is strongly innervated by the CEAm and CEAc (Petrovich et al., 2001),

and in agreement we observed similar patterns in the current study after injections into the dorsal LHA. The second field is a caudolateral portion of the LHA, and is strongly innervated by the CEAm and CEAc and lightly by the BMAa and BLAp (Petrovich et al., 2001). However, neither the dorsal nor ventral LHA injections in the present study were centered in that region. The third field is ventromedial LHA (including the TU), which is moderately innervated by the BLAp and BMAp (Petrovich et al., 2001; Petrovich et al., 1996); our ventral LHA injections were placed within this field, and produced labeling consistent with this pattern.

The present study found substantial retrograde labeling within the CEA and basolateral area nuclei, but after tracer injections into different parts of the LHA. This is consistent with prior observations that the CEA and BLA send parallel fibers to the LHA (Krettek & Price, 1978a), and that the CEA sends substantial projections into the dorsal LHA (Ono et al., 1985; Petrovich et al., 2001; Yoshida et al., 2006). Retrograde labeling in the CEA was dense after injections into the dorsal LHA and light to moderate following injections into the ventral LHA, but only when injections included the regions directly adjacent to fornix, suggesting the CEA preferentially targets the perifornical region (for CEA projections to far lateral regions see: Petrovich et al. 2001). Light labeling following ventral LHA injections is consistent with prior work that found sparse labeling after discrete injections into the dorsal and ventral zones of the juxtaventromedial LHA (LHAjvd, LHAjvv) (Hahn & Swanson, 2015) and no labeling after injections into TU (Toth, Fuzesi, Halasz, Tulogdi, & Haller, 2010). Our findings that the rostral half of the CEAl has much stronger projections to the LHA than the

caudal CEAl is consistent with a previous study that did not find significant labeling within the LHA from the caudal CEAl (Petrovich & Swanson, 1997). Light to moderately dense projections from the basolateral area of the amygdala to the LHA have also been reported previously (Ono et al., 1985; Petrovich et al., 2001), and in general agreement we found substantial labeling in distinct nuclei within this area. Specifically, the BMAa projects to both dorsal and ventral LHA, while caudal regions (BMAp, BLAp, LA) project to only the ventral LHA. Early anterograde work (Krettek & Price, 1978a) did not find LHA labeling after injections restricted to the BMA. However, consistent with the current results, a later anterograde tracing study (Petrovich et al., 1996) with a more sensitive tracer (Lanciego & Wouterlood, 2011) and a recent study with retrograde injections into discrete ventral LHA cell groups (LHAjvd or LHAjvv) (Hahn & Swanson, 2015), showed moderate to dense input from the BMAa and BMAp.

The LHA is a highly differentiated region (Swanson, 2004) and it is important to determine which specific cell groups receive inputs from the CEA, and particularly from the dense cluster of neurons we identified (across CEAm/CEAl; Fig. 2.7a, 2.8c) after tracer injections into the dorsal LHA. Recent work has started to systematically examine inputs and outputs of discrete LHA cell groups (Hahn & Swanson, 2010, 2012, 2015). Of particular interest are two regions, suprafornical (LHAs) and juxtadorsomedial (LHAjd), which are included within the dorsal LHA of the present study. Retrograde tracer injections confined to LHAs resulted in the labeling of a dense group of neurons in the CEAl, and sparse labeling in CEAm, CEAc, BMAa, and caudal BLAp (Hahn & Swanson, 2010). In contrast, retrograde tracer deposits restricted to the LHAjd did not

label the CEAl, and resulted in low labeling of the CEAm, CEAc, and all regions of the basolateral area of the amygdala (Hahn & Swanson, 2012). Thus, the dense labeling within the CEA we observed after dorsal LHA retrograde tracer injections is, at least in part, due to specific projections to the LHAs.

The specific phenotype of CEA neurons projecting to LHA has not been characterized, however CEA neurons are nearly exclusively GABAergic (Swanson & Petrovich, 1998), and additionally express various neuropeptides, especially within the CEAl (e.g., Cassell et al., 1986; Day, Curran, Watson, & Akil, 1999; Haubensak et al., 2010; H. Li et al., 2013; Marchant, Densmore, & Osborne, 2007; Roberts, Woodhams, Polak, & Crow, 1982; Wray & Hoffman, 1983). Based on topographical distribution, the CEAm/CEAl group of neurons that strongly projects to the LHA may contain enkephalin (Cassell et al., 1986; Day et al., 1999; Wray & Hoffman, 1983). A subpopulation of CEAl neurons expresses protein kinase C-δ (PKCδ), a substantial proportion of which coexpress enkephalin (Haubensak et al., 2010). Interestingly, recent work found that the PKCδ-positive neurons are critical for fear (Haubensak et al., 2010), and for the inhibition of feeding (Cai et al., 2014). Nevertheless, other neuropeptides are also densely expressed within portions of this area (e.g., somatostatin, corticotropin-releasing hormone, neurotensin), and CEA to LHA pathways are likely heterogeneous in terms of neuropeptide content. In that regard, neurons in the LHA are responsive to many of the neuropeptides and the neurotransmitter expressed by the CEA (Stanley, Urstadt, Charles, & Kee, 2011; Tsujino & Sakurai, 2009).

Within the LHA, the targets of CEA inputs include neurons that express two orexigenic neuropeptides: melanin-concentrating hormone (MCH) and orexin/hypocretin (Broberger et al., 1998; de Lecea et al., 1998; Griffond & Risold, 2009; Hahn, 2010; Nahon, Presse, Bittencourt, Sawchenko, & Vale, 1989; Sakurai et al., 1998; Swanson et al., 2005). Anterograde tract tracing combined with orexin detection showed that the CEA (specifically the CEAl) innervates a substantial proportion of orexin neurons in the LHA, especially within the perifornical region, which somewhat overlaps with our dorsal LHA and includes LHAs (Yoshida et al., 2006). Additional detailed analyses revealed that GABAergic CEA terminals innervate orexin and MCH neurons (Nakamura, Tsumori, Yokota, Oka, & Yasui, 2009). Interestingly, the BMAa—the only other amygdalar nucleus that sends substantial input to the dorsal LHA (current study)—also innervates MCH neurons, and these projections are glutamatergic (Niu, Yokota, Tsumori, Oka, & Yasui, 2012). It remains to be determined whether BMAa neurons also innervate orexin neurons.

mPFC projections to the LHA. The current study found that the entire rostrocaudal and dorsoventral extent of the mPFC projects to the dorsal LHA, while only a restricted ventrocaudal region of the mPFC (i.e., ILA and adjacent PL and ORBv) also projects to the ventral LHA. This is consistent with other studies that reported labeling along the dorsoventral extent of the mPFC (Gabbott, Warner, Jays, Salway, & Busby, 2005; Kita & Oomura, 1982), and laterally across the orbital regions (Gabbott et al., 2005) after retrograde tracer injections that included both dorsal and ventral LHA, and studies with deposits restricted to cell groups ventral to fornix that reported labeling in

caudal PL, ILA, and ORBv (Hahn & Swanson, 2015; Toth et al., 2010). Also consistent with prior work, most of the labeled neurons were in layer 5, with moderate labeling in layer 6 (Gabbott et al., 2005).

Current findings also align with previous observations with anterograde tract tracing (Floyd, Price, Ferry, Keay, & Bandler, 2001; Hoover & Vertes, 2011). These studies have shown stronger projections to the perifornical and lateral regions of the LHA from the ventral compared to the dorsal mPFC (Hoover & Vertes, 2011; Hurley et al., 1991; Sesack et al., 1989; Takagishi & Chiba, 1991; Vertes, 2004). Similarly, we found that the ventral mPFC had more projections to the LHA, compared to the dorsal mPFC. In general agreement with a previously demonstrated rostrocaudal gradient of projections from the mPFC (specifically from PL) to the LHA (Floyd et al., 2001), we observed more labeled neurons in rostral than caudal PL following retrograde injections into dorsal LHA. Taken together, prior and current findings suggest that the density of mPFC inputs to the LHA increases along two axes to create a dorsorostral to ventrocaudal gradient of light to dense innervation.

Recent, high-resolution analyses of discrete dorsal LHA regions provide additional topographical specificity to the patterns of mPFC to LHA projections. Retrograde tracer deposits in regions medial to (LHAjd) or directly above (LHAs) fornix moderately labeled the entire medial wall of the mPFC and lightly labeled the rostromedial orbital area (Hahn & Swanson, 2010, 2012), while deposits lateral to fornix in a region that corresponds to LHAd (Swanson, 2004) resulted in labeling that was restricted to the ILA (Hurley et al., 1991). Together with the present report, these findings

suggest that ACAd, PL, and rostromedial orbital regions project specifically to the LHAjd and LHAs, while the ILA projects to the entire dorsal area of LHA. Finally, the mPFC inputs to the LHA include the area with neurons that express the peptides MCH and orexin. Anterograde tracing combined with orexin detection confirmed that ILA neurons directly innervate orexin neurons across the entire orexin field (Yoshida et al., 2006). Whether projections from other mPFC areas also innervate orexin neurons, and whether any mPFC neurons innervate MCH neurons, remains unknown.

Functional significance. It is instructive to review the organization of the amygdala-prefrontal-lateral hypothalamic system delineated in the current study within larger structural and functional frameworks. The two large amygdalar areas examined are differentiated parts of the striatum or cortex that belong to different functional systems—autonomic (CEA), main olfactory (BMAa, BMAp, BLAp), or frontotemporal (BLAa, LA) (Swanson & Petrovich, 1998). In agreement with this organization, the most substantial output to the LHA was from the striatal, autonomic system (CEA) and the nuclei that belong to the main olfactory cortex (BMAa, BMAp, BLAp). The nuclei that belong to the frontotemporal cortex (BLAa and LA) did not send direct input to the LHA (except for a small, ventrolateral group of neurons within the LA), and they also do not send pathways to the bed nuclei of the stria terminalis (BST) (Dong, Petrovich, & Swanson, 2001), which would provide an indirect route to the LHA (Dong, Petrovich, & Swanson, 2000; Dong, Petrovich, Watts, & Swanson, 2001; Dong & Swanson, 2003, 2004a, 2004b, 2006a, 2006b, 2006c). A reverse pattern was observed for amygdalar pathways to the mPFC. The cortical (except BMAa), but not striatal (CEA), nuclei sent

topographically organized projections to the mPFC, and the strongest inputs were from the BLAa, BLAp, and BMAp, while the LA input was more limited.

Nevertheless, the LA sends substantial projections to another cortical region, the hippocampal formation (HF), which provides access to the hypothalamus (Canteras & Swanson, 1992; Cenquizca & Swanson, 2006; Petrovich et al., 2001; Risold & Swanson, 1996). Interestingly, the only part of the LA that has direct projections to the LHA (current study) —the ventrolateral region— does not project to the HF (Petrovich et al., 2001). This topography suggests parallel LA pathways reach the LHA directly and indirectly via the HF, as different LA regions send direct pathways to the LHA and the HF. In contrast, the BLAa does not send any direct projections to the HF (Petrovich et al., 2001). The two frontotemporal cortical nuclei, therefore, preferentially innervate either the mPFC or the HF. This dichotomy is also reflected in their outputs to the striatum. Neither sends direct projections to the CEA (except for a limited input to the capsular part, from LA) (Pitkänen, Savander, & LeDoux, 1997; Swanson & Petrovich, 1998); instead they substantially innervate other parts of the striatum. Similar to its widespread innervation of the mPFC, the BLAa sends widespread output to the striatum, including the nucleus accumbens and large portions of the caudoputamen not innervated by other parts of the amygdala (Kita & Kitai, 1990). The LA, on the other hand, most substantially projects to the nucleus accumbens (Kita & Kitai, 1990).

The connectional patterns described in the current study also agree with the organization of cerebral hemisphere, defined by Larry Swanson, that controls motivated behaviors through a triple descending projection—cortical, striatal, and pallidal

(Swanson, 2000, 2005). Here, we found that the LHA receives converging striatal (CEA) and cortical (BMA, BLA, mPFC) inputs, which are topographically organized (dorsal LHA: CEA, BMAa, entire mPFC; ventral LHA: BMAa, BMAp, BLAp, ILA). The third (pallidal) descending component, from the BST, has been defined anatomically (Dong et al., 2000; Dong, Petrovich, & Swanson, 2001; Dong, Petrovich, Watts, et al., 2001; Dong & Swanson, 2003, 2004a, 2004b, 2006a, 2006b, 2006c), and was recently functionally tested for the control of feeding (Jennings, Rizzi, Stamatakis, Ung, & Stuber, 2013).

The present study found that different amygdalar neurons send direct projections to the mPFC and LHA, and thus parallel pathways, from different amygdalar subsystems, provide direct and indirect (via mPFC) inputs to the LHA. This framework suggests the amygdala influences the mPFC and LHA independently. Similar organization has been shown for amygdalar projections to the mediodorsal thalamus (MD) and mPFC (a target of the MD) (McDonald, 1987). Parallel BLA pathways (originating mainly from different neurons) to the mPFC and ventral hippocampus were also recently reported (Senn et al., 2014). In contrast, many BLA (and adjacent BMA and LA) neurons send collaterals to simultaneously innervate the PFC and striatum (McDonald, 1991).

Nearly all projections from the BLAa to mPFC arise from principal pyramidal neurons (McDonald, 1992). Quantitative ultrastructural analyses of these BLA projections have shown that a vast majority (>95%) of terminals synapse onto glutamatergic mPFC neurons in layers 2 and 5, but they also terminate (~5%) onto inhibitory interneurons (Gabbott, Warner, & Busby, 2006). This pattern of connections suggests the BLA could monosynaptically innervate mPFC output neurons and therefore

influence their targets, including the LHA, as was recently demonstrated for layer 5 mPFC neurons which project to the spinal cord (Gabbott et al., 2012). Even though most BLA inputs synapse onto pyramidal mPFC neurons, and fewer directly innervate interneurons (Gabbott et al., 2006), electrical stimulation of BLA neurons can inhibit mPFC neuronal firing through monosynaptic (as well as polysynaptic) pathways (Dilgen, Tejeda, & O'Donnell, 2013; Perez-Jaranay & Vives, 1991). Thus, BLA inputs could guide mPFC outputs through excitation or inhibition of pyramidal neurons.

Consistent with structural evidence, BLA inputs have been shown to influence mPFC during aversive- and reward-driven associative learning and subsequent behaviors, either through activation of pyramidal mPFC neurons or through inhibitory mechanisms. Pyramidal mPFC (PL, ILA) neurons which receive BLA (mostly BLAp) input showed increased activity (spiking and bursting) in response to a cue (odor) that predicts footshocks, but not to a control cue, at post-conditioning tests as well as during acquisition, while activity in mPFC neurons that were not responsive to BLA stimulation was unchanged (Laviolette et al., 2005). Furthermore, BLA inactivation significantly reduced the firing rate of pyramidal PL neurons in response to a conditioned fear cue (tone) and during conditioned lever pressing for food (Sotres-Bayon et al., 2012). Interestingly, the PL and ILA were differentially activated during the expression and extinction of conditioned fear (Sierra-Mercado, Padilla-Coreano, & Quirk, 2011), and correspondingly, the BLA neurons projecting to the PL were activated in response to an aversively conditioned stimulus (CS) while those projecting to the ILA were activated in response to an extinguished CS (Senn et al., 2014). Similarly, the BLAa was suggested to

guide mPFC activity during the acquisition of cue-food associations, because its recruitment preceded that of the mPFC and BLAa-mPFC pathways (specifically PL) were activated during this learning (Cole, Hobin, & Petrovich, 2015; Cole et al., 2013; Keefer et al. 2014).

In accordance with BLA influence via inhibitory interneurons, spontaneous mPFC firing (specifically in rostral PL) was suppressed during presentations of an aversive conditioned cue, and this suppression was eliminated with BLA lesions (Garcia, Vouimba, Baudry, & Thompson, 1999). Other work has shown that GABA, but not glutamate, transmission in the mPFC increased due to activation of inhibitory interneurons when rats were placed in a cocaine-associated environment, and that this inhibitory transmission could be blocked by basolateral area inactivation prior to context re-exposure (Chefer, Wang, & Shippenberg, 2011). Similarly, inactivation of the BLA-mPFC pathway via optogenetic inhibition of BLA terminals in PL inhibited cue-induced reinstatement of drug seeking behavior (Stefanik & Kalivas, 2013). Thus, the BLA can control both the activation (Sotres-Bayon et al., 2012) and suppression (Garcia et al., 1999) of mPFC neurons in response to conditioned stimuli (appetitive and aversive). Importantly, separate populations of pyramidal mPFC neurons exhibited profiles of either monosynaptic excitation or suppression of baseline firing following BLA stimulation, and these two populations were under differential control of the dopamine system (Floresco & Tse, 2007). Given that multiple, topographically organized pathways arise from different parts of the BLA and send pathways to different mPFC areas, it is likely that these two neuronal populations are parts of different BLA-mPFC subsystems.

Characterizing the precise subsystems is essential given the heterogeneity of the amygdala and mPFC (Heidbreder & Groenewegen, 2003; Swanson & Petrovich, 1998). These caveats in regard to comparisons across functional studies and inconsistencies in nomenclature, unfortunately, are a much broader concern.

Sensory and associative processing within the BLA-mPFC system could, in turn, control feeding and other motivated behaviors through mPFC-hypothalamic connections. For example, stimulation of μ-opioid- (Mena et al., 2011; Mena et al., 2013) or dopamine D1- (Land et al., 2014) receptor containing mPFC neurons has been shown to drive food consumption. Within the hypothalamus, sites of their action include the dorsal (perifornical) LHA and orexin neurons. The effects of mPFC μ-opioid elicited feeding were blocked by antagonism of NMDA glutamate receptors in the dorsal (perifornical) LHA (Mena et al., 2013), and stimulation of the mPFC μ-opioid system, in the absence food intake, recruited orexin and other neurons within the dorsomedial LHA (Mena et al., 2013). Additionally, D1-receptor containing mPFC neurons were shown to sparsely innervate the LHA (Land et al., 2014).

The LHA, especially the dorsal (perifornical) area, which contains orexin and MCH neurons, has been proposed to integrate cognitive and environmental influences with physiological drives underlying the motivation to eat (e.g., Berthoud & Münzberg, 2011; Petrovich, 2013). For example, MCH and orexin have been implicated in feeding driven by learned food cues in the absence of hunger (Petrovich, Hobin, & Reppucci, 2012; Sherwood, Holland, Adamantidis, & Johnson, 2015). Central orexin administration increases intake and motivation (breakpoint in progressive ratio responding) for palatable

food, while peripheral administration of an orexin antagonist blocks these effects (Borgland et al., 2009; Cason & Aston-Jones, 2013, 2014; Choi, Davis, Fitzgerald, & Benoit, 2010; Clegg, Air, Woods, & Seeley, 2002; Nair, Golden, & Shaham, 2008). Orexin neurons are recruited by environments and cues that predict food (and other rewards) (Choi et al., 2010; Harris, Wimmer, & Aston-Jones, 2005; Petrovich et al., 2012) as well as during the acquisition of cue-food associations (Cole et al., 2015). The BLA-mPFC system, can therefore access LHA feeding regulatory mechanisms as well as other motivational systems (e.g., Arvanitogiannis, Tzschentke, Riscaldino, Wise, & Shizgal, 2000; Wise, 1974).

In conclusion, here we defined topographically organized connections for amygdalar influence on the lateral hypothalamus via direct and mPFC routes. Precisely delineated organization of anatomical connections is an essential framework upon which functional studies can build (Khan, 2013). We focused on the control of feeding behavior, but the BLA-mPFC system could ultimately provide access for cognitive processing influence on hypothalamic circuitries underlying other motivated behaviors (Swanson, 2000, 2005). The amygdala-prefrontal-hypothalamic network function is adaptive and necessary for survival, but also susceptible to potential dysregulation (Likhtik & Paz, 2015; Petrovich, 2013). For example, environmental learned signals engaging the BLA-mPFC systems can override internal homeostatic signals regulating feeding behavior (Petrovich, 2013). More broadly, disruptions of this circuitry, particularly of the BLA-mPFC system, can result in maladaptive learning (Likhtik & Paz, 2015), and thus suboptimal expression of motivated behaviors.

III. Study 2: Fos Induction Maps

Introduction

Cessation of eating in response to fear is an adaptive physiological response (Cannon, 1915), however it may become maladaptive if persistent. This phenomenon can be replicated in the laboratory setting; previously neutral cues can come to signal a fearful event through Pavlovian conditioning, and these cues can later inhibit eating in hungry subjects. Importantly, this inhibition of feeding is a general effect of fear which can be elicited by both simple, discrete cues (Petrovich & Lougee, 2011; Petrovich et al., 2009) as well as complex, contextual stimuli (Reppucci et al., 2013) associated with past aversive events. The current study began the investigation of where in the brain fear-cues override the body's homeostatic hunger signals to inhibit feeding.

The ability of learned cues to modulate feeding behavior has been well-established (for review see: Petrovich, 2013). Specifically, it has been demonstrated that learned cues from the environment can induce consumption despite satiation (e.g., Grant & Milgram, 1973; Petrovich, Ross, Gallagher, et al., 2007; Reppucci & Petrovich, 2012; Weingarten, 1983, 1984), or inhibit consumption despite acute food deprivation (e.g., Bouton & Bolles, 1980; Petrovich & Lougee, 2011; Reppucci et al., 2013). The importance of an amygdala-prefrontal-lateral hypothalamic network in the conditioned potentiation of feeding has been established using diverse approaches, including lesion, functional disconnection, and functional circuit mapping techniques (Holland et al., 2002; Petrovich et al., 2005; Petrovich, Ross, Holland, et al., 2007; Petrovich et al., 2002). In contrast, the neural circuitry underlying the conditioned inhibition of feeding is less well

understood. Lesion work has demonstrated that the central nucleus of the amygdala (CEA), but not the basolateral area of the amygdala, is critical for fear-cue inhibited feeding (Petrovich et al., 2009). However, the importance of the medial prefrontal cortex (mPFC) and the lateral hypothalamic area (LHA) during the inhibition of feeding remain unknown. Here, we investigated activation within the amygdala (CEA and basolateral area), mPFC, and LHA to assess their recruitment when a learned fear-cue inhibits eating despite physiological hunger.

To accomplish this we used a behavioral training procedure recently developed in our laboratory (Petrovich & Lougee, 2011). In brief, this protocol consisted of alternating appetitive and aversive training sessions, which occurred in distinct contexts. During the appetitive sessions rats consumed food, while during the aversive sessions rats in the experimental groups received tone-shock pairings and rats in the control groups received only tones. During test day, consumption was monitored during tone presentations in the appetitive context and no footshocks were delivered. Rats were sacrificed following the test to determine brain activation patterns associated with the inhibition of the feeding as measured by immunohistochemical detection of the immediate early gene (IEG) *c-fos'* protein product (Fos) induction. IEGs are rapidly induced in response to extracellular stimuli and under diverse behavioral circumstances, and the resulting protein products often act as transcription factors to modify gene expression in response to the triggering event (Curran & Morgan, 1995; Morgan & Curran, 1991). As such, IEGs, like Fos, are considered indirect markers of recent neuronal activity (Chaudhuri, 1997).

In addition to food consumption, expression of another behavior—freezing—was also assessed during the test. Freezing is a fear-related behavioral response typically expressed by rodents in these settings, and is considered an index of conditioned fear learning (Blanchard & Blanchard, 1969; Bouton & Bolles, 1980; Fanselow, 1984). To aid in the interpretation of the Fos induction patterns two additional control groups were added to the previously established behavioral paradigm (Petrovich & Lougee, 2011). These groups underwent training and testing identical to that of the experimental and control groups, except they did not have access to food (no-food experimental and no-food control groups). The no-food experimental group helped dissociate Fos patterns associated with the inhibition of feeding from patterns associated with freezing. The no-food control group helped isolate the effects of feeding when compared to the control group.

Importantly, we completed a comprehensive comparison of Fos induction patterns in males and females. Few studies compare behavior and brain activation patterns of intact males and females (Cahill, 2006; Zucker & Beery, 2010), even though it is a necessary step in characterizing differences between the sexes (McCarthy et al., 2012). Thus, the current study intended to begin to remedy the gross underrepresentation of female subjects in both basic and clinical research (Zucker & Beery, 2010), which is especially relevant for the current behavioral paradigm given that women have higher reported rates of anxiety and eating disorders (Becker et al., 2007; McCarthy et al., 2012; McLean & Anderson, 2009). Thus, our goals were two-fold. First, we aimed to replicate prior behavioral findings that fear-cues can override hunger signals triggered by food-

deprivation to inhibit feeding in both male and female rats. Second, we aimed to map the patterns of activation within an amygdala-prefrontal-lateral hypothalamic network during the expression of this behavior, and assess whether these patterns of activation were similar between males and females.

Methods & Materials

Subjects. Sixty-four experimentally naïve adult male and female Long-Evans rats (225-250g at arrival; Charles River Laboratories; Portage, MI) were individually caged and maintained on a 12 h light/dark cycle (lights on at 6:00). Following arrival, rats were acclimated to the colony rooms for at least one week and handled daily prior to behavioral training; male and female rats were housed in separate colony rooms. Rats had *ad libitum* access to standard laboratory chow (Prolab, RMH 3000, 5P00; LabDiet, St. Louis, MO; 3.2 kcal/g; 26% protein, 14% fat, 60% carbohydrate) and water, except as otherwise noted. During the experiment rats were returned to *ad libitum* access to chow for at least 24 hours between consecutive food deprivations. Body weights and vaginal smears (to verify normal estrous cycling) were obtained six days a week. All housing and testing procedures were in compliance with the *National Institute of Health Guidelines for Care and Use of Laboratory Animals*, and approved by the Boston College Animal Care and Use Committee.

Apparatus. Training and testing were conducted in a set of eight identical behavioral chambers (30 x 28 x 30 cm; Coulbourn Instruments, Allentown, PA) located in a room different from the colony housing rooms. The chambers had aluminum top and sides, a transparent Plexiglas back and front, a grid floor, as well as a recessed food cup

(3.2 × 4.2 cm) on one wall. Each chamber was enclosed in an isolation cubicle (79 x 53 x 53 cm; Coulbourn Instruments, Allentown, PA) composed of monolithic rigid foam walls, which isolated from ambient sound and light. A ventilation fan, located on the back wall of each isolation cubicle, provided masking noise (55 dB). Video cameras controlled by Digital Video Security System Digital Video Recorder software program (Coulbourn Instruments, Allentown, PA) were located on the back wall of each isolation cubicle and recorded behavior during training and testing. Rats were pre-exposed to ~1 g of the training food pellets (45mg, 5TUL; Test Diets; Richmond, Indiana; 3.4 kcal/g; 20% protein, 13% fat, 67% carbohydrate) the day before the start of the behavioral training procedure. These food pellets have a similar caloric density and macronutrient energy composition to the standard laboratory chow, with the exception that the carbohydrates are from starch in the chow and sucrose in the pellets.

Behavioral training procedure. The training procedure consisted of 9 sessions conducted on separate days (Fig. 3.1): 6 appetitive sessions (S1, S2, S4, S6, S8, S9) and 3 aversive sessions (S3, S5, S7). The appetitive and aversive training sessions took place in two distinct contexts (Context A and B, respectively). Context A was used for appetitive sessions and consisted of a Plexiglas insert over the grid flooring, an illuminated house light, closed isolation chamber doors, a glass dish (107 x 87 x 70 mm), and the odor of 1% acetic acid. Context B was used for aversive sessions and consisted of open isolation chamber doors, a tee-pee shaped Plexiglas insert that obscured the aluminum sides, and the odor of 5% ammonium hydroxide.

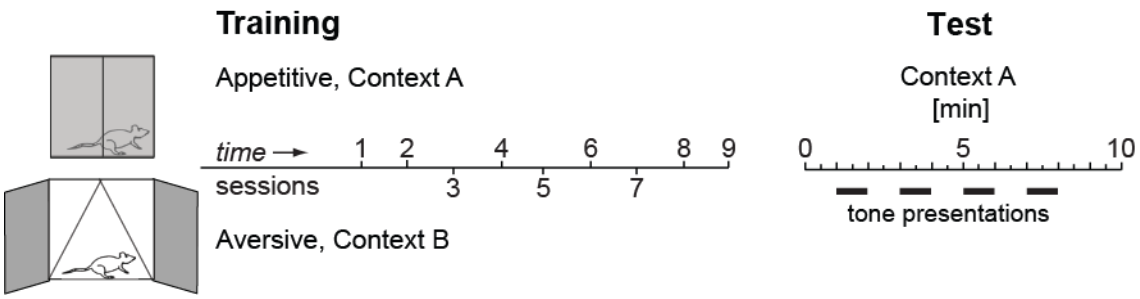

Group	Appetitive Training Sessions	Aversive Training Sessions	Test Session
Experimental	access to food	tone-shock	access to food; tones
Control	access to food	tone-only	access to food; tones
No-Food Experimental	food in home cage	tone-shock	tones
No-Food Control	food in home cage	tone-only	tones

Fig. 3.1 Experimental design. The behavioral protocol consisted of alternating appetitive and aversive sessions conducted in distinct contexts. During the appetitive sessions half of rats were allowed to consume food pellets (food access condition), while the other half of rats did not have food access (no-food access condition). Tones were played during the aversive sessions, and for half of the rats (experimental condition) each tone was followed by a mild electric footshock while the other half of the rats received only tones (control condition). At test, behavior was monitored during tone presentations in the appetitive context; no footshocks were delivered. Rats were perfused and brains collected 90 minutes following the start of test for analyses of Fos induction (figure adapted from: Petrovich & Lougee, 2011).

Appetitive sessions. Rats were acutely food deprived (~22 hours) prior to each appetitive session. During these sessions all rats were placed inside the behavioral chamber for 10 minutes and half were allowed to consume food pellets located in the glass dish while the other half of the rats did not have access to food pellets (no-food groups). At the end of each session rats were removed from the chambers, placed in their home cages, and returned to their respective colony rooms. When applicable, the food remaining was weighed and the amount consumed calculated. Rats in the no-food groups received food pellets in their home cage 30-60 minutes following each session, and the amount given was matched to that eaten by rats of the same sex and experimental condition.

Aversive sessions. Aversive training occurred under non-food deprived conditions, and each session was 10 minutes long. The first session was habituation to the new context; no shocks were administered. During each of the remaining two sessions, half of the male and female rats (experimental and no-food experimental groups) received two tone-shock pairings (tone: 75 dB, 2 kHz, 60s each; shock: 1 mA, 1 second each, Precision Adjustable Shocker, Coulbourn Instruments, Allentown, PA), while the other half of the rats (control and no-food control groups) received only tone presentations. All tones were presented using a variable inter-trial interval of 4 minutes ± 50%.

Food consumption test. Rats were acutely food deprived (~22 hours) prior to test. Testing occurred in Context A, the context used during appetitive sessions, which allowed us to isolate the effects of the tone (conditioned stimulus, CS) from possible confounding effects of the aversive training context. During test, rats were placed in the

behavioral chamber for 10 minutes and the tone was presented four times (at minutes 1, 3, 5, and 7); no footshocks were administered. Rats in the experimental and control groups had access to food in the glass dish during the test, while the no-food experimental and no-food control groups did not have access to food. When applicable, the food remaining at the end of the test was weighed and the amount consumed calculated. Rats were immediately returned to the colony room, and left undisturbed without access to food for ~80 min at which time they were sacrificed (i.e., 90 minutes from the start of the test session, when Fos levels peak (Morgan & Curran, 1991)) in order to measure test-specific Fos induction.

Behavioral measures. Food consumption was monitored during all training sessions and at test for the control and experimental groups. By monitoring food consumption across the appetitive training sessions, we were able to determine if there were any generalized effects of footshock experience on consumption in a context where no aversive stimuli were ever received. Although rats arrived at the same weight, males gained weight at a substantially greater rate (see Results, Table 3.1; Charles River Laboratories, n.d.). To control for this weight difference, and the resulting possible differences in gastric capacity (Bull & Pitts, 1971), consumption data were analyzed as the actual amount consumed (g) and also as an expression of the percent consumption of the same-sex control group (see: Petrovich & Lougee, 2011; Reppucci et al., 2013). This calculation was done by dividing the consumption for each subject, control and experimental, by the mean consumption of the control group for the same sex and then

multiplying the result by 100; this calculation preserved the existing variance in consumption for all groups.

Additionally, videos recorded during the test were analyzed for freezing behavior for all subjects. Freezing behavior is a species-typical defense response that is characterized by the cessation of all movement except that required for breathing (Blanchard & Blanchard, 1969; Fanselow, 1984). Observers were "blind" with respect to the sex and training conditions of the rats observed. The observer recorded the behavior of each rat every 1.25 seconds, paced by a metronome, for the 60 seconds prior to the first tone presentation (pre-CS period), and during each of the four tone presentations (CS period). The percentage of time rats exhibited freezing behavior during each of the sampling periods was then calculated.

Histological procedures. Rats were briefly anesthetized with isoflurane (5%; Baxter Healthcare Corporation, Deerfield, IL), and then deeply anesthetized with an intraperitoneal injection of tribromoethanol (375 mg/kg; Sigma-Aldrich, St. Louis, MO). Rats were then transcardially perfused with 0.9% saline followed by 4% paraformaldehyde in 0.1 M borate buffer. Brains were extracted and post-fixed overnight in a solution of 12% sucrose dissolved in the perfusion liquid. The brains were then rapidly frozen in hexanes cooled in dry ice, and stored at −80°C. Brains were sliced in 30μm sections using a Leica SM2000R sliding microtome and collected into four, adjacent series.

The first series was stained using standard immunohistochemical procedures for visualization of Fos. Free-floating tissue sections were incubated in a blocking solution

for 1 hour at room temperature to minimize nonspecific binding. The blocking solution contained 0.02M potassium phosphate-buffered saline (KPBS), 0.3% Triton X-100 (Sigma-Aldrich, St. Louis, MO), 2% normal goat serum (S-1000; Vector Laboratories, Burlingame, CA), and 10% non-fat milk (M-0841; LabScientific, Livingston, New Jersey). After blocking, the tissue was incubated in the blocking solution with the primary antibody, anti-*c-fos* raised in rabbit (1:2000; SC-52; Santa Cruz Biotechnology Inc, Santa Cruz, CA or 1:30,000; Ab-5; Calbiochem, EMD Millipore, Billerica, MA; counterbalanced across training conditions) for 72 hours at 4°C. The tissue was then incubated in the blocking solution with the secondary antibody, biotinylated goat anti-rabbit IgG (1:500; BA-1000; Vector Laboratories, Burlingame, CA) for 45 minutes. Subsequently, the tissue was reacted with avidin-biotin complex (PK-6100; Vector Laboratories, Burlingame, CA) for 45 minutes. This was followed by a second 30 minute incubation in the secondary antibody solution, and a second 30 minute incubation in the ABC solution to improve specific binding. To produce a color reaction, the tissue was incubated in a diaminobenzidine solution (SK-4100; Vector Laboratories, Burlingame, CA) for 1-2 minutes with constant, manual agitation. Tissue was rinsed with washes in KPBS between each solution change in the processing protocol. Immunohistochemically stained tissue was then mounted onto SuperFrost Plus slides (Fisher Scientific, Pittsburgh, PA) and air-dried, followed by oven-drying at 45^{o}C overnight. Tissue was then dehydrated through alcohols, cleared in xylenes, and coverslipped with DPX (13512; Electron Microscopy Sciences, Hatfield, PA).

The second series was collected into a 0.02 M KPBS solution, mounted onto gelatin-subbed slides, and Nissl-stained with thionin (Simmons & Swanson, 1993) for identification of cytoarchitectonic borders of brain structures, as defined in Swanson's rat brain atlas (Swanson, 2004). The remaining series were collected into trays containing a cryoprotectant solution (0.025 M sodium phosphate buffer with 30% ethylene glycol and 20% glycerol) and stored at −20°C for later use. Brain perfusions, collection, slicing, and storage were counterbalanced across training conditions.

Image acquisition and analysis. Images were taken at 10X with an Olympus BX51 light microscope and attached Olympus DP72 camera using DP2-BSW software (Olympus America Inc, Center Valley, PA), which was controlled by a PC computer. Using the ImageJ software program (NIH), borders for regions of interest were drawn onto the Nissl-stained image, and then transposed to the adjacent immunohistochemically stained tissue to allow for semi-automated counting of Fos-positive neurons. The analysis followed the parcellation and nomenclature as defined in the Swanson atlas (2004), except for the LHA (see description below). A detailed examination across the rostrocaudal extent of all parts of the CEA (lateral (CEAl), medial (CEAm), capsular (CEAc); Levels 24-28, -1.33 to -2.45 mm from bregma, Fig. 3.4a; all subsequent measurements refer to mm from bregma) was completed since this nucleus was previously shown to be critical for fear-cue inhibited feeding (Petrovich et al., 2009). However, the patterns of activation did not differ across the levels analyzed, and thus the analyses of subsequent regions were conducted at a single mid-rostrocaudal level.

The five cell groups that comprise the basolateral area of the amygdala were examined (Fig. 3.5a): the lateral amygdalar nucleus (LA; Level 30, -3.25 mm), anterior part of the basolateral amygdalar nucleus (BLAa; Level 27, -2.00 mm), posterior part of the basolateral amygdalar nucleus (BLAp; Level 30, -2.00 mm), anterior part of the basomedial amygdalar nucleus (BMAa; Level 26, -1.78 mm), and posterior part of the basomedial amygdalar nucleus (BMAp; Level 30, -3.25 mm). Within the mPFC, three regions were analyzed: the dorsal part of the anterior cingulate (ACAd), prelimbic (PL), and infralimbic (ILA) areas (all Level 9, +2.80 mm, Fig. 3.6a). Analysis was also completed for the LHA (Level 29, -2.85 mm, Fig. 3.7a). At this anatomical level ten distinct LHA cell groups were identified in the most recent parcellation (Swanson, 2004), however, in order to reliably sample across brains we defined three areas for our analysis. The cell groups above fornix, in an area known to contain orexigenic peptides (Broberger et al., 1998; Hahn, 2010; Swanson et al., 2005), were divided into two sampling areas due to reports of topographical differences in function (see: Harris & Aston-Jones, 2006) and differential recruitment in other feeding paradigms (e.g. Cole et al., 2015; Mena et al., 2013; Petrovich et al., 2012). We defined these areas as the dorsomedial area (dmLHA) which included the juxtadorsomedial (LHAjd) and suprafornical (LHAs) regions (Hahn & Swanson, 2010, 2012; Swanson, 2004), and the dorosolateral area (dlLHA) which included the dorsal region (LHAd) and magnocellular nucleus (LHAm; Swanson, 2004). The third sampling area was defined as the ventral area (vLHA) and was comprised of all cell groups located ventral to fornix at this level: the dorsal and ventral zones of the juxtaventromedial region (LHAjvd, jvv), posterior zone of the subfornical region

(LHAsfp), medial zone of the ventral region (LHAvm), and the intermediate and lateral parts of the tuberal nucleus (TUi, l; Swanson, 2004).

Statistical analysis. Behavioral data were analyzed using two-way (sex by experimental condition) analysis of variances (ANOVAs) for food consumption measures, and three-way (sex by experimental condition by food access condition) ANOVAs for freezing behavior and body weights. Due to baseline differences in body weight and food consumption (see Results), Fos counts for males and females were analyzed separately using two-way (experimental condition by food access condition) ANOVAs. *Post hoc* independent-samples t-Tests were completed to clarify reported effects, as needed. For brain regions that showed effects of experimental or food access condition, partial correlations were completed for the food access groups and collapsed across the sexes in a single analysis (plots can be found in Appendix). These correlations examined the relationship between Fos induction and each of the two primary behavioral measures at test while controlling for the effects of the other behavioral measure (Fos correlation with grams consumed, controlling for freezing; Fos correlation with freezing, controlling for grams consumed). Five rats were excluded from analyses due to poor health or technical malfunction during perfusion (1 male experimental, 1 female no-food control, 3 female no-food experimental; see Table 3.1 for final group sizes). Additionally, data for the following were not collected due to tissue damage: CEA (2 male no-food control, 1 female no-food control, 1 female no-food experimental), LA, BLAp, BMAp (2 male no-food control), BMAa (2 female no-food experimental), mPFC (1 female experimental), and LHA (1 female experimental, 1 female no-food experimental). All

statistics were computed using SPSS software, and in all cases $p \leq 0.05$ was considered significant.

Results

Training. Food pellet consumption increased across appetitive training sessions for all groups that had access to food (Fig. 3.2). Males increased consumption across training sessions faster than females and thus consumed more food than females by the end of training. A repeated ANOVA across training sessions confirmed a significant within-subjects main effect of session ($F(5, 27)=35.825$, $p<0.001$) and interaction of session with sex ($F(5, 27)=5.867$, $p<0.001$), as well as a significant between-subjects main effect of sex ($F(1, 27)=16.963$, $p<0.001$). Importantly, control and experimental groups of the same sex consumed similar amounts of pellets. There were no effects or interactions with experimental condition ($p >0.05$, all); experience with footshocks in Context B did not affect consumption in Context A.

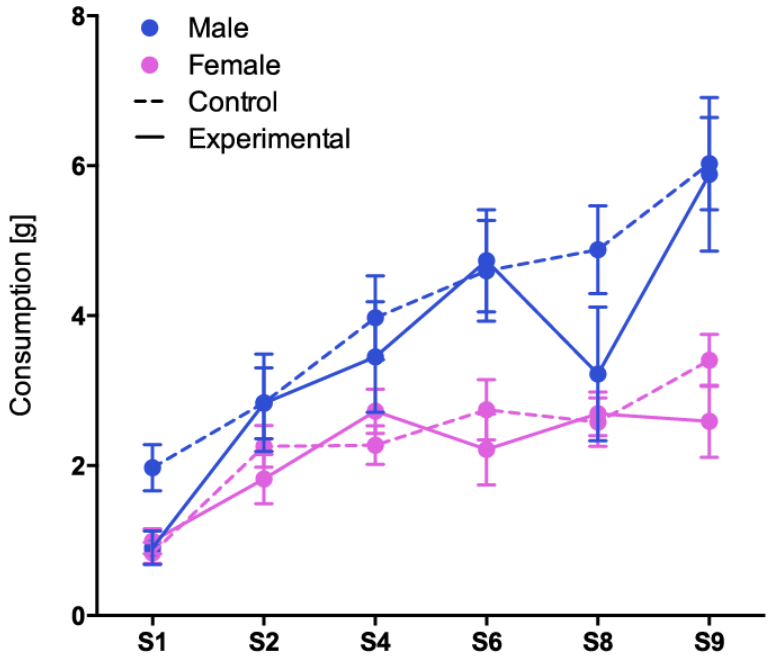

Fig. 3.2 Consumption during training. Mean (± SEM) food pellet consumption in grams is shown for each appetitive training session.

All subjects were the same weight at arrival, however males gained weight much more rapidly than females and thus weighed significantly more than females prior to training ($F(1, 58)=81.377$, $p<0.001$) and prior to test ($F(1,58)=163.99$, $p<0.001$; Table 3.1). There were no effects or interactions with experimental condition on body weights at either time point ($p>0.05$, all). The ANOVAs revealed an unexpected effect of food access condition, with the no-food groups weighing significantly less than the corresponding groups at each time point ($F(1,58)>8.853$, $p<0.01$, both). However, this study was conducted in multiple replications, and closer inspection noted that one replication, which did not include no-food groups, had rats heavier than the other replications. When replication was added as an additional factor into the ANOVAs, the main effect of food access was eliminated ($p>0.05$, both) and the replication effect was confirmed ($F(1,58)>27.047$, $p<0.001$, both). All female rats were observed to be cycling normally, and all stages of estrous were represented at test. Although not directly analyzed due to sample size, results suggest that estrous cycle stage did not affect female feeding or freezing behavior since behavioral data variability (as interpreted by the SEM) was no greater in females than in males (see Food consumption test: Behavioral results below). Thus, neither access to food in the chamber during training sessions, nor the experience of receiving footshocks during training produced changes in body weight or estrous cycling.

Table 3.1 Body weights. Data presented as mean ± SEM in grams.

Group	n	Prior to Training	Prior to Test
Male Control	8	343.88 ± 20.98	383.38 ± 20.21
Male Experimental	7	343.86 ± 17.09	386.43 ± 14.09
Male No-Food Control	8	304.88 ± 7.20	345.38 ± 9.15
Male No-Food Experimental	8	315.75 ± 6.31	351.75 ± 8.60
Female Control	8	262.25 ± 7.47	275.25 ± 9.18
Female Experimental	8	260.88 ± 5.91	272.00 ± 4.91
Female No-Food Control	7	244.86 ± 2.87	259.71 ± 5.01
Female No-Food Experimental	5	249.40 ± 3.82	248.40 ± 3.63

Food consumption test: Behavioral results. Subjects in the experimental groups strongly inhibited food intake compared to the control groups during the test with presentations of a learned fear-cue ($F(1,30)=23.247$, $p<0.001$). *Post hoc* t-Tests confirmed that both the male ($t(1,13)=4.431$, $p=0.001$) and female ($t(1,14)=2.110$, $p=0.05$) experimental groups significantly inhibited food intake compared to the corresponding control groups (Fig. 3.3a, left). The baseline difference in food consumption observed during training was also evident at test; males consumed significantly more food pellets than females ($F(1,30)=9.316$, $p<0.01$). This baseline difference in grams consumed led to a significant sex by experimental condition interaction ($F(1,30)=4.801$, $p<0.05$), as the exact difference between the control and experimental groups was greater in males than females (3.57g vs. 1.34g). To account for baseline sex differences in consumption, and to determine if there were differences in the extent of food intake inhibition between the sexes, we re-calculated the amount consumed and expressed it as the percent of the mean consumption of the control group of the same sex (see Methods & Materials: Behavioral measures). The resulting ANOVA showed that both males and females in the experimental groups inhibited food intake compared to the corresponding control groups ($F(1,30)=18.615$, $p<0.001$), and that extent of this inhibition was statistically similar between the sexes (Fig. 3a, right). There was no main effect or interaction with sex ($p>0.05$, both) when consumption was analyzed as a percent of the same sex control group.

All subjects who received tone-shock pairings during training acquired a conditioned fear response specific to the tone CS; there were no instances of freezing by

any subject prior to the first CS presentation at test (0 ± 0 % of time for all groups). Subjects in the experimental condition showed robust freezing behavior during CS presentations, while subjects in the control condition showed negligible amounts of freezing behavior ($F(1,51)=77.062$, $p<0.001$; Fig. 3.3b). There were no effects or interactions with sex or food access condition on the expression freezing during CS presentations ($p>0.05$). Thus, any positive contextual associations with food consumption from training did not dampen the freezing response for subjects with access to food compared to the no-food groups, nor did the presence of food at test influence the expression of the conditioned freezing response to the CS.

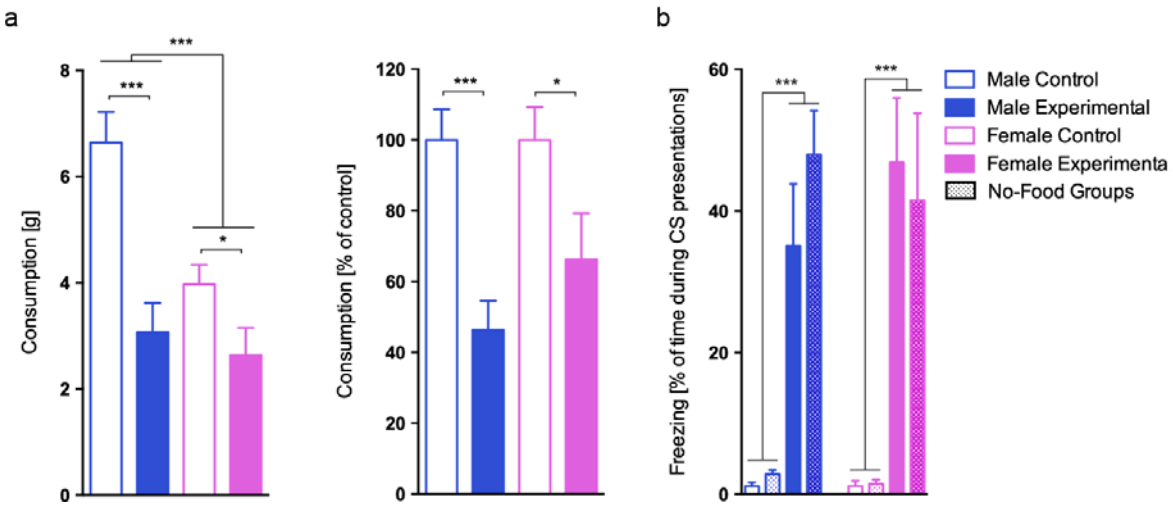

Fig. 3.3 Behavioral results from the food consumption test. **a** The amount of food pellets consumed expressed in grams (left), and as the percent of the consumption of the control group of the same sex (right). **b** The percent of time expressing freezing behavior during CS presentations. All data are shown as mean ± SEM; *p≤0.05; ***p<0.001.

Food consumption test: Fos induction. Within the CEA, Fos induction patterns corresponded to food consumption, specifically within the CEAl and CEAm (Fig. 3.4b). For both regions, Fos induction was significantly greater in the groups with access to food compared to the no-food groups for males ($F(1,28)>21.521$, $p<0.001$, both) and females ($F(1,25)>17.528$, $p<0.001$, both). In males, rats in the control condition also had significantly greater Fos induction than those in the experimental condition in both the CEAl ($F(1,28)=4.686$, $p<0.05$) and CEAm ($F(1,28)=5.271$, $p<0.05$). *Post hoc* t-Tests confirmed this was due to differences between the male control group, which consumed substantial amounts of food, compared to the male experimental group, which was inhibiting food intake (CEAl: $t(1,13)=2.082$, $p=0.06$; CEAm $t(1, 13)=2.628$, $p<0.05$; Fig. 3.4d); the no-food groups had similar Fos induction ($p>0.05$, both). There was no effect of experimental condition on Fos induction in females ($p>0.05$, both). Partial correlations using the data from all subjects with access to food showed that food consumption was significantly, and positively, correlated with Fos induction in CEAl and CEAm ($r(28)>0.485$, $p<0.01$, both; collapsed data for the entire CEA depicting the simple correlation relationship is shown in Fig. 3.4c). Freezing behavior did not correlate with Fos induction in either region ($p>0.05$, both). In contrast to the CEAl and CEAm, Fos induction in the CEAc was low and similar across all conditions for both sexes ($p>0.05$, all).

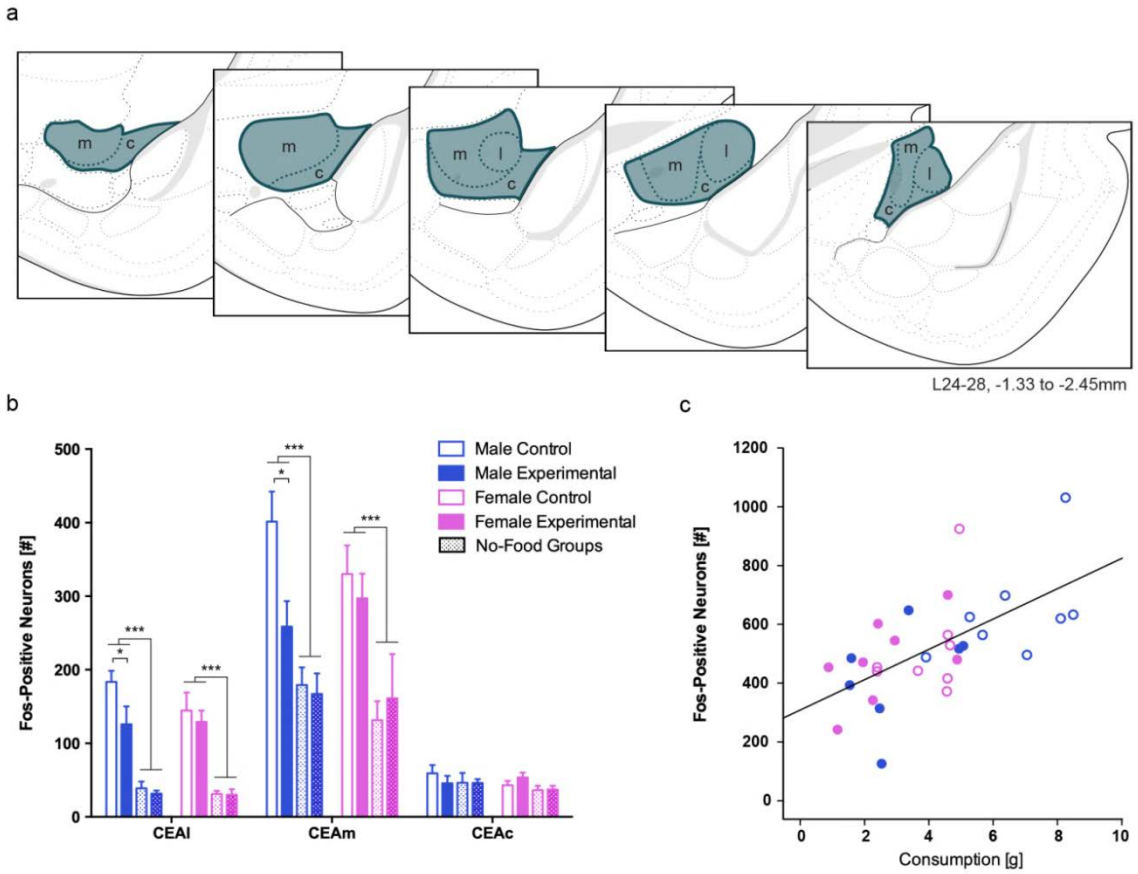

Fig. 3.4 Fos induction in the CEA. **a** Sampling regions for analysis shown on rat brain templates derived from Swanson (2004). **b** Total number of Fos-positive neurons within each division of the CEA are shown as mean ± SEM; *p≤0.05; ***p<0.001. **c** Scatter plot depicting the relationship between the total number of Fos-positive neurons in the CEA and food consumption (g) for all subjects with access to food during the test. **d** Photomicrographs of CEA showing Fos induction in a distinct group of neurons within the CEAl/CEAm; scale bars = 100µm. (continued on next page)

d

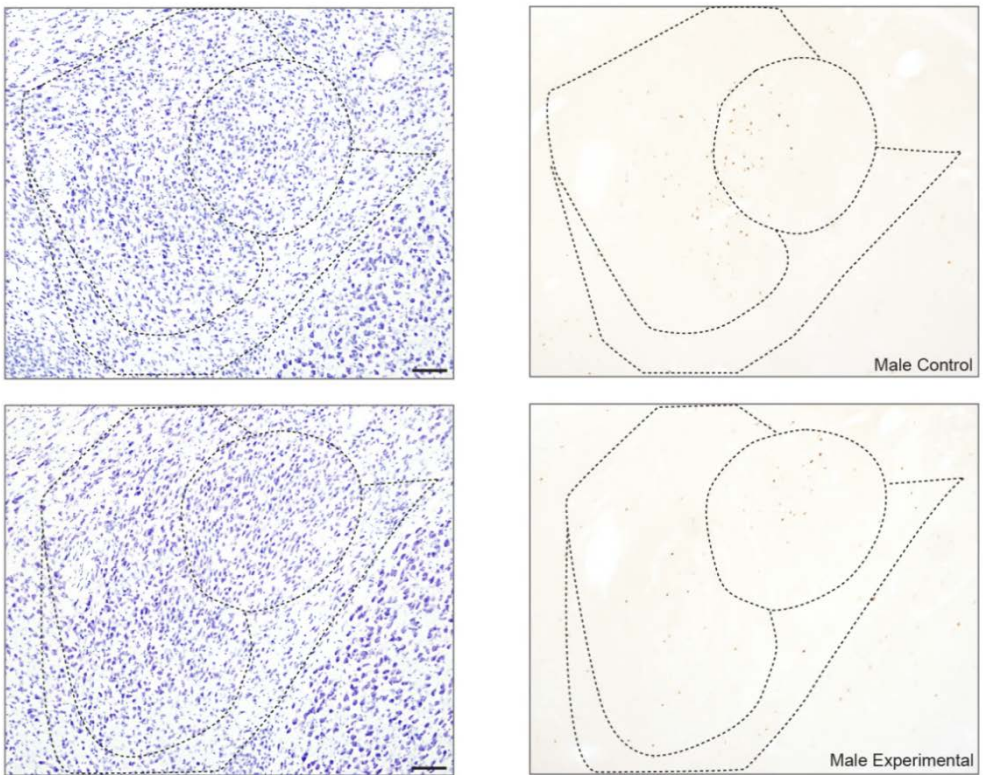

Fig. 3.4, continued

Fos induction patterns were different for each of the five cell groups which comprise the basolateral area of the amygdala, however, three general patterns emerged. The pattern in one cell group (BLAa) corresponded with food access condition. Two cell groups (LA and BMAp) had Fos patterns that corresponded with experimental condition. The last two cell groups (BLAp, BMAa) had similar patterns of Fos induction across all conditions; there were no significant effects of experimental or food access condition on Fos induction in the BLAp or BMAa for either sex ($p>0.05$, all; Fig. 3.5d).

Fos induction in the BLAa was significantly greater in groups with access to food compared to the no-food groups for males ($F(1,30)=5.291$, $p<0.05$). In females, the pattern was similar and approached significance ($F(1,27)=3.817$, $p=0.06$). For both sexes, this difference was irrespective of experimental condition ($p>0.05$, both; Fig. 3.5b). Fos induction in BLAa did not significantly correlate with food consumption or freezing behavior ($p>0.05$, both; data from all subjects with access to food). Thus, unlike the CEAl and CEAm, where Fos induction corresponded with food consumption, Fos in the BLAa corresponded to only the presence or absence of food.

Fos induction in LA was greater in rats in the experimental condition, which exhibited robust freezing to the tone CS during test, compared to rats in the control condition, which exhibited negligible amounts of freezing behavior (Fig. 3.5c). This difference between rats in the experimental and control conditions was significant for males ($F(1,28)=6.411$, $p<0.05$) and approached significance for females ($F(1,27)=3.268$, $p=0.08$). Fos induction in LA was not influenced by food access condition for either sex ($p>0.05$, both). Partial correlations using the data from all subjects with access to food

showed that Fos induction in LA was significantly, and positively, correlated with freezing behavior ($r(28)=0.400$, $p<0.05$), and not correlated to food consumption ($p>0.05$).

The BMAp had a similar pattern of Fos induction as the LA, with greater Fos induction in the experimental compared to the control condition (Fig. 3.5c). However, this effect was not as strong as in the LA and only approached significance in both males ($F(1,28)=3.072$, $p=0.09$) and females ($F(1,27)=3.827$, $p=0.06$). For males this effect was driven by a significant difference between the no-food groups ($t(1, 12)= 2.238$, $p<0.05$), while in females this effect was driven by a significant difference between the groups with food access ($t(1, 14)= 2.848$, $p<0.05$). There was no main effect or interaction with food access condition in males, but in females there was a significant experimental condition by food access condition interaction ($F(1, 27)=5.007$, $p<0.05$). *Post hoc* t-Tests showed that in addition to lower Fos induction than the female experimental group (see above), the female control group also had significantly lower Fos induction than the female no-food control group ($t(1, 13)= 2.142$, $p= 0.05$). Interestingly, partial correlations using the data from all subjects with access to food showed the Fos induction in BMAp was positively associated with both freezing ($r(28)=0.346$, $p=0.06$) and food consumption ($r(28)=0.323$, $p=0.08$).

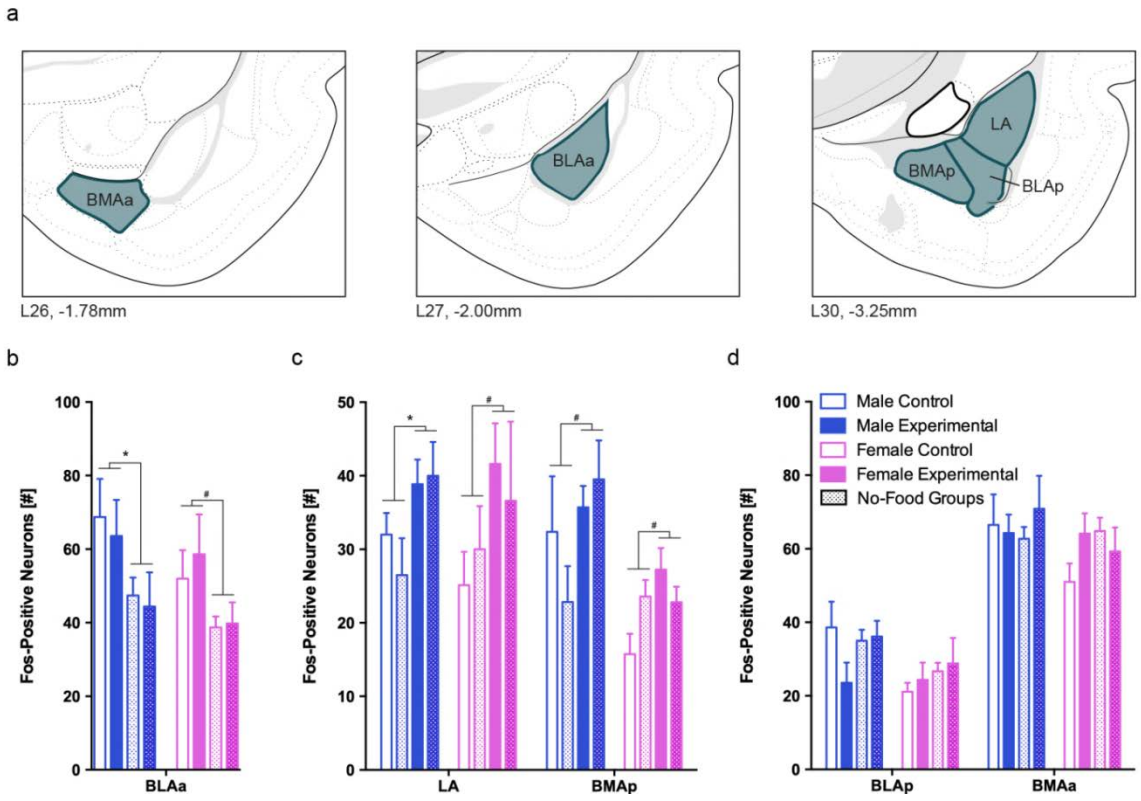

Fig. 3.5 Fos induction in the nuclei that comprise the basolateral area of the amygdala. **a** Sampling regions for analysis shown on rat brain templates derived from Swanson (2004). Fos induction corresponded with food access condition in BLAa (**b**), with experimental condition in LA and BMAp (**c**), and did not correspond with either condition in BLAp or BMAa (**d**). Total number of Fos-positive neurons within each cell group are shown as mean ± SEM; #p<0.10, *p<0.05.

Within the mPFC, overall Fos induction was much greater in the PL and ILA compared to the ACAd for both sexes (Fig. 3.6b). In males and females, repeated (across the three mPFC regions) two-way (experimental condition by food access condition) ANOVAs confirmed a significant within-subjects effect of region ($F(2, 46)>91.009$, $p<0.001$, both), and showed that this effect did not depend or interact with experimental or food access condition ($p>0.05$, all). However, mPFC Fos induction patterns across experimental and food access conditions were very different between the sexes. In females, the repeated ANOVA revealed that rats in the experimental condition had significantly greater Fos induction than those in the control condition ($F(1,23)=8.375$, $p<0.01$), and there was no effect of food access condition on Fos induction ($p>0.05$). In contrast, all male groups showed similar amounts of mPFC Fos induction ($p>0.05$, all). Since there were no effects of food access or experimental condition on Fos induction in males, partial correlations were completed using only the data from females with access to food. These correlations revealed that, in females, mPFC Fos induction significantly, and positively, correlated with both consumption ($r(12)=0.724$, $p<0.01$) and freezing behavior ($r(12)=0.629$, $p<0.05$).

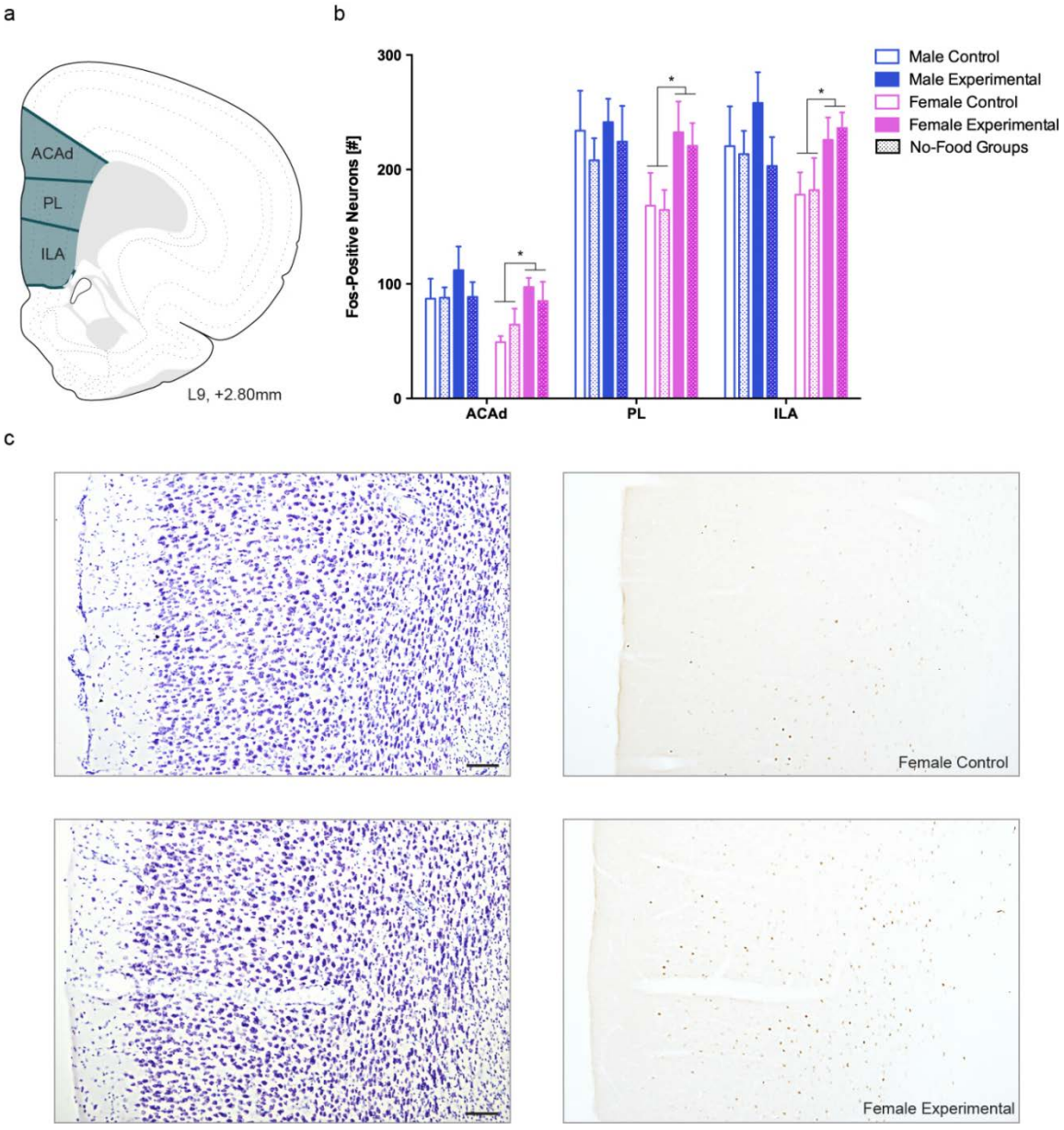

Fig. 3.6 Fos induction in the mPFC. **a** Sampling regions for analysis shown on rat brain templates derived from Swanson (2004). **b** Total number of Fos-positive neurons within each division of the mPFC are shown as mean ± SEM; *p<0.01 across all three divisions. **c** Representative photomicrographs of PL; scale bars = 100µm.

Within the LHA, Fos induction patterns were related to food consumption at test. In the dorsomedial LHA, Fos induction was significantly greater in the male groups with access to food compared to the male no-food groups ($F(1, 30)=5.262$, $p<0.05$), irrespective of experimental condition ($p>0.05$). In the dorsolateral LHA a main effect of experimental condition approached significance in males ($F(1,30)=3.136$, $p=0.09$), and this effect was driven by more Fos in the control compared to the experimental group ($t(1,13)=2.113$, $p=0.05$), while the no-food groups had similar Fos induction ($p>0.05$). There were no significant effects of food access or experimental condition on dorsomedial or dorsolateral LHA Fos induction in females ($p>0.05$, all). In the ventral LHA, there was greater Fos induction in groups with access to food compared to the no-food groups, and qualitatively, this effect appeared to be driven by activation of a specific group of neurons (LHAsfp) within this sampling region (Fig. 3.7d). However, in the ventral LHA the main effect of food access condition only approached significance for males ($F(1,30)=3.763$, $p=0.06$) and females ($F(1,25)=3.413$, $p=0.08$). An experimental condition by food access condition interaction also approached significance in females ($F(1,23)=3.922$, $p=0.06$); the female no-food experimental group had lower Fos induction in the ventral LHA than both the female experimental group ($t(1,9)=2.846$, $p<0.05$) and the female no-food control group ($t(1,9)=2.207$, $p=0.06$). Partial correlations using the data from all subjects with access to food showed that Fos induction in the dorsolateral ($r(27)=0.395$, $p<0.05$) and ventral ($r(27)=0.387$, $p<0.05$), but not dorsomedial ($p>0.05$), LHA significantly correlated with food consumption (simple correlation relationships are shown in Fig. 3.7c); in no region did Fos correlate with freezing ($p>0.05$, all).

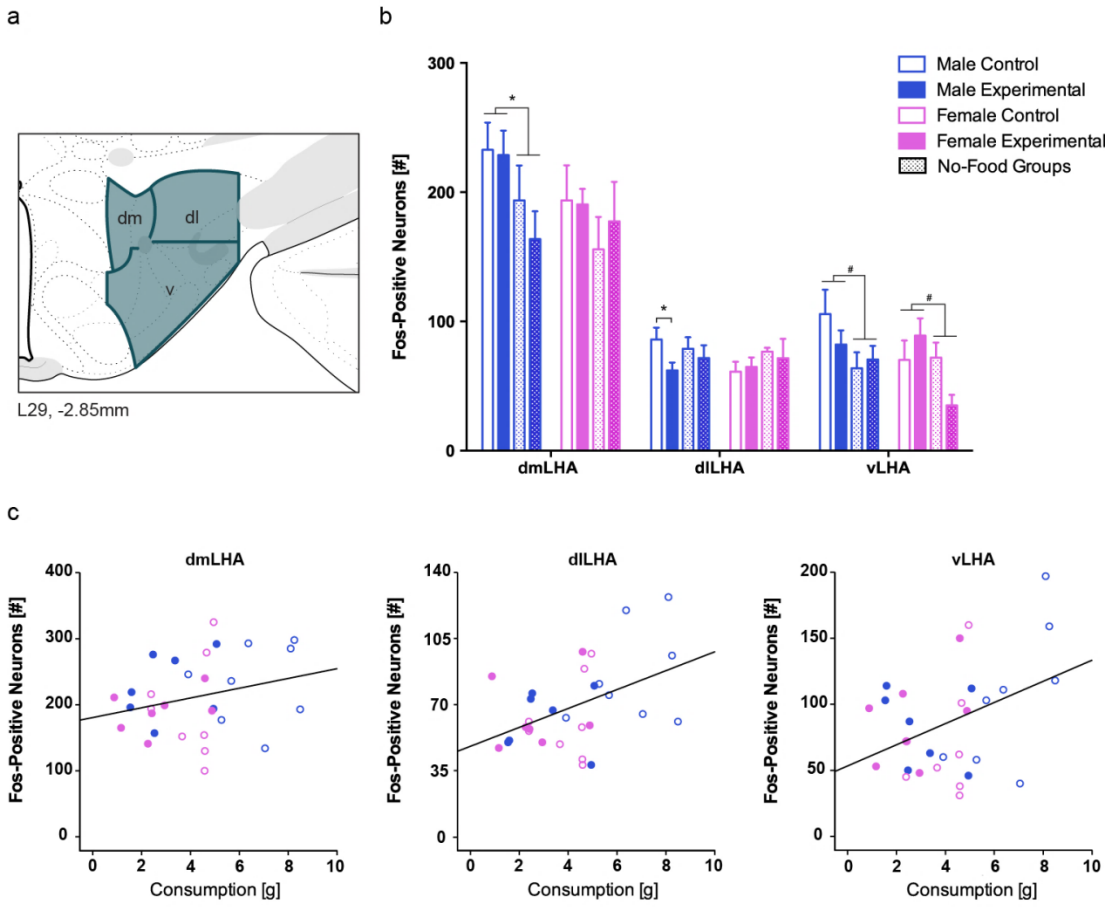

Fig. 3.7 Fos induction in the LHA. **a** Sampling areas for analysis shown on rat brain templates derived from Swanson (2004). **b** Total number of Fos-positive neurons within the three areas analyzed are shown as mean ± SEM; #p<0.01, *p≤0.05. **c** Scatter plots depicting the relationship between food consumption (g) and the total number of Fos-positive neurons in each LHA sampling region for all subjects with access to food during the test. **d** Photomicrographs from the ventral LHA sampling area showing that Fos is mainly contained within LHAsfp; scale bars = 100µm. (continued on next page)

d

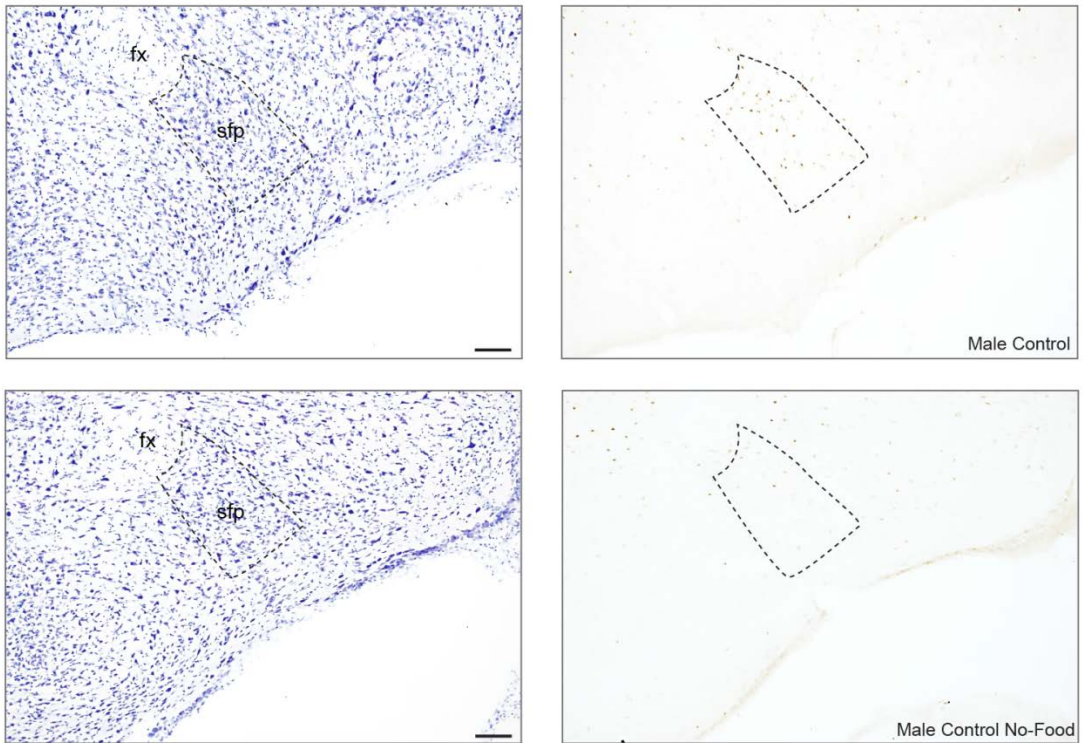

Fig. 3.7, continued

Discussion

Here, the aim was to replicate prior evidence that a learned fear-cue can override physiological hunger and inhibit food intake in food-deprived rats, and to examine the recruitment of an amygdala-prefrontal-lateral hypothalamic network during the expression of this behavior. Using Fos induction as a marker of neural activity, we aimed to determine how and where the fear-cue acts within this network to alter food intake, and whether the pattern of neural activation was similar in males and females.

We demonstrated that a learned fear-cue inhibited food intake in food-deprived rats, and that the extent of this inhibition of intake was comparable in males and females, replicating prior results (Petrovich & Lougee, 2011). Importantly, this inhibition was driven by the presentation of the conditioned fear-cue; there was no evidence that prior experience with footshocks alone affected food intake during the training period. This is consistent with recent reports that footshock delivery in one context did not affect food consumption in a different context previously associated with food (Holmes & Westbrook, 2014; Reppucci et al., 2013). There was, however, a large baseline difference in consumption between males and females that emerged during training and was evident during the food consumption test. We have reported this previously in similar behavioral preparations (Petrovich & Lougee, 2011; Reppucci et al., 2013), and it may be linked to significant differences in body weight (see Methods & Materials: Behavioral measures) and resulting gastric capacity (Bull & Pitts, 1971) or other factors (see: Asarian & Geary, 2013; Fukushima et al., 2015). In addition to their similar inhibited feeding response, males and females in the experimental condition also expressed equal levels of freezing

behavior in the presence of the learned fear-cue. Prior reports have also shown that males and females of other outbred strains of rats exhibited similar freezing responses to aversively conditioned discrete cues (Barker & Galea, 2010; Gruene, Roberts, Thomas, Ronzio, & Shansky, 2014; Maren, De Oca, & Fanselow, 1994; Pryce, Lehmann, & Feldon, 1999), and similar behavioral responses across a variety of measures following footshock experience (Viviani, Haegler, Strasser, & Steiner, 2012).

It is important to note that the inhibition of feeding observed in the present study was not merely a consequence of immobilization due to conditioned freezing behavior. Instead, these two behaviors are elicited by the same CS, and their expression is at least partially dissociable. In a behavioral paradigm similar to the current study, lesions of the periaqueductal gray (Petrovich, Ross, Holland & Gallagher, 2006) or basolateral area of the amygdala (Petrovich et al., 2009) abolished CS-induced freezing, while CS-induced inhibition of feeding remained intact. Additionally, we have previously reported that during repeated food consumption tests with presentations of a fear-cue, females will continue to inhibit food intake even after they have extinguished conditioned freezing behavior (Petrovich & Lougee, 2011; Reppucci & Petrovich, 2014). Further, in a study using contextual fear conditioning the occurrence of freezing and feeding behaviors was sampled across the entire test session. There it was found that rats in the aversively conditioned context had a sufficient amount of time that they were not freezing during which they could have consumed food, but that they did not utilize it as such (Reppucci et al., 2013). It is likely that activation of different brain regions or circuits may give rise

to the behavioral dissociation between CS-induced inhibited food intake and CS-induced freezing.

We found that distinct cell groups within an amygdala-prefrontal-lateral hypothalamic network were differentially activated across groups within the current study. This study was the first to examine recruitment of brain substrates during the inhibition of feeding by a learned fear-cue, and importantly compared neural activation in both males and females. In accordance with the behavioral findings, typically the patterns of activation were similar between males and females, with mPFC patterns as a notable exception. Four general patterns of activation emerged: association with 1) the amount of food consumed (CEAl, CEAm, mPFC, LHA), 2) the presence or absence of food (BLAa), 3) experimental condition (LA, BMAp, mPFC), or 4) no differential activation across conditions (CEAc, BLAp, BMAa).

Amygdala. The CEA and basolateral area of the amygdala are both critical for aversive and appetitive associative learning and the subsequent control of behavior (e.g. Pare & Duvarci, 2012; Petrovich, 2013). However, they are structurally, phenotypically, and connectionally distinct (Swanson & Petrovich, 1998), and as such, these two regions have been shown to play opposing roles in the control of feeding by learned cues. The basolateral area of the amygdala, but not the CEA, was critical for the ability of a learned cue to elicit feeding in sated rats (Holland et al., 2002), while the CEA, but not the basolateral area, was critical in the inhibition of feeding by a learned fear-cue in food deprived rats (Petrovich et al., 2009). In the current study we found differential Fos induction across distinct groups in both the CEA and basolateral area of the amygdala

during the inhibition of feeding; each region's recruitment was more closely associated to different aspects of the behavioral paradigm, in agreement with their structural and connectional differences.

Fos induction in CEA, specifically CEAl and CEAm, corresponded to food consumption during test. Fos was robustly induced in rats with access to food compared to the no-food subjects, and for males this robust activation was blunted in the experimental group (i.e., rats that strongly inhibited food intake). The baseline difference in food intake between the sexes resulted in difference in grams consumed between the male control and experimental groups being > 2.5-fold greater than the difference in grams consumed between the female control and experimental groups during the test (3.57g vs. 1.34g, respectively). This difference may be why the male, but not female, groups had significantly different Fos induction patterns. That is, the smaller difference in grams consumed between the two female groups was not sufficient to produce differences in Fos at the group level, even if at the individual level CEA Fos was associated with feeding in females. In support of this, Fos induction in CEA significantly correlated with the amount of food subjects consumed at test—both sexes included, when freezing was controlled.

The pattern of CEA activation in the current study is consistent with reports of increased CEA Fos induction following ingestion driven by homeostatic need (J. Li et al., 2012) or by learned cues (Holland & Hsu, 2014). Moreover, exposure to contexts previously associated with food (Schiltz, Bremer, Landry, & Kelley, 2007), and administration of a substance known to promote food intake (2-Deoxy-d-glucose, 2-DG;

Ritter & Dinh, 1994) have also been shown to increase Fos induction in the CEA. In the latter case, this induction was specific to the CEAl (Ritter & Dinh, 1994). In addition to recruitment by appetite-promoting (orexigenic) stimuli, the CEA is also recruited by appetite-reducing (anorexigenic) stimuli. Specifically, a subpopulation of CEAl neurons, which is marked by the expression protein kinase C- δ (PKC-δ), was recently implicated in the inhibition of feeding. These neurons were activated by (as measured with Fos induction) well-characterized anorexigenic stimuli (e.g., lithium chloride, cholecystokinin, quinine) (Cai et al., 2014). Further, optogenetic stimulation of these neurons inhibited food intake in food-deprived subjects without eliciting anxiety or freezing behaviors (Cai et al., 2014). Orexigenic and anorexigenic stimuli likely activate separate populations of CEA neurons. The CEA is a highly diverse nucleus; although nearly exclusively GABAergic, neurons often co-express at least one neuropeptide (Cassell et al., 1986; H. Li et al., 2013; Marchant et al., 2007; Roberts et al., 1982; Swanson & Petrovich, 1998; Wray & Hoffman, 1983). This heterogeneity is one potential mechanism by which different CEA neurons could respond differently to stimuli that promote or inhibit food intake.

The CEA is well-recognized as the amygdalar output for conditioned fear (for reviews see: Ehrlich et al., 2009; Ledoux, 2012; Maren, 2001; Pare & Duvarci, 2012), however Fos induction patterns within this nucleus during conditioned fear expression have been inconsistent. Prior reports have shown increases, decreases, or no change (Beck & Fibiger, 1995; Day, Kryskow, Nyhuis, Herlihy, & Campeau, 2008; Hall, Thomas, & Everitt, 2001; Pezzone, Lee, Hoffman, & Rabin, 1992; Rosen, Fanselow,

Young, Sitcoske, & Maren, 1998; Scicli, Petrovich, Swanson, & Thompson, 2004). These reported differences are likely due to differences in behavioral preparations used across studies and/or inconsistences in the parts of CEA that were compared.

In the current study CEA Fos induction did not correlate with freezing behavior and there was no differential Fos induction across the experiment and control conditions, including the no-food groups. Thus we found that Fos induction corresponded with food consumption but not the expression of freezing behavior. The lack of Fos induction associated with freezing during conditioned fear expression in the current study may be due to differences in behavioral protocols on test day compared to prior experiments where such a difference was reported (Beck & Fibiger, 1995; Hall et al., 2001; Scicli et al., 2004). Here, the test period was only 10 minutes long compared to the 30 minute tests of contextual fear that induced Fos (Beck & Fibiger, 1995; Scicli et al., 2004). Consistent with the current findings, an 8 minute long contextual fear test did not produce detectable Fos induction (Scicli et al., 2004). Similarly, subjects in a prior study that showed Fos induction received significantly longer CS presentations compared to current study (8 minutes vs. 4 x 10 seconds, respectively). Additionally, unlike any of the aforementioned studies, here the test was in an appetitive context that had previously been paired with food over multiple sessions.

As mentioned, decreases in CEA IEG expression in response to a conditioned fear-cue have been reported (Day et al., 2008), and the current study's CEA activation pattern is in agreement with this. Day and colleagues found that fear-cues suppressed robust amphetamine-induced *c-fos* mRNA expression in the CEA (Day et al., 2008).

Similarly, the present results suggest that the fear-cue suppressed feeding-induced Fos expression. Thus, fear-cues may activate some populations of neurons in the CEA (as seen in: Beck & Fibiger, 1995; Hall et al., 2001; Scicli et al., 2004), and inhibit the activation other populations of neurons.

Fos induction patterns across the five cell groups in the basolateral area of the amygdala were distinct. Within the BLAa, Fos induction was greater in subjects with access to food compared to the no-food groups, irrespective of experimental condition. Interestingly, unlike the pattern in the CEA, Fos induction in BLAa did not correlate with consumption, which suggests it could be due to the presence of food and/or learned associations related to the food. This pattern was unique to the BLAa, which is particularly intriguing given our group's recent reports that the BLAa was the only cell group, out of more than 30 analyzed areas that showed selective recruitment during early tone-food learning (Cole et al., 2015; Cole et al., 2013). Related to this, potentiated feeding in response to a discrete CS which predicted sucrose delivery was associated with increased Fos induction in the BLA (sampling region included BLAa and BLAp) compared to an unconditioned stimulus (Holland & Hsu, 2014). But, in these prior preparations, the cue and the food were both presented, so it is unclear whether the increased Fos was due to the conditioned properties of cue, the food presentation, or consumption. However, earlier work did not find changes in BLA Fos induction following ingestion of a palatable meal (Park & Carr, 1998), in agreement with current findings that BLAa Fos induction was not correlated with consumption. Thus, it seems likely that the BLAa Fos induction in the current study was driven by the learned

associations with food. Indeed, exposure to a food-associated context was previously shown to increase Fos expression in the BLA (Schiltz et al., 2007).

Physiological state has been shown to influence Fos induction in the BLAa. Fos induction was increased in the BLAa after 12 or 36hrs of food deprivation compared to sated controls, but when these subjects were allowed to consume food Fos induction was similar across groups (Moscarello, Ben-Shahar, & Ettenberg, 2009). This suggests there is no additive effect of food deprivation and food consumption on Fos induction. Thus, the pattern of Fos induction observed in the current study could not be explained by the hunger state of the subjects at the end of test (i.e., still food-deprived for the no-food groups, and at least partially sated for the food access groups).

BLAa Fos patterns in the present study were specific to food access condition and unaffected by experimental condition. However, prior reports observed that fear expression increased Fos induction in the BLAa in response to contextual (Beck & Fibiger, 1995; Scicli et al., 2004) or discrete (Hall et al., 2001; Senn et al., 2014) conditioned fear-cues. As discussed above, this may be due to differences between the behavioral preparations and/or sampling region (BLAa-alone, or BLAa + BLAp).

Within the LA, Fos induction was greater in the experimental compared to the control condition, irrespective of food access. This is consistent with prior studies that showed increased LA Fos induction following presentation of discrete (Senn et al., 2014; but see Hall et al., 2001) or contextual (Scicli et al., 2004) fear-cues. The LA (including its functional relationship with the CEA, as revealed by contralateral lesions) is critical for conditioned fear expression (Campese, Gonzaga, & LeDoux, 2014; Jimenez &

Maren, 2009). The LA is considered the primary amygdalar input region in regards to conditioned fear learning, receiving auditory and somatosensory information (for reviews see: Ehrlich et al., 2009; Pare & Duvarci, 2012; Pare et al., 2004; Sigurdsson, Doyere, Cain, & LeDoux, 2007). A recent study employing optogenetic techniques highlighted the importance of the convergence of these sensory inputs into the LA by showing that pairing activation of auditory input terminals in LA with an aversive event was sufficient to create a fear memory, and that reactivation of these same inputs was sufficient to elicit conditioned fear behaviors (Kwon et al., 2014). This suggests an intriguing possibility that the LA Fos induction in the experimental condition in the current study may reflect reactivation of the same neurons that were recruited by the tone (auditory) and footshock (somatosensory) stimuli during the initial tone-shock conditioning.

Within the BMAp, Fos induction was greater in the experimental compared to the control condition, similar to the patterns of Fos induction observed in the LA. This similarity is consistent with dense reciprocal connections between these cell groups and that the BMAp may be a relay node for LA to CEA communication (Pare & Duvarci, 2012; Petrovich et al., 1996; Pitkänen et al., 1995; Savander, Go, Ledoux, & Pitkänen, 1996; Swanson & Petrovich, 1998). Reports of increased BMAp Fos induction during the expression of conditioned fear have been inconsistent across studies (Beck & Fibiger, 1995; Hall et al., 2001; Senn et al., 2014), and again this is likely due to differences between preparations or inconsistencies in sampling regions. However, neurons within the BMA have been shown to acquire excitatory responses to discrete fear-cues, and they were also activated during the expression of conditioned fear (Amano, Duvarci, Popa, &

Pare, 2011). There is evidence to suggest that this activation may be critical for fear expression; post-training lesions (Anglada-Figueroa & Quirk, 2005) or temporary inactivation (Amano et al., 2011) of an area which encompassed the BLA and BMA blocked the expression of conditioned freezing behavior. Further work is needed to better elucidate the role of the BMAp, specifically, in conditioned fear learning and expression.

mPFC. We found sex-specific Fos induction in the mPFC. Females in the experimental condition had significantly greater Fos induction than those in the control condition, while in contrast, all male groups showed similar amounts of Fos induction. Interestingly, Fos induction in females correlated with both food consumption and freezing during the test suggesting that the mPFC is involved in both the appetitive (feeding) and aversive (freezing) aspects of this particular behavioral paradigm.

The mPFC is has been implicated in fear-related behaviors and its different parts are associated with different functions. The dorsal mPFC (ACAd and dorsal PL) has been linked to the expression of conditioned fear, while the ventral mPFC (ventral PL and ILA) has been linked to the inhibition of conditioned fear especially during extinction (for reviews see: Courtin, Bienvenu, Einarsson, & Herry, 2013; Sotres-Bayon & Quirk, 2010). The Fos patterns in females in the current study were consistent with these functions. Greater activation of the ACAd and PL in the experimental compared to control condition may have resulted from presentation of the conditioned fear-cue and subsequent expression of conditioned fear responses (i.e., freezing). While greater activation of the ILA in the experimental compared to control condition may have

resulted from subjects trying to inhibit the conditioned response to the fear-cue in order to consume food.

The mPFC is also involved in food- and reward-related behaviors. The mPFC is necessary for the potentiation of feeding by learned contextual cues (Petrovich, Ross, Holland, et al., 2007), and exposure to a context previously associated with food induced significant Fos induction in mPFC compared control conditions (Choi et al., 2010; Schiltz et al., 2007). Furthermore, the mPFC's roles in learning and the cognitive guidance of behaviors (Dalley, Cardinal, & Robbins, 2004; Euston et al., 2012; Gilmartin, Balderston, & Helmstetter, 2014), including fear expression and feeding, are diverse. Thus, separate populations of mPFC neurons that subserve these different functions were likely differentially recruited during the feeding tests under fear, which may explain why Fos induction was high, but not different, across all the male groups in the current study.

Comparisons between males and females in other mPFC-dependent paradigms have found that the sexes are similar in some instances but not in others. For example, stress-induced reinstatement of operant responding for palatable food pellets was associated with increased activation of mPFC for both males and females (Cifani et al., 2012; Nair et al., 2011), and in females this effect was not dependent on ovarian hormones (Cifani et al., 2012). In contrast, exposure to stress facilitates classical eyeblink conditioning in males but impairs learning in females, and the effect was at least partially dependent on ovarian hormones (Wood & Shors, 1998). This deficit in females was alleviated by functional disconnection of the mPFC and BLA (Maeng, Waddell, & Shors, 2010) or bilateral temporary inactivation of the PL during the stressor (Maeng & Shors,

2013), which suggested that the behavioral sex difference may have been due to an overactivation of the mPFC in females. Similar mechanisms might underlie greater Fos induction in females in the experimental compared to the control condition in the current study.

LHA. Fos induction patterns in the LHA were associated with food consumption during the test. More specifically, Fos in the dorsomedial LHA was significantly greater for males with access to food compared to males in the no-food groups, and there a similar pattern in the ventral LHA (but it did not reach statistical significance for either sex). Within the dorsolateral LHA, the only statistically significant difference was reduced Fos in the male experimental group compared to the male control group. These groups ate differential amounts of food and in accordance, Fos within the dorsolateral LHA correlated with food consumption but not freezing behavior. Similar to the CEA, Fos induction in the dorsolateral and ventral LHA correlated with food consumption within the food access groups for both sexes. These results are consistent with the LHA's critical role in feeding behavior (reviewed in: Elmquist et al., 1999). The LHA is important for feeding elicited by both homeostatic and non-homeostatic drives, as it is anatomically positioned to integrate cognitive and environmental influences with physiological signals contributing to the motivation to eat (e.g., Berthoud & Münzberg, 2011; Petrovich, 2013; Swanson, 2000, 2005). Meal anticipation (Poulin & Timofeeva, 2008; Verhagen et al., 2011), food-associated contexts (Choi et al., 2010; Schiltz et al., 2007), well-learned tone-food associations (Cole et al., 2015), and ingestion of a palatable meal (Park & Carr, 1998) have all been shown to increase Fos induction in the

LHA. Thus, the Fos induction observed in rats with food access in the current study could be driven by both consumption of food, as well as the contextual cues associated with the food.

The dorsal area of the LHA (dorsomedial and dorsolateral sampling areas in the current study) contains two populations of neurons that express orexigenic neuropeptides: melanin-concentrating hormone (MCH) and orexin/hypocretin (Broberger et al., 1998; de Lecea et al., 1998; Hahn, 2010; Nahon et al., 1989; Sakurai et al., 1998; Swanson et al., 2005). Both MCH and orexin have been implicated in feeding driven by learned cues (Petrovich et al., 2012; Sherwood et al., 2015), and orexin neurons are activated by food-associated cues (Choi et al., 2010; Wheeler et al., 2014). In addition to feeding behavior, orexin neurons are also recruited during a range of processes including reward, stress, and arousal (e.g., Berridge, Espana, & Vittoz, 2010; Cason & Aston-Jones, 2013, 2014; Harris & Aston-Jones, 2006; Rodgers et al., 2000). Of particular relevance to the current study, expression of conditioned fear has been shown to increase Fos induction in the LHA (Beck & Fibiger, 1995), including within orexin neurons (Furlong, Vianna, Liu, & Carrive, 2009). Thus, Fos induction in the current study could represent activation of neurons which express orexigenic neuropeptides, or other neurons which influence these populations through local circuits (see: Brown, Woodworth, & Leinninger, 2015; Burt, Alberto, Parsons, & Hirasawa, 2011). Nevertheless, MCH and orexin are not the only populations of LHA neurons that are important in the regulation of feeding. For example, recent work using opto- and pharmaco-genetic techniques revealed a subpopulation of GABAergic neurons (marked by the presence of the vesicular GABA transporter, and

which do not co-express orexigenic neuropeptides) that when activated, increased both appetitive and consummatory measures of feeding behavior (Jennings et al., 2015). This diversity of neuronal phenotypes and the variety of circumstances under which they are activated make it clear that further work is needed to better define the role, or roles, of the LHA in inhibition of feeding by a learned fear-cue.

Clinical Implications. The term anorexia refers to a loss or lack of appetite, even though colloquially it is most commonly associated with the eating disorder. Anorexia can result from homeostatic perturbations (e.g., internal states like dehydration, or external pressures like fear and stress), or as a symptom of various pathologies (e.g., wasting disease states, psychological disorders) (Watts, Salter, & Neuner, 2007). The behavioral paradigm in the current study provided a model with which to interrogate the neural circuits underlying one of these anorexia triggers—external homeostatic challenge, and as such yielded insight into the neural mechanisms underlying short-term fear-induced anorexia. Although direct translational application of our model to anorexia nervosa (AN), the eating disorder in humans, is not possible, it is useful regarding at least one aspect of the disease—fear processing and extinction. It has been proposed that alterations in fear processing may contribute to the disease and that rapid fear learning and resistance to extinction may predispose people to the disease and/or inhibit their recovery (Strober, 2004).

Intense fear of gaining weight is a primary symptom of AN, and this eating disorder shares high co-morbidity with anxiety disorders (American Psychiatric Association, 2000). Indeed, high trait anxiety often predates illness onset (Kaye, 2008),

and may contribute to a feed-forward perpetuation of AN symptoms in patients suffering from the disease (Attia, 2010). Additionally, both state and trait anxiety levels have been shown to negatively correlate with meal size in in-patient weight-restored AN patients, but not in BMI-matched healthy control comparisons (Steinglass et al., 2010). In an fMRI study, women with AN rated food images as more fear-inducing and had greater BOLD responses in the mPFC compared to healthy control subjects (Uher et al., 2004). This is particularly interesting, since the mPFC is where we found in the current study that female rats who were expressing fear anorexia had greater activation compared to the control subjects. Together this suggests that fear-related mPFC overactivation may be a female-specific susceptibility factor, consistent with higher reported rates of eating and anxiety disorders in women (Becker et al., 2007; McCarthy et al., 2012; McLean & Anderson, 2009).

Conclusion. The present study replicated prior behavioral findings that learned fear-cues can inhibit food intake in both male and female rats despite physiological hunger and prior history of eating in the test context. Additionally, this study provided the first evidence for the recruitment of the brain substrates underlying this phenomenon. Using Fos induction as a measure of activation, we found recruitment of distinct regions within an amygdala-prefrontal-lateral hypothalamic system that represented various conditions of this experiment (i.e., feeding, freezing, learned associations). In both males and females, CEA and LHA activation was associated with the amount of food consumed, BLAa activation with food-associated cues, and LA and BMAp activation with fear expression. Selective recruitment of the mPFC in female, but not male, rats in

the experimental condition was associated with both feeding and freezing behavior, and offers an interesting avenue for future research regarding female susceptibility in anxiety and eating disorders. These Fos induction analyses were an important first step in identifying the network of regions which is engaged during fear-cue inhibited feeding. However, it should be noted that Fos analyses have limitations; neurons may use IEGs other than Fos to regulate activity-induced transcription, and Fos is expressed in a variety of phenotypically distinct populations of neurons (Chaudhuri, 1997; Curran & Morgan, 1995; Morgan & Curran, 1991). Thus, null results from a Fos analysis cannot necessarily be interpreted as a negative finding in regards to a region's involvement in a particular behavior. If minimal Fos is observed, then one could test for induction of other IEGs. If similar amounts of Fos are observed across conditions, then combining Fos with pathway- and/or neurochemical-specific techniques could distinguish between populations of neurons that were differentially recruited. Nevertheless, the results from the current study provide important functional maps for future interrogation of the circuitry underlying the inhibition of feeding by a learned fear-cue.

IV: General Discussion

Anatomical organization of the amygdala-prefrontal-lateral hypothalamic network

It is useful to first review the anatomical organization of the amygdala-prefrontal-lateral hypothalamic network and how it relates to the circuitry underlying motivated behaviors before discussing the functional recruitment of this network during fear-cue inhibited feeding (Fig. 4.3). The organization of the cerebral networks which support motivated behaviors, including the defensive and feeding behaviors of interest in the

current work, is conceptualized as a triple descending pathway. This pathway consists of converging input from cortical, striatal, and pallidal regions to hypothalamic "behavioral control columns" that coordinate behavioral expression by integrating this converging input (Swanson, 2000, 2005). The amygdalar regions examined within this dissertation are considered highly differentiated parts of the cortex (basolateral area) or striatum (CEA) (McDonald, 2003; Swanson & Petrovich, 1998). With respect to the triple descending pathway, and in agreement with the classification of the cortical and striatal components of the amygdala, Study 1 found that the cortical input from the mPFC and cortical parts of the amygdala (i.e., basolateral area nuclei: LA, BLA, BMA; Swanson & Petrovich, 1998), and striatal input from the amygdala (i.e., CEA; Swanson & Petrovich, 1998) send converging pathways to the LHA. This convergence of information can reach the LHA via direct pathways from each of these cortical and striatal cell groups, or via indirect pathways following cotico-cortico (i.e., between the mPFC and basolateral area, and between distinct cell groups within the basolateral area) or cortico-striatal (i.e., mPFC or basolateral area to CEA) processing. In return, the LHA can influence these and other forebrain regions from which it receives input, via ascending projections.

Direct descending projections to the LHA. The LHA receives direct inputs from the amygdala and mPFC. The LHA receives projections from all parts of the basolateral area of the amygdala (glutamatergic), as well as from all parts of the CEA (GABAergic + peptidergic) (Hahn & Swanson, 2010, 2012, 2015; Kita & Oomura, 1982; Krettek & Price, 1978a; Ono et al., 1985; Petrovich et al., 2001; Petrovich et al., 1996). The entire mPFC sends direct glutamatergic projections to the LHA (Floyd et al., 2001;

Gabbott et al., 2005; Hahn & Swanson, 2010, 2012, 2015; Hurley et al., 1991; Kita & Oomura, 1982; Sesack et al., 1989; Takagishi & Chiba, 1991; Vertes, 2004). Interestingly, the dorsal and ventral LHA receive the majority of their inputs from different subsets of amygdalar and mPFC regions. As shown in Study 1, these projections are organized such that the dorsal LHA receives input from the entire mPFC and from the CEA (especially the CEAl and CEAm), while the ventral LHA receives input from a restricted ventrocadual region of the mPFC (mostly ILA) and the basolateral area (especially the BMA, but also the LA). Thus, in accordance with the triple descending pathway (Swanson, 2000, 2005), the LHA is anatomically positioned to integrate converging information from these cortical and striatal cell groups and coordinate the expression of motivated behaviors accordingly.

Cortico-cortico processing. The mPFC and basolateral area of the amygdala are reciprocally connected, and processing within this system could subsequently influence hypothalamic circuitries that function as behavioral controllers (Likhtik & Paz, 2015; Petrovich, 2013; Swanson, 2000, 2005). The basolateral area of the amygdala (predominately the BLAa and BLAp, but also the LA and BMAp) sends projections to the entire mPFC (Hoover & Vertes, 2007; Kita & Kitai, 1990; Krettek & Price, 1977; McDonald, 1987, 1991; Petrovich et al., 1996). These projections are topographically organized along both rostrocaudal to rostrocaudal, and rostrocaudal to dorsoventral gradients (see Study 1: Pathway Tracing; Hoover & Vertes, 2007). Thus, distinct regions within the basolateral area preferentially target specific regions of the mPFC. Nearly all projections from the BLA to the mPFC arise from glutamatergic principal pyramidal

neurons, which make up ~85% of the BLA neuronal population (McDonald, 1992). A vast majority of these projections (>95%) synapse onto glutamatergic mPFC neurons, suggesting that the BLA could monosynaptically influence mPFC output neuron firing, which was recently demonstrated for mPFC neurons that receive BLA input and project to the spinal cord (Gabbott et al., 2012). In addition to extensive innervation of pyramidal neurons, ~5% of BLA inputs innervate interneurons (Gabbott et al., 2006), and stimulation of BLA neurons can inhibit mPFC neuronal firing through monosynaptic, as well as polysynaptic, pathways (Dilgen et al., 2013; Perez-Jaranay & Vives, 1991). In that regard, separate populations of pyramidal mPFC neurons have been shown to exhibit profiles of either monosynaptic excitation or suppression of baseline firing following BLA stimulation (Floresco & Tse, 2007).

In return, the mPFC sends direct projections to the basolateral area of the amygdala (Cassell, Chittick, Siegel, & Wright, 1989; Gabbott et al., 2005). These projections are most likely glutamatergic, however a very small population of mPFC GABAergic projecting neurons has been identified (Lee, Vogt, Rubenstein, & Sohal, 2014). Although all basolateral area cell groups receive mPFC inputs, these pathways are arranged such that the ACAd and PL more heavily project to the BLA (Cassell & Wright, 1986; McDonald, 1998; McDonald, Mascagni, & Guo, 1996; Sesack et al., 1989; Vertes, 2004), while the ILA more heavily projects to the BMA (McDonald, 1998; McDonald et al., 1996; Vertes, 2004). These mPFC inputs typically result in an inhibition of processing within the basolateral area. mPFC (PL/ILA) stimulation was more likely to induce excitatory responses from interneurons in the LA and BLA, while stimulation of

another cortical area, sensory cortex, was more likely to induce excitatory responses from primary projection neurons within these nuclei (Rosenkranz & Grace, 2001). Consistent with the activation of inhibitory interneurons and the timecourse of a disynaptic pathway, mPFC stimulation often caused a suppression of firing in BLA projection neurons (Rosenkranz & Grace, 2001, 2002). Indeed, local interneurons are well-positioned to influence BLA output firing—half of the synapses formed on projection neurons in the BLA are from local interneurons (Muller, Mascagni, & McDonald, 2006), which comprise ~15% of the BLA neuronal population (McDonald, 1992).

The reciprocal pattern of connections between the basolateral area of the amygdala and the mPFC, as described above, are arranged and matched by strength; the BLA more strongly projects to the dorsal mPFC (ACAd, PL), which preferentially innervates the BLA, and the BMA more strongly projects the ILA, which preferentially innervates the BMA. Indeed, basolateral area neurons have been shown to preferentially innervate basolateral area-projecting mPFC neurons (Little & Carter, 2013), and thus basolateral projections to the mPFC could potentially influence their own firing. These patterns of connections provides structural support for the possibility of both excitatory feedforward processing via synapses onto principle projecting neurons, and inhibitory feedback processing via connections onto local inhibitory interneurons within each component of this basolateral area-mPFC circuitry. The bidirectional connections between the basolateral area and mPFC could enhance processing within this system and result in increased output to targets like the LHA.

Information processing between the different cells group within the basolateral area is highly organized (Fig. 4.1). The cell groups that comprise the BLA (BLAa, BLAp) are densely interconnected (Krettek & Price, 1978b; Savander et al., 1995), while connections between the BMA cell groups are predominately unidirectional (BMAp to BMAa) (Petrovich et al., 1996; Savander et al., 1996). The LA and BMAp are very strongly, and reciprocally, connected (Krettek & Price, 1978b; Petrovich et al., 1996; Pitkänen et al., 1995; Savander et al., 1996; Wakefield, 1979). In contrast, the LA is weakly bidirectionally connected with the BLAa, BLAp and BMAa (Krettek & Price, 1978b; Pitkänen et al., 1995; Savander et al., 1995, 1996). Lastly, the BLA and BMA nuclei are weakly connected with each other (Petrovich et al., 1996; Savander et al., 1995, 1996). The processing between basolateral area cell groups follows similar cortico-cortico processing principles discussed above for the basolateral area-mPFC system. The projection neurons in these nuclei are nearly exclusively glutamatergic, but their connections could innervate either glutamatergic principal pyramidal neurons or synapse onto inhibitory GABAergic local interneurons (McDonald, 1992; Muller et al., 2006) and subsequently excite or reduce the output from the target nucleus.

Cortico-striatal processing. The mPFC projects to the CEA. The ILA sends a strong projection to the CEA (especially to the CEAm and CEAc) (Hurley et al., 1991; McDonald, 1998; McDonald et al., 1996; McDonald, Shammah-Lagnado, Shi, & Davis, 1999; Vertes, 2004), while the PL projects only lightly to the CEAc (Vertes, 2004); these mPFC projections are mostly glutamatergic. The CEA, like other striatal regions, does

not send projections to any part of the mPFC or other cortical regions (Study 1: Pathway Tracing; Hoover & Vertes, 2007; Swanson & Petrovich, 1998).

In addition to mPFC inputs, the CEA receives cortical input from amygdalar nuclei. Each of the cell groups within the basolateral area can directly or indirectly (including via other intraamygdalar connections) influence the CEA, via glutamatergic projections (Fig. 4.1) (Ledoux, 2012; Pitkänen et al., 1997; Swanson & Petrovich, 1998). The BLAp, BMAa, and BMAp send strong projections to the CEA, particularly to the CEAc but also to the CEAm (Bienkowski & Rinaman, 2013; Petrovich et al., 1996; Savander et al., 1995, 1996). The CEAc additionally receives input from the LA, which sends only weak projections to the CEAm and CEAl (Bienkowski & Rinaman, 2013; Krettek & Price, 1978b; Pitkänen et al., 1995). In contrast to the other basolateral area cell groups, the BLAa projects only very weakly to the CEA (Bienkowski & Rinaman, 2013; Krettek & Price, 1978b; Pitkänen et al., 1997; Savander et al., 1995), if at all (Swanson & Petrovich, 1998). Processing within the CEA consists of GABAergic pathways organized such that the CEAl projects to the CEAc, and more importantly, both of these divisions project to the CEAm (Jolkkonen & Pitkänen, 1998; Petrovich & Swanson, 1997), which serves as the major amygdalar output region to hypothalamic, midbrain, and hindbrain targets (Maren, 2001; Pitkänen et al., 1997; Swanson & Petrovich, 1998). This connectional organization allows for information integrated within the CEA to be relayed to the LHA.

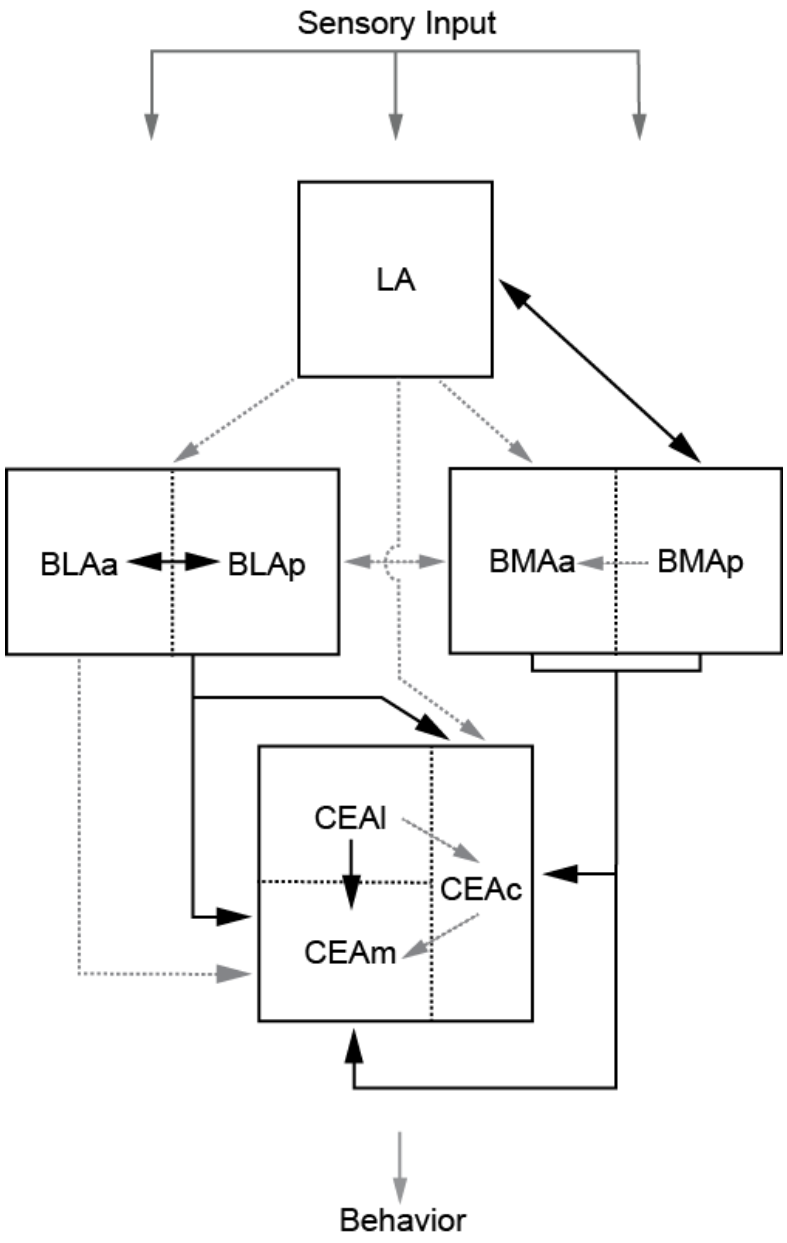

Fig.4.1 Intraamygdalar connections between the basolateral area cell groups and the CEA. Strong projections are indicated by solid lines, and weaker projections by dashed lines.

Ascending projections from the LHA. The LHA is considered a coordinator of behavioral expression for feeding and other motivated behaviors due to its descending projections to the mid- and hindbrain, and its ascending projections to the forebrain, including to forebrain regions from which it receives input (Saper, 2000). In general, the LHA innervates striatal regions more heavily than cortical regions. The CEA receives a moderately strong projection from the LHA (Allen & Cechetto, 1993; Berk & Finkelstein, 1982; Hahn & Swanson, 2010; Saper, Swanson, & Cowan, 1979; Schmitt et al., 2012; Veening, 1978; Villalobos & Ferssiwi, 1987). In contrast, although LHA projections to the basolateral area of the amygdala exist, they are very weak (Allen & Cechetto, 1993; Hahn & Swanson, 2012; Schmitt et al., 2012; Veening, 1978; Villalobos & Ferssiwi, 1987). The LHA sends weak projections to the mPFC (Allen & Cechetto, 1993; Goto et al., 2005; Hahn & Swanson, 2012, 2015; Hoover & Vertes, 2007; Saper, 1985; Villalobos & Ferssiwi, 1987). The neurotransmitters in these ascending projections have not been fully characterized; the LHA is a heterogeneous structure and projection neurons to amygdalar and mPFC regions could be glutamatergic or GABAergic, and may also contain neuropeptides (Berthoud & Münzberg, 2011; Burt et al., 2011; Meister, 2007; Schone & Burdakov, 2012). These ascending projections provide a mechanism for the LHA to supply feedback to forebrain regions through which it could influence cognitive processes that modulate the expression of motivated behaviors.

Functional recruitment of the amygdala-prefrontal-lateral hypothalamic network during fear-cue inhibited feeding

In Study 2, we found that distinct cell groups within the amygdala-prefrontal-lateral hypothalamic network were differentially recruited by fear- and feeding- related processing during the food consumption test in the presence of a learned fear-cue. We observed Fos induction patterns associated with 1) the amount of food consumed (CEAl, CEAm, LHA), 2) the presence of food-cues (BLAa), 3) the presence of fear-cues (LA, BMAp), 4) no differential activation (CEAc, BLAp, BMAa), or 5) a combination of these patterns (mPFC).

Fos induction in the CEA correlated with consumption, and was greater for subjects in groups with access to food compared to subjects in groups without food access. Considering prior work showed that the CEA was critical for fear-cues to inhibit feeding (Petrovich et al., 2009), this pattern of Fos induction suggests that the CEA is critically recruited during fear-cue inhibited feeding. Since less Fos was observed in subjects that were inhibiting food intake in the presence of fear-cues, a suppression of CEA activation resulting from the integration of information from the mPFC and basolateral area cell groups, may be necessary for the expression of fear-cue inhibited feeding behavior. This explanation is consistent with the CEA's role in the output of information following amygdalar information processing (Ledoux, 2012; Pitkänen et al., 1997; Swanson & Petrovich, 1998). Specifically, that information about the fear stimulus (from the LA/BMAp where Fos induction was greater in the presence of a fear-cue) and food/food-associated context (from the BLAa, where Fos induction was greater in

presence of food-cues) were relayed to the CEA where this integration of information resulted in Fos induction that corresponded to food intake. Connections between the basolateral area cell groups to the CEA are important for both fear and feeding behaviors. For example, functional disconnection of the LA and CEA (via contralateral lesions) abolished conditioned fear expression (Campese, Gonzaga, & LeDoux, 2014; Jimenez & Maren, 2009). This could be due to the direct unidirectional pathway from the LA to the CEA, or more likely, given the weakness of that pathway, via the BMAp (see Fig. 4.1). Optogenetic inhibition of LA and BLA projections to the CEA differentially modulated the learning of aversive and appetitive associations: the inhibition of this pathway impaired cue-shock fear conditioning, but promoted cue-sucrose learning (Namburi et al., 2015). Interestingly, LA and BLA inputs to the CEA can compete, similar to the competition between mPFC and sensory cortex inputs to the basolateral area, which is described below. Electrophysiological investigations showed that activation of a subset of BLA neurons blocked LA-stimulation induced excitation of the CEAm (Jasnow et al., 2013).

mPFC (especially ILA) pathways to the CEA are also important for the expression of conditioned fear responses. Electrolytic lesions of ILA, but not PL, switched behavior from shuttling to freezing in an active avoidance paradigm, and increased Fos induction in the CEA suggesting that the ILA typically suppresses CEA-mediated conditioned freezing responses (Moscarello & LeDoux, 2013). In support of the idea of "top-down" mPFC suppression of amygdalar processing, stimulation of the mPFC

(ventral PL and ILA) blocked the ability of electrical stimulation of LA, BLA, or BMA to excite CEA neurons (Quirk, Likhtik, Pelletier, & Pare, 2003).

Similar to the CEA, Fos induction in the LHA was associated with how much food subjects consumed during the test session in Study 2, and the similarities in Fos patterns are consistent with the reciprocal connections between these two regions (reviewed above). This Fos pattern is also consistent with the LHA as a critical component of the network underlying feeding behavior, which it regulates by integrating cognitive, environmental, and physiological information (Berthoud & Münzberg, 2011; Elmquist et al., 1999; Petrovich, 2013; Swanson, 2000, 2005). Interestingly, the neurons with robust CEA Fos induction observed in the subjects who were consuming large amounts of food were located in a specific region (Fig. 4.2 b', d'), which topographically overlaps with the region where we observed strong retrograde labeling following tracer injection into the dorsal LHA (Study 1; Fig. 4.2 a', c'). This suggests CEA neurons that project to the dorsal LHA might have been recruited during the consumption of food. CEA neurons are GABAergic, but could activate the LHA via disinhibition or through the release of neuropeptides (Burt et al., 2011; Charles & Hales, 2004; Crain & Shen, 1990; Stowe & Nemeroff, 1991). The LHA sends reciprocal projections to the CEA, and this ascending pathway could further drive the activation of CEA neurons during food consumption. Consistent with this, it was recently reported that unilateral lesions of the LHA suppressed food-cue induced Fos expression in the CEA (Wheeler et al., 2014).

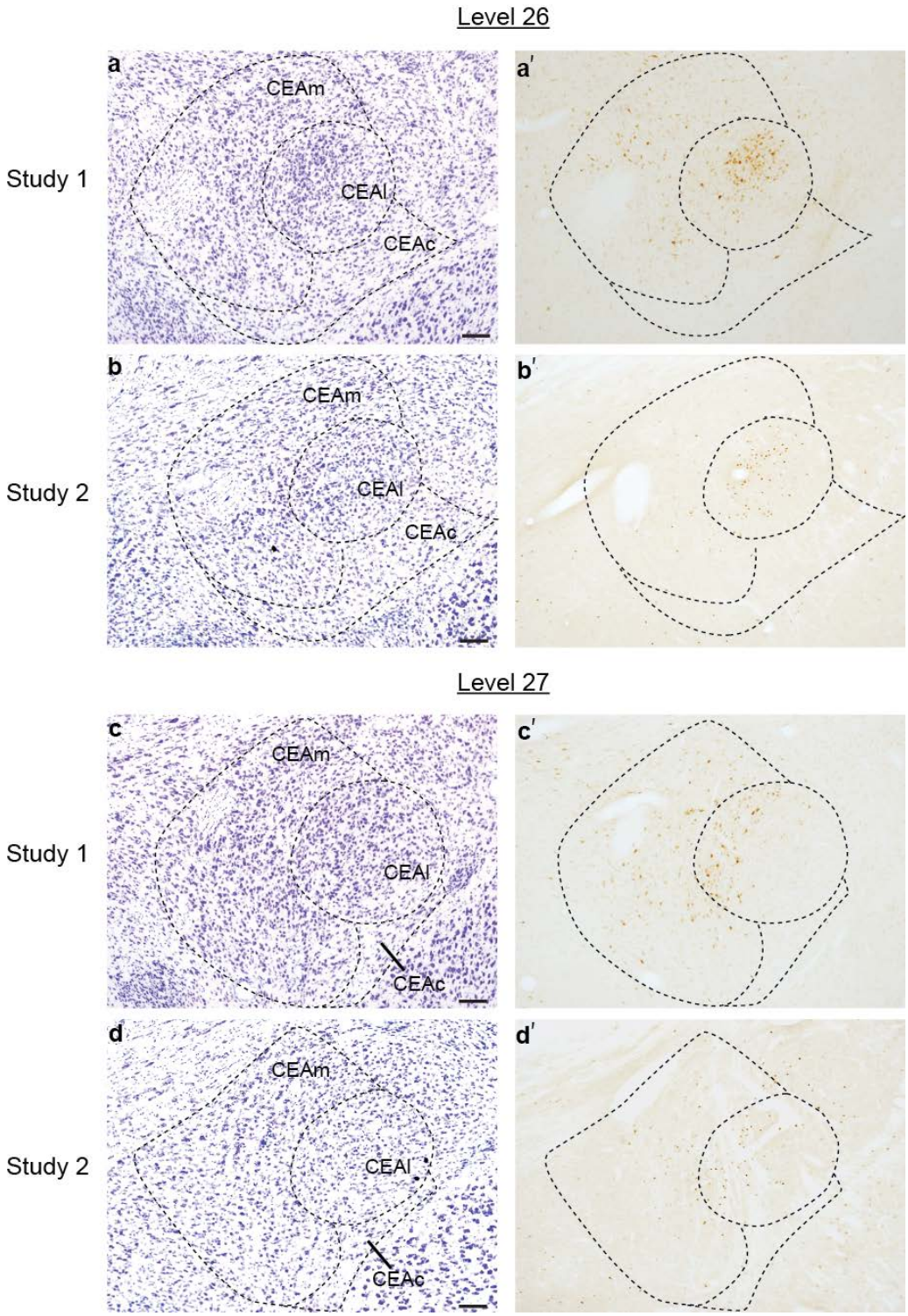

Fig. 4.2 Comparisons of the locations of the CEA-LHA projection neurons identified in Study 1 (**a'**, **c')** and Fos induction during feeding tests under fear-cue in Study 2 (**b'**, **d'**). Adjacent Nissl-stained tissue (**a**, **b**, **c**, **d**). Scale bars = 100μm.

Multiple, topographically organized pathways exist between the basolateral amygdala and mPFC, thus it is very likely that different pathways between these cortical regions were differentially engaged by fear- and feeding-related processing during the test in Study 2. Specifically, three different patterns of Fos induction were observed for these cortical regions: Fos that corresponded to the presence of fear-cues (LA, BMAp, and in females—mPFC), Fos that corresponded to the presence of food-cues (BLAa), or no differential activation (BMAa, BLAp, and in males—mPFC). These patterns will be discussed next, with respect to the anatomical organization of, and prior evidence regarding the function of processing within, the basolateral area-mPFC system.

Consistent with structural evidence, basolateral area inputs influence the mPFC during the expression of behavior following both aversive (e.g., fear-related) and appetitive (e.g., food-related) learning. For example, a population of BLA neurons that projects to the mPFC was activated during the expression of conditioned fear (Herry et al., 2008), and inactivation of the BLA significantly reduced the firing rate of pyramidal PL neurons in response to an aversively conditioned fear-cue (Sotres-Bayon et al., 2012). Further, pyramidal mPFC (PL, ILA) neurons that receive BLA input showed increased activity in response to a conditioned cue that predicts footshocks (Laviolette et al., 2005). Interestingly, the PL and ILA are differentially activated during the expression and extinction of conditioned fear (Sierra-Mercado et al., 2011), and correspondingly, BLA neurons projecting to the PL were activated in response to an aversively conditioned stimulus (CS), while those projecting to the ILA were activated in response to an extinguished CS (Senn et al., 2014). Similar to the recruitment of BLA pathways to the

mPFC during aversive learning, BLAa neurons that send direct projections to the PL were activated during appetitive (tone-food) learning (Keefer, Reppucci, Mayer, & Petrovich, 2014). Furthermore, BLA inactivation significantly reduced the firing rate of pyramidal PL neurons during conditioned lever pressing for food (Sotres-Bayon et al., 2012). Based on this prior work, it is feasible to suggest that during the food consumption test with fear-cues in Study 2 the BLAa was relaying information regarding the presence of appetitively conditioned contextual cues, while the LA and BMAp were relaying information regarding the aversively conditioned tone cue to the mPFC (especially to the PL given its role in the expression of conditioned behaviors).

Projections from the mPFC to the basolateral area are also functionally engaged during the expression of fear- and feeding-related behaviors. For example, food intake by food-deprived mice induced activation of a subset of mPFC neurons and optogenetic stimulation of these neurons' terminal ends in the BLA increased food intake (Land et al., 2014). Activation of this pathway could account for some of the Fos induction observed in the BLAa for groups with access to food, compared to Fos patterns in this cell group for subjects without food access. Consistent with the differential roles of the PL and ILA in the expression and extinction of conditioned fear, retrieval of a fear memory was associated with activation of PL inputs to the LA, while retrieval of an extinction memory was associated with activation of ILA inputs to the LA (Knapska et al., 2012). Given the role of the ILA in extinction processes, ILA pathways to the LA and BMAp may have been recruited in Study 2 during feeding tests under a fear-cue, which were conducted under extinction conditions (tones presented without shocks). Consistent with

this idea, an electrophysiological investigation showed that stimulation of the mPFC prior to stimulation of sensory cortex reduced the response of BLA projection neurons to the input from sensory cortex (Rosenkranz & Grace, 2001), which provides evidence for "top-down" mPFC pathways that could suppress amygdalar firing in response to "bottom-up" sensory stimuli information.

It is clear from the functional studies reviewed thus far, that the mPFC was likely an active contributor and recipient of information processing during the expression of fear and feeding behaviors in Study 2; a supposition which is supported by the anatomical organization of the amygdala-prefrontal-lateral hypothalamic network. Indeed, there was robust Fos induction within the mPFC across groups (shown in Fig. 3.6). Hence, the most parsimonious explanation for why differential Fos induction was not observed in males would be that separate populations of mPFC neurons were being recruited. The mPFC was the only region examined in Study 2 where males and females had different patterns of Fos induction. Interestingly, the findings from studies examining classical eyeblink conditioning suggest that this sex difference could be due to differential information processing within the basolateral amygdala-mPFC system. Stress impaired eyeblink conditioning in females, but not males, and this deficit was alleviated by functional disconnection of the mPFC and BLA (Maeng et al., 2010; Wood & Shors, 1998).

The connectional organization of the amygdala-prefrontal-lateral hypothalamic network allows for processing within the basolateral area-mPFC system to, in turn, influence the LHA. As previously discussed, the LHA is a critical region in the circuitry which regulates feeding behavior, and consequently basolateral area and mPFC inputs

could influence its control of feeding in response to a conditioned fear-cue. Functional disconnection of the BLA and LHA blocked the ability of a learned cue to potentiate feeding (Petrovich et al., 2002), and a subsequent study that combined retrograde tracing and immediate early gene induction showed that LHA-projecting BMA/BLA neurons were activated during feeding driven by a learned cue for food (Petrovich et al., 2005). LHA-projecting mPFC neurons were also activated during feeding driven by this cue (Petrovich et al., 2005), and stimulation of a subset of mPFC neurons has been shown to elicit robust feeding which can blocked by antagonism of glutamate receptors in the LHA (Mena et al., 2011; Mena et al., 2013). Thus, input from the basolateral area-mPFC system could have, like the CEA, promoted activation of LHA behavioral controllers that regulate the expression of feeding behavior.

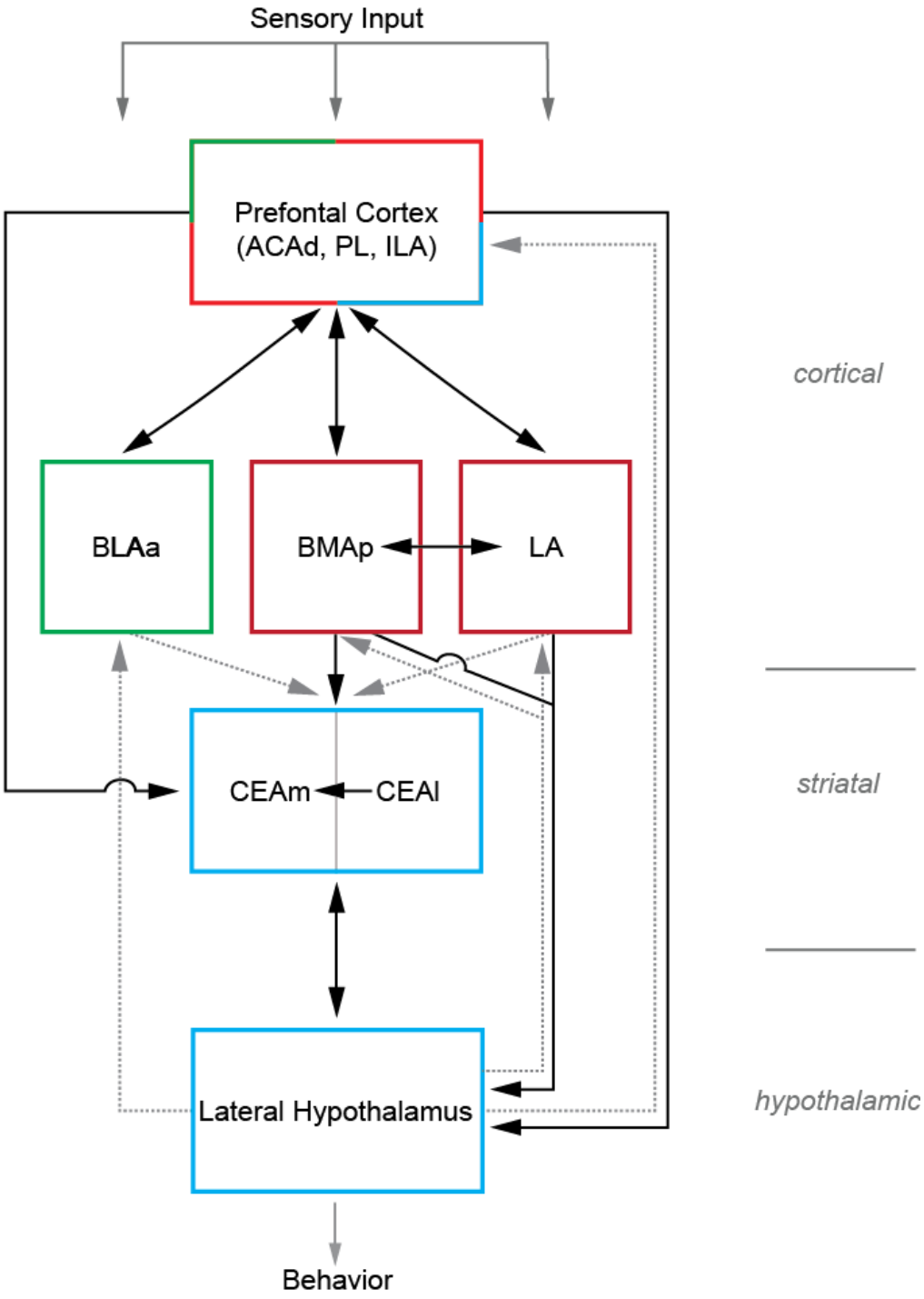

Fig. 4.3 Summary of the organization of connections between brain areas that showed differential Fos induction in Study 2 (red=fear, green=food/food-cues, blue=consumption). Moderate to strong projections are indicated by solid lines, and weak projections by dashed lines.

Sex differences in the amygdala-prefrontal-lateral hypothalamic network and fear-cue inhibited feeding.

It is clear that males and females differ in a wide variety of ways. The etiology of these sex differences is a combination of gonadal hormone (organizational or activational effects), genetic (sex chromosome linked), and epigenetic (often hormonally mediated) factors (Davies & Wilkinson, 2006; Nugent & McCarthy, 2011). Despite clear differences between the sexes, within most disciplines of basic biological research, studies have overwhelming and disproportionately used male subjects (Zucker & Beery, 2010). Even when female subjects are included, few studies directly compare behavior and brain activation patterns between males and females, despite the fact that many diseases are more prevalent in a particular sex (Cahill, 2006; Zucker & Beery, 2010) and that including both males and females is a necessary step in characterizing differences between the sexes (McCarthy et al., 2012). To help remedy this gap, the National Institutes of Health recently released new guidelines to balance the use of male and female subjects in animal research (Clayton & Collins, 2014). Here, sex differences in the recruitment of the amygdala-prefrontal-lateral hypothalamic network during the expression of fear-cue inhibited feeding behavior were examined; typically the patterns of activation were similar between males and females, with one notable exception being activation patterns in the mPFC.

Study 1 was completed using male subjects in part for ease of comparison since the neuroanatomical tract tracing literature, not unlike many other disciplines of basic research, has predominately used male subjects. However, there is little evidence to

suggest that the structural pathways investigated in Study 1 using male subjects would not also exist in female subjects. Although some amygdalar and hypothalamic nuclei are known to be sexually dimorphic (Simerly, 2002), none of those regions were examined here. Even so, projections arising from or going to highly sexually dimorphic brain regions are typically present in both sexes (e.g., Cavalcante, Bittencourt, & Elias, 2014; Gu, Cornea, & Simerly, 2003; Kang, McCarthy, Cherry, & Baum, 2011). In regard to the specific regions and pathways of the amygdala-prefrontal-lateral hypothalamic network examined in Study1, a number of comparison anatomy studies referenced within this dissertation included female subjects and made no reports of sex differences in the basic organization of these pathways (Berk & Finkelstein, 1982; Cassell & Wright, 1986; Hurley et al., 1991; Kita & Oomura, 1982; Krettek & Price, 1977, 1978a, 1978b; McDonald, 1987, 1991; Pitkänen et al., 1995; Veening, 1978; Villalobos & Ferssiwi, 1987). Thus, whether two regions are directly connected—the most basic level of neuroanatomical pathways—appears to be highly conserved across the sexes. Nevertheless, many aspects of these pathways can differ structurally between the sexes. For instance, the relative strength of these projections can depend on, and be measured by, the number of projecting neurons, the number of synapses, the amount of neurochemical released from the presynaptic membranes, the number of receptors on the postsynaptic membranes, *et cetera*. Further, even if males and females have identical pathways in terms of structure, these pathways can be differentially recruited in male versus female brains by the same stimuli, or under different circumstances. Sexual dimorphisms in the structure or functional recruitment of neuroanatomical pathways

could parsimoniously explain observed sex differences in behavior, but that might not always be in the case. In some instances sex differences in the brain could represent compensatory mechanisms that prevent the expression of sex differences in behavior (Cahill, 2006; De Vries, 2004; de Vries & Sodersten, 2009).

In Study 2, it was particularly important to include both sexes in the functional investigation of the amygdala-prefrontal-lateral hypothalamic network during fear-cue inhibited feeding. This was in part because women have higher reported rates of anxiety and eating disorders compared to men (Becker et al., 2007; McCarthy et al., 2012; McLean & Anderson, 2009), and in part because our group had previously described sex differences in certain aspects of fear-induced inhibition of feeding. Specifically, females were slower to extinguish fear-cue inhibited feeding compared to males (Petrovich & Lougee, 2011), and males selectively inhibited food intake in an aversive-associated context while females consumed similar amounts of food in both neutral and aversive-associated contexts (Reppucci et al., 2013). In the current study, we observed very similar behavior in our male and female subjects—subjects in the experimental condition inhibited their food intake and expressed freezing behavior in the presence of a learned fear-cue compared to subjects in the control condition, irrespective of sex. Prior reports had also shown that males and females of outbred strains of rats exhibited similar freezing responses to aversively conditioned discrete cues (Barker & Galea, 2010; Gruene et al., 2014; Maren et al., 1994; Pryce et al., 1999). However, sex differences in fear learning, expression, and extinction have all been documented (see: Andreano & Cahill, 2009; Dalla & Shors, 2009; Lebron-Milad & Milad, 2012). These differences are

particularly pronounced in studies using aversively conditioned contextual cues (Barker & Galea, 2010; Chang et al., 2009; Gupta, Sen, Diepenhorst, Rudick, & Maren, 2001; Lynch, Cullen, Jasnow, & Riccio, 2013; Maren et al., 1994), and appear to be driven by circulating gonadal hormones in females (Chang et al., 2009; Gupta et al., 2001; Lynch et al., 2013), but not in males (Anagnostaras et al., 1998; but see: Graham & Milad, 2014). Interestingly, fear conditioning differences between the sexes might not reflect differences in learning *per se*, and may instead represent differences in employed strategy (Andreano & Cahill, 2009; Archer, 1975; Dalla & Shors, 2009) which could partially explain the dissimilar findings for cued versus contextual fear conditioning.

Although we observed a similar inhibition of food intake in males and females there was a large baseline difference in consumption between the sexes. This difference is most easily explained by significant differences in body weight between the sexes and resulting gastric capacity (Bull & Pitts, 1971). However, other factors, most notably activational effects of circulating gonadal hormones, could also have contributed to this difference. Estradiol has been well-characterized as anorexigenic and testosterone as orexigenic, especially in feminized and masculinized brains, respectively. In adult rats, testosterone levels are relatively constant in males, but circulating levels of gonadal hormones in females vary with phase of their 4-5 day estrous cycle (for review see: Asarian & Geary, 2013). The subjects in Study 2 were all gonadally intact. Thus, the activational effects of testosterone were likely similar for all male subjects, but the activational effects of estradiol could have unequally affected female subjects depending on cycle phase. Females in high estrogen phases at test could have been consuming less

food in part because of their hormonal status, which could have attenuated consumption for subjects in the experimental condition and blunted consumption for subjects in the control condition compared to female subjects in low estrogen phases at test. Although the effect of estrous phase could not directly be analyzed due to sample size, our results suggested it did not significantly affect female feeding or freezing behavior since behavioral data variability (as interpreted by the SEM) was no greater in females than in males. However, future studies employing gonadectomized subjects with and without hormone replacement could be done to directly address the role(s) of circulating gonadal hormones on fear-cue inhibited feeding behavior and the neural network that is recruited during its expression.

The mPFC was the only region examined in Study 2 where males and females had different patterns of Fos induction. Interestingly, similar findings were reported for studies examining classical eyeblink conditioning. Exposure to stress facilitated classical eyeblink conditioning in males but impaired learning in females (Wood & Shors, 1998). The deficit in females could be alleviated by functional disconnection of the mPFC and BLA (Maeng et al., 2010) or bilateral temporary inactivation of the mPFC during the stressor (Maeng & Shors, 2013). These findings suggested that the behavioral sex difference in eyeblink conditioning following stress exposure may have been due to an overactivation of the mPFC in females as a result of differential processing within the amgydala-mPFC system compared to males. A similar mechanism could underlie the greater Fos induction seen in females in the experimental compared to the control condition in the current study. This female-specific effect could be predictive of a

behavioral sex difference that had yet to emerge (i.e., under extinction conditions, females exhibit a prolonged inhibition of food intake compared to males (Petrovich & Lougee, 2011)). Alternatively, it could indicate the existence of compensatory mechanisms that prevented the expression of behavioral sex differences during the test (Cahill, 2006; De Vries, 2004; de Vries & Sodersten, 2009). Regardless, this finding provides an important starting point for further anatomical and functional interrogation of the neural circuits that are recruited when a learned fear-cue inhibits feeding behavior. For example, an interesting question arises regarding differences in the activation of afferent or efferent projections of the mPFC during the expression of this behavior. Differences between the sexes in the recruitment or strength of specific mPFC pathways (including those involving the BLA) could explain why female groups showed differential mPFC activation between experimental conditions while the male groups showed similar levels of mPFC activation across conditions.

Conclusion

The brain network which orchestrates feeding is complex, and requires integration of the neural processes that control the homeostatic regulation of feeding, and the processes that allow environmental influences, including learned environmental cues, to override it. The studies in this dissertation examined one model of environmental control of feeding: fear-cue inhibited feeding. This model and the underlying neural circuitry mediating environmental inhibition of food intake despite hunger may have important clinical implications for anxiety and eating disorders. Here, we identified three forebrain regions: the amygdala, mPFC, and LHA, as critical components of a network that

supports a fear-cue's ability to inhibit feeding by overriding homeostatic hunger signals triggered by food-deprivation. The current studies assessed how this network is organized (anatomically; Study 1), and how it is recruited (functionally) during the expression of fear-cue inhibited feeding (Study 2). We showed that this is a complex network composed of multiple, topographically organized pathways, and provided the first evidence that amygdalar pathways to the mPFC and LHA are parallel and almost exclusively arise from different neurons. We also found that distinct cell groups within the amygdala-prefrontal-lateral hypothalamic network were differentially recruited with the presence of fear-cues, food- cues, and by food consumption. Together, the studies in this dissertation provide anatomical and functional maps for future interrogation of the forebrain circuitry underlying fear-cue inhibited feeding.

V. References

Allen, G. V., & Cechetto, D. F. (1993). Functional and anatomical organization of cardiovascular pressor and depressor sites in the lateral hypothalamic area. II. Ascending projections. *J Comp Neurol, 330*(3), 421-438.

Amano, T., Duvarci, S., Popa, D., & Pare, D. (2011). The fear circuit revisited: contributions of the basal amygdala nuclei to conditioned fear. *J Neurosci, 31*(43), 15481-15489.

American Psychiatric Association. (2000). *Diagnostic and statistical manual of mental disorders: DSM-IV-TR* (4th ed.). Washington, DC: American Psychiatric Association.

Anagnostaras, S. G., Maren, S., DeCola, J. P., Lane, N. I., Gale, G. D., Schlinger, B. A., et al. (1998). Testicular hormones do not regulate sexually dimorphic Pavlovian fear conditioning or perforant-path long-term potentiation in adult male rats. *Behav Brain Res, 92*(1), 1-9.

Andreano, J. M., & Cahill, L. (2009). Sex influences on the neurobiology of learning and memory. *Learn Mem, 16*(4), 248-266.

Anglada-Figueroa, D., & Quirk, G. J. (2005). Lesions of the basal amygdala block expression of conditioned fear but not extinction. *J Neurosci, 25*(42), 9680-9685.

Archer, J. (1975). Rodent sex differences in emotional and related behavior. *Behav Biol, 14*(4), 451-479.

Arvanitogiannis, A., Tzschentke, T. M., Riscaldino, L., Wise, R. A., & Shizgal, P. (2000). Fos expression following self-stimulation of the medial prefrontal cortex. *Behav Brain Res, 107*(1-2), 123-132.

Asarian, L., & Geary, N. (2013). Sex differences in the physiology of eating. *Am J Physiol Regul Integr Comp Physiol, 305*(11), R1215-1267.

Ashwell, R., & Ito, R. (2014). Excitotoxic lesions of the infralimbic, but not prelimbic cortex facilitate reversal of appetitive discriminative context conditioning: the role of the infralimbic cortex in context generalization. *Front Behav Neurosci, 8*, 63.

Attia, E. (2010). Anorexia nervosa: current status and future directions. *Annu Rev Med, 61*, 425-435.

Barker, J. M., & Galea, L. A. (2010). Males show stronger contextual fear conditioning than females after context pre-exposure. *Physiol Behav, 99*(1), 82-90.

Beck, C. H., & Fibiger, H. C. (1995). Conditioned fear-induced changes in behavior and in the expression of the immediate early gene c-fos: with and without diazepam pretreatment. *J Neurosci, 15*(1 Pt 2), 709-720.

Becker, J. B., Monteggia, L. M., Perrot-Sinal, T. S., Romeo, R. D., Taylor, J. R., Yehuda, R., et al. (2007). Stress and disease: is being female a predisposing factor? *J Neurosci, 27*(44), 11851-11855.

Berk, M. L., & Finkelstein, J. A. (1982). Efferent connections of the lateral hypothalamic area of the rat: an autoradiographic investigation. *Brain Res Bull, 8*(5), 511-526.

Berridge, C. W., Espana, R. A., & Vittoz, N. M. (2010). Hypocretin/orexin in arousal and stress. *Brain Res, 1314*, 91-102.

Berthoud, H. R., & Münzberg, H. (2011). The lateral hypothalamus as integrator of metabolic and environmental needs: from electrical self-stimulation to opto-genetics. *Physiol Behav, 104*(1), 29-39.

Bienkowski, M. S., & Rinaman, L. (2013). Common and distinct neural inputs to the medial central nucleus of the amygdala and anterior ventrolateral bed nucleus of stria terminalis in rats. *Brain Struct Funct, 218*(1), 187-208.

Blanchard, R. J., & Blanchard, D. C. (1969). Crouching as an index of fear. *J Comp Physiol Psychol, 67*(3), 370-375.

Borgland, S. L., Chang, S. J., Bowers, M. S., Thompson, J. L., Vittoz, N., Floresco, S. B., et al. (2009). Orexin A/hypocretin-1 selectively promotes motivation for positive reinforcers. *J Neurosci, 29*(36), 11215-11225.

Bouton, M. E., & Bolles, R. C. (1980). Conditioned fear assessed by freezing and by the suppression of 3 different baselines. *Animal Learning & Behavior, 8*(3), 429-434.

Broberger, C., De Lecea, L., Sutcliffe, J. G., & Hokfelt, T. (1998). Hypocretin/orexin- and melanin-concentrating hormone-expressing cells form distinct populations in the rodent lateral hypothalamus: relationship to the neuropeptide Y and agouti gene-related protein systems. *J Comp Neurol, 402*(4), 460-474.

Brown, J. A., Woodworth, H. L., & Leinninger, G. M. (2015). To ingest or rest? Specialized roles of lateral hypothalamic area neurons in coordinating energy balance. *Front Syst Neurosci, 9*, 9.

Bull, L. S., & Pitts, G. C. (1971). Gastric capacity and energy absorption in the force-fed rat. *J Nutr, 101*(5), 593-596.

Burgos-Robles, A., Bravo-Rivera, H., & Quirk, G. J. (2013). Prelimbic and infralimbic neurons signal distinct aspects of appetitive instrumental behavior. *PLoS One, 8*(2), e57575.

Burt, J., Alberto, C. O., Parsons, M. P., & Hirasawa, M. (2011). Local network regulation of orexin neurons in the lateral hypothalamus. *Am J Physiol Regul Integr Comp Physiol, 301*(3), R572-580.

Cahill, L. (2006). Why sex matters for neuroscience. *Nat Rev Neurosci, 7*(6), 477-484.

Cai, H., Haubensak, W., Anthony, T. E., & Anderson, D. J. (2014). Central amygdala PKC-delta(+) neurons mediate the influence of multiple anorexigenic signals. *Nat Neurosci, 17*(9), 1240-1248.

Campese, V., Gonzaga, R. & LeDoux J.E. Facilitation and suppression of instrumental responding require connections between the lateral and central amygdala. Program No. 747.25. 2014 Neuroscience Meeting Planner. Washington, DC: Society for Neuroscience, 2014. Online.

Cannon, W. B. (1915). *Bodily changes in pain, hunger, fear, and rage; an account of recent researches into the function of emotional excitement*. New York, London,: D. Appleton and Company.

Canteras, N. S., & Swanson, L. W. (1992). Projections of the ventral subiculum to the amygdala, septum, and hypothalamus: a PHAL anterograde tract-tracing study in the rat. *J Comp Neurol, 324*(2), 180-194.

Cason, A. M., & Aston-Jones, G. (2013). Role of orexin/hypocretin in conditioned sucrose-seeking in rats. *Psychopharmacology (Berl), 226*(1), 155-165.

Cason, A. M., & Aston-Jones, G. (2014). Role of orexin/hypocretin in conditioned sucrose-seeking in female rats. *Neuropharmacology, 86*, 97-102.
Cassell, M. D., Chittick, C. A., Siegel, M. A., & Wright, D. J. (1989). Collateralization of the amygdaloid projections of the rat prelimbic and infralimbic cortices. *J Comp Neurol, 279*(2), 235-248.
Cassell, M. D., Gray, T. S., & Kiss, J. Z. (1986). Neuronal architecture in the rat central nucleus of the amygdala: a cytological, hodological, and immunocytochemical study. *J Comp Neurol, 246*(4), 478-499.
Cassell, M. D., & Wright, D. J. (1986). Topography of projections from the medial prefrontal cortex to the amygdala in the rat. *Brain Res Bull, 17*(3), 321-333.
Cavalcante, J. C., Bittencourt, J. C., & Elias, C. F. (2014). Distribution of the neuronal inputs to the ventral premammillary nucleus of male and female rats. *Brain Res, 1582*, 77-90.
Cenquizca, L. A., & Swanson, L. W. (2006). Analysis of direct hippocampal cortical field CA1 axonal projections to diencephalon in the rat. *J Comp Neurol, 497*(1), 101-114.
Chang, Y. J., Yang, C. H., Liang, Y. C., Yeh, C. M., Huang, C. C., & Hsu, K. S. (2009). Estrogen modulates sexually dimorphic contextual fear extinction in rats through estrogen receptor beta. *Hippocampus, 19*(11), 1142-1150.
Charles, A. C., & Hales, T. G. (2004). From inhibition to excitation: functional effects of interaction between opioid receptors. *Life Sci, 76*(5), 479-485.
Charles River Laboratories (n.d.). Long-Evans Rats. Retrieved from: http://www.criver.com/files/pdfs/rms/us-model-pricing/rm_rm_c_long_evans_rats.aspx.
Chaudhuri, A. (1997). Neural activity mapping with inducible transcription factors. *Neuroreport, 8*(16), v-ix.
Chefer, V. I., Wang, R., & Shippenberg, T. S. (2011). Basolateral amygdala-driven augmentation of medial prefrontal cortex GABAergic neurotransmission in response to environmental stimuli associated with cocaine administration. *Neuropsychopharmacology, 36*(10), 2018-2029.
Choi, D. L., Davis, J. F., Fitzgerald, M. E., & Benoit, S. C. (2010). The role of orexin-A in food motivation, reward-based feeding behavior and food-induced neuronal activation in rats. *Neuroscience, 167*(1), 11-20.
Cifani, C., Koya, E., Navarre, B. M., Calu, D. J., Baumann, M. H., Marchant, N. J., et al. (2012). Medial prefrontal cortex neuronal activation and synaptic alterations after stress-induced reinstatement of palatable food seeking: A study using c-fos-GFP transgenic female rats. *J Neurosci, 32*(25), 8480-8490.
Clayton, J. A., & Collins, F. S. (2014). Policy: NIH to balance sex in cell and animal studies. *Nature, 509*(7500), 282-283.
Clegg, D. J., Air, E. L., Woods, S. C., & Seeley, R. J. (2002). Eating elicited by orexin-a, but not melanin-concentrating hormone, is opioid mediated. *Endocrinology, 143*(8), 2995-3000.

Cole, S., Hobin, M. P., & Petrovich, G. D. (2015). Appetitive associative learning recruits a distinct network with cortical, striatal, and hypothalamic regions. *Neuroscience, 286*, 187-202.
Cole, S., Powell, D. J., & Petrovich, G. D. (2013). Differential recruitment of distinct amygdalar nuclei across appetitive associative learning. *Learn Mem, 20*(6), 295-299.
Courtin, J., Bienvenu, T. C., Einarsson, E. O., & Herry, C. (2013). Medial prefrontal cortex neuronal circuits in fear behavior. *Neuroscience, 240*, 219-242.
Crain, S. M., & Shen, K. F. (1990). Opioids can evoke direct receptor-mediated excitatory effects on sensory neurons. *Trends Pharmacol Sci, 11*(2), 77-81.
Curran, T., & Morgan, J. I. (1995). Fos: an immediate-early transcription factor in neurons. *J Neurobiol, 26*(3), 403-412.
Dalla, C., & Shors, T. J. (2009). Sex differences in learning processes of classical and operant conditioning. *Physiol Behav, 97*(2), 229-238.
Dalley, J. W., Cardinal, R. N., & Robbins, T. W. (2004). Prefrontal executive and cognitive functions in rodents: neural and neurochemical substrates. *Neurosci Biobehav Rev, 28*(7), 771-784.
Davies, W., & Wilkinson, L. S. (2006). It is not all hormones: alternative explanations for sexual differentiation of the brain. *Brain Res, 1126*(1), 36-45.
Day, H. E., Curran, E. J., Watson, S. J., Jr., & Akil, H. (1999). Distinct neurochemical populations in the rat central nucleus of the amygdala and bed nucleus of the stria terminalis: evidence for their selective activation by interleukin-1beta. *J Comp Neurol, 413*(1), 113-128.
Day, H. E., Kryskow, E. M., Nyhuis, T. J., Herlihy, L., & Campeau, S. (2008). Conditioned fear inhibits c-fos mRNA expression in the central extended amygdala. *Brain Res, 1229*, 137-146.
de Lecea, L., Kilduff, T. S., Peyron, C., Gao, X., Foye, P. E., Danielson, P. E., et al. (1998). The hypocretins: hypothalamus-specific peptides with neuroexcitatory activity. *Proc Natl Acad Sci U S A, 95*(1), 322-327.
De Vries, G. J. (2004). Minireview: Sex differences in adult and developing brains: compensation, compensation, compensation. *Endocrinology, 145*(3), 1063-1068.
de Vries, G. J., & Sodersten, P. (2009). Sex differences in the brain: the relation between structure and function. *Horm Behav, 55*(5), 589-596.
Dilgen, J., Tejeda, H. A., & O'Donnell, P. (2013). Amygdala inputs drive feedforward inhibition in the medial prefrontal cortex. *J Neurophysiol, 110*(1), 221-229.
Dong, H. W., Petrovich, G. D., & Swanson, L. W. (2000). Organization of projections from the juxtacapsular nucleus of the BST: a PHAL study in the rat. *Brain Res, 859*(1), 1-14.
Dong, H. W., Petrovich, G. D., & Swanson, L. W. (2001). Topography of projections from amygdala to bed nuclei of the stria terminalis. *Brain Res Rev, 38*(1-2), 192-246.
Dong, H. W., Petrovich, G. D., Watts, A. G., & Swanson, L. W. (2001). Basic organization of projections from the oval and fusiform nuclei of the bed nuclei of the stria terminalis in adult rat brain. *J Comp Neurol, 436*(4), 430-455.

Dong, H. W., & Swanson, L. W. (2003). Projections from the rhomboid nucleus of the bed nuclei of the stria terminalis: implications for cerebral hemisphere regulation of ingestive behaviors. *J Comp Neurol, 463*(4), 434-472.
Dong, H. W., & Swanson, L. W. (2004a). Organization of axonal projections from the anterolateral area of the bed nuclei of the stria terminalis. *J Comp Neurol, 468*(2), 277-298.
Dong, H. W., & Swanson, L. W. (2004b). Projections from bed nuclei of the stria terminalis, posterior division: implications for cerebral hemisphere regulation of defensive and reproductive behaviors. *J Comp Neurol, 471*(4), 396-433.
Dong, H. W., & Swanson, L. W. (2006a). Projections from bed nuclei of the stria terminalis, anteromedial area: cerebral hemisphere integration of neuroendocrine, autonomic, and behavioral aspects of energy balance. *J Comp Neurol, 494*(1), 142-178.
Dong, H. W., & Swanson, L. W. (2006b). Projections from bed nuclei of the stria terminalis, dorsomedial nucleus: implications for cerebral hemisphere integration of neuroendocrine, autonomic, and drinking responses. *J Comp Neurol, 494*(1), 75-107.
Dong, H. W., & Swanson, L. W. (2006c). Projections from bed nuclei of the stria terminalis, magnocellular nucleus: implications for cerebral hemisphere regulation of micturition, defecation, and penile erection. *J Comp Neurol, 494*(1), 108-141.
Ehrlich, I., Humeau, Y., Grenier, F., Ciocchi, S., Herry, C., & Luthi, A. (2009). Amygdala inhibitory circuits and the control of fear memory. *Neuron, 62*(6), 757-771.
Elmquist, J. K., Elias, C. F., & Saper, C. B. (1999). From lesions to leptin: hypothalamic control of food intake and body weight. *Neuron, 22*(2), 221-232.
Euston, D. R., Gruber, A. J., & McNaughton, B. L. (2012). The role of medial prefrontal cortex in memory and decision making. *Neuron, 76*(6), 1057-1070.
Fanselow, M. S. (1984). What is conditioned fear? *TINS, 7*(12), 460-462.
Floresco, S. B., & Tse, M. T. (2007). Dopaminergic regulation of inhibitory and excitatory transmission in the basolateral amygdala-prefrontal cortical pathway. *J Neurosci, 27*(8), 2045-2057.
Floyd, N. S., Price, J. L., Ferry, A. T., Keay, K. A., & Bandler, R. (2001). Orbitomedial prefrontal cortical projections to hypothalamus in the rat. *J Comp Neurol, 432*(3), 307-328.
Fukushima, A., Hagiwara, H., Fujioka, H., Kimura, F., Akema, T., & Funabashi, T. (2015). Sex differences in feeding behavior in rats: the relationship with neuronal activation in the hypothalamus. *Front Neurosci, 9*, 88.
Furlong, T. M., Vianna, D. M., Liu, L., & Carrive, P. (2009). Hypocretin/orexin contributes to the expression of some but not all forms of stress and arousal. *Eur J Neurosci, 30*(8), 1603-1614.
Gabbott, P. L., Warner, T. A., Brown, J., Salway, P., Gabbott, T., & Busby, S. (2012). Amygdala afferents monosynaptically innervate corticospinal neurones in rat medial prefrontal cortex (mPFC). *J Comp Neurol*.

Gabbott, P. L., Warner, T. A., & Busby, S. J. (2006). Amygdala input monosynaptically innervates parvalbumin immunoreactive local circuit neurons in rat medial prefrontal cortex. *Neuroscience, 139*(3), 1039-1048.

Gabbott, P. L., Warner, T. A., Jays, P. R., Salway, P., & Busby, S. J. (2005). Prefrontal cortex in the rat: projections to subcortical autonomic, motor, and limbic centers. *J Comp Neurol, 492*(2), 145-177.

Garcia, R., Vouimba, R. M., Baudry, M., & Thompson, R. F. (1999). The amygdala modulates prefrontal cortex activity relative to conditioned fear. *Nature, 402*(6759), 294-296.

Gilmartin, M. R., Balderston, N. L., & Helmstetter, F. J. (2014). Prefrontal cortical regulation of fear learning. *Trends Neurosci, 37*(8), 455-464.

Goosens, K. A., & Maren, S. (2001). Contextual and auditory fear conditioning are mediated by the lateral, basal, and central amygdaloid nuclei in rats. *Learn Mem, 8*(3), 148-155.

Goto, M., Canteras, N. S., Burns, G., & Swanson, L. W. (2005). Projections from the subfornical region of the lateral hypothalamic area. *J Comp Neurol, 493*(3), 412-438.

Graham, B. M., & Milad, M. R. (2014). Inhibition of estradiol synthesis impairs fear extinction in male rats. *Learn Mem, 21*(7), 347-350.

Grant, D. P., & Milgram, N. W. (1973). Plasticity of normal feeding: situational and individual factors. *Can J Psychol, 27*(3), 305-316.

Griffond, B., & Risold, P. Y. (2009). MCH and feeding behavior-interaction with peptidic network. *Peptides, 30*(11), 2045-2051.

Gruene, T. M., Roberts, E., Thomas, V., Ronzio, A., & Shansky, R. M. (2014). Sex-Specific Neuroanatomical Correlates of Fear Expression in Prefrontal-Amygdala Circuits. *Biol Psychiatry*.

Gu, G., Cornea, A., & Simerly, R. B. (2003). Sexual differentiation of projections from the principal nucleus of the bed nuclei of the stria terminalis. *J Comp Neurol, 460*(4), 542-562.

Gupta, R. R., Sen, S., Diepenhorst, L. L., Rudick, C. N., & Maren, S. (2001). Estrogen modulates sexually dimorphic contextual fear conditioning and hippocampal long-term potentiation (LTP) in rats. *Brain Res, 888*(2), 356-365.

Hahn, J. D. (2010). Comparison of melanin-concentrating hormone and hypocretin/orexin peptide expression patterns in a current parceling scheme of the lateral hypothalamic zone. *Neurosci Lett, 468*(1), 12-17.

Hahn, J. D., & Swanson, L. W. (2010). Distinct patterns of neuronal inputs and outputs of the juxtaparaventricular and suprafornical regions of the lateral hypothalamic area in the male rat. *Brain Res Rev, 64*(1), 14-103.

Hahn, J. D., & Swanson, L. W. (2012). Connections of the lateral hypothalamic area juxtadorsomedial region in the male rat. *J Comp Neurol, 520*(9), 1831-1890.

Hahn, J. D., & Swanson, L. W. (2015). Connections of the juxtaventromedial region of the lateral hypothalamic area in the male rat. *Front Syst Neurosci, 9*(66).

Hall, J., Thomas, K. L., & Everitt, B. J. (2001). Fear memory retrieval induces CREB phosphorylation and Fos expression within the amygdala. *Eur J Neurosci, 13*(7), 1453-1458.

Harris, G. C., & Aston-Jones, G. (2006). Arousal and reward: a dichotomy in orexin function. *Trends Neurosci, 29*(10), 571-577.

Harris, G. C., Wimmer, M., & Aston-Jones, G. (2005). A role for lateral hypothalamic orexin neurons in reward seeking. *Nature, 437*(7058), 556-559.

Haubensak, W., Kunwar, P. S., Cai, H., Ciocchi, S., Wall, N. R., Ponnusamy, R., et al. (2010). Genetic dissection of an amygdala microcircuit that gates conditioned fear. *Nature, 468*(7321), 270-276.

Heidbreder, C. A., & Groenewegen, H. J. (2003). The medial prefrontal cortex in the rat: evidence for a dorso-ventral distinction based upon functional and anatomical characteristics. *Neurosci Biobehav Rev, 27*(6), 555-579.

Herry, C., Ciocchi, S., Senn, V., Demmou, L., Muller, C., & Luthi, A. (2008). Switching on and off fear by distinct neuronal circuits. *Nature, 454*(7204), 600-606.

Holland, P. C., & Hsu, M. (2014). Role of amygdala central nucleus in the potentiation of consuming and instrumental lever-pressing for sucrose by cues for the presentation or interruption of sucrose delivery in rats. *Behav Neurosci, 128*(1), 71-82.

Holland, P. C., Petrovich, G. D., & Gallagher, M. (2002). The effects of amygdala lesions on conditioned stimulus-potentiated eating in rats. *Physiol Behav, 76*(1), 117-129.

Holmes, N. M., & Westbrook, R. F. (2014). Appetitive context conditioning proactively, but transiently, interferes with expression of counterconditioned context fear. *Learn Mem, 21*(11), 597-605.

Hoover, W. B., & Vertes, R. P. (2007). Anatomical analysis of afferent projections to the medial prefrontal cortex in the rat. *Brain Struct Funct, 212*(2), 149-179.

Hoover, W. B., & Vertes, R. P. (2011). Projections of the medial orbital and ventral orbital cortex in the rat. *J Comp Neurol, 519*(18), 3766-3801.

Hurley, K. M., Herbert, H., Moga, M. M., & Saper, C. B. (1991). Efferent projections of the infralimbic cortex of the rat. *J Comp Neurol, 308*(2), 249-276.

Jasnow, A. M., Ehrlich, D. E., Choi, D. C., Dabrowska, J., Bowers, M. E., McCullough, K. M., et al. (2013). Thy1-expressing neurons in the basolateral amygdala may mediate fear inhibition. *J Neurosci, 33*(25), 10396-10404.

Jennings, J. H., Rizzi, G., Stamatakis, A. M., Ung, R. L., & Stuber, G. D. (2013). The inhibitory circuit architecture of the lateral hypothalamus orchestrates feeding. *Science, 341*(6153), 1517-1521.

Jennings, J. H., Ung, R. L., Resendez, S. L., Stamatakis, A. M., Taylor, J. G., Huang, J., et al. (2015). Visualizing hypothalamic network dynamics for appetitive and consummatory behaviors. *Cell, 160*(3), 516-527.

Jimenez, S. A., & Maren, S. (2009). Nuclear disconnection within the amygdala reveals a direct pathway to fear. *Learn Mem, 16*(12), 766-768.

Jolkkonen, E., & Pitkänen, A. (1998). Intrinsic connections of the rat amygdaloid complex: projections originating in the central nucleus. *J Comp Neurol, 395*(1), 53-72.

Kang, N., McCarthy, E. A., Cherry, J. A., & Baum, M. J. (2011). A sex comparison of the anatomy and function of the main olfactory bulb-medial amygdala projection in mice. *Neuroscience, 172*, 196-204.
Kaye, W. (2008). Neurobiology of anorexia and bulimia nervosa. *Physiol Behav, 94*(1), 121-135.
Keefer, S. E., Reppucci, C. J., Mayer, H. S., & Petrovich, G. D. Plasticity within the basolateral amygdala pathways to the prelimbic cortex during Pavlovian appetitive conditioning. Program No. 650.11. 2014 Neuroscience Meeting Planner. Washington, DC: Society for Neuroscience, 2014. Online.
Khan, A. M. (2013). Controlling feeding behavior by chemical or gene-directed targeting in the brain: what's so spatial about our methods? *Front Neurosci, 7*, 182.
Kita, H., & Kitai, S. T. (1990). Amygdaloid projections to the frontal cortex and the striatum in the rat. *J Comp Neurol, 298*(1), 40-49.
Kita, H., & Oomura, Y. (1982). An HRP study of the afferent connections to rat lateral hypothalamic region. *Brain Res Bull, 8*(1), 63-71.
Knapska, E., Macias, M., Mikosz, M., Nowak, A., Owczarek, D., Wawrzyniak, M., et al. (2012). Functional anatomy of neural circuits regulating fear and extinction. *Proc Natl Acad Sci U S A, 109*(42), 17093-17098.
Krettek, J. E., & Price, J. L. (1977). Projections from the amygdaloid complex to the cerebral cortex and thalamus in the rat and cat. *J Comp Neurol, 172*(4), 687-722.
Krettek, J. E., & Price, J. L. (1978a). Amygdaloid projections to subcortical structures within the basal forebrain and brainstem in the rat and cat. *J Comp Neurol, 178*(2), 225-254.
Krettek, J. E., & Price, J. L. (1978b). A description of the amygdaloid complex in the rat and cat with observations on intra-amygdaloid axonal connections. *J Comp Neurol, 178*(2), 255-280.
Kwon, J. T., Nakajima, R., Kim, H. S., Jeong, Y., Augustine, G. J., & Han, J. H. (2014). Optogenetic activation of presynaptic inputs in lateral amygdala forms associative fear memory. *Learn Mem, 21*(11), 627-633.
Lanciego, J. L., & Wouterlood, F. G. (2011). A half century of experimental neuroanatomical tracing. *J Chem Neuroanat, 42*(3), 157-183.
Land, B. B., Narayanan, N. S., Liu, R. J., Gianessi, C. A., Brayton, C. E., Grimaldi, D. M., et al. (2014). Medial prefrontal D1 dopamine neurons control food intake. *Nat Neurosci, 17*(2), 248-253.
Laviolette, S. R., Lipski, W. J., & Grace, A. A. (2005). A subpopulation of neurons in the medial prefrontal cortex encodes emotional learning with burst and frequency codes through a dopamine D4 receptor-dependent basolateral amygdala input. *J Neurosci, 25*(26), 6066-6075.
Lebron-Milad, K., & Milad, M. R. (2012). Sex differences, gonadal hormones and the fear extinction network: implications for anxiety disorders. *Biol Mood Anxiety Disord, 2*(1), 3.
Ledoux, J. (2012). Rethinking the emotional brain. *Neuron, 73*(4), 653-676.
Lee, A. T., Vogt, D., Rubenstein, J. L., & Sohal, V. S. (2014). A class of GABAergic neurons in the prefrontal cortex sends long-range projections to the nucleus

accumbens and elicits acute avoidance behavior. *J Neurosci, 34*(35), 11519-11525.
Li, H., Penzo, M. A., Taniguchi, H., Kopec, C. D., Huang, Z. J., & Li, B. (2013). Experience-dependent modification of a central amygdala fear circuit. *Nat Neurosci, 16*(3), 332-339.
Li, J., Chen, K., Yan, J., Wang, Q., Zhao, X., Yang, X., et al. (2012). Increased sucrose intake and corresponding c-Fos in amygdala and parabrachial nucleus of dietary obese rats. *Neurosci Lett, 525*(2), 111-116.
Likhtik, E., & Paz, R. (2015). Amygdala-prefrontal interactions in (mal)adaptive learning. *Trends Neurosci*.
Little, J. P., & Carter, A. G. (2013). Synaptic mechanisms underlying strong reciprocal connectivity between the medial prefrontal cortex and basolateral amygdala. *J Neurosci, 33*(39), 15333-15342.
Lynch, J., 3rd, Cullen, P. K., Jasnow, A. M., & Riccio, D. C. (2013). Sex differences in the generalization of fear as a function of retention intervals. *Learn Mem, 20*(11), 628-632.
Maeng, L. Y., & Shors, T. J. (2013). The stressed female brain: neuronal activity in the prelimbic but not infralimbic region of the medial prefrontal cortex suppresses learning after acute stress. *Front Neural Circuits, 7*, 198.
Maeng, L. Y., Waddell, J., & Shors, T. J. (2010). The prefrontal cortex communicates with the amygdala to impair learning after acute stress in females but not in males. *J Neurosci, 30*(48), 16188-16196.
Marchant, N. J., Densmore, V. S., & Osborne, P. B. (2007). Coexpression of prodynorphin and corticotrophin-releasing hormone in the rat central amygdala: evidence of two distinct endogenous opioid systems in the lateral division. *J Comp Neurol, 504*(6), 702-715.
Maren, S. (2001). Neurobiology of Pavlovian fear conditioning. *Annu Rev Neurosci, 24*, 897-931.
Maren, S., Aharonov, G., & Fanselow, M. S. (1996). Retrograde abolition of conditional fear after excitotoxic lesions in the basolateral amygdala of rats: absence of a temporal gradient. *Behav Neurosci, 110*(4), 718-726.
Maren, S., De Oca, B., & Fanselow, M. S. (1994). Sex differences in hippocampal long-term potentiation (LTP) and Pavlovian fear conditioning in rats: positive correlation between LTP and contextual learning. *Brain Res, 661*(1-2), 25-34.
Martinez, R. C., Gupta, N., Lazaro-Munoz, G., Sears, R. M., Kim, S., Moscarello, J. M., et al. (2013). Active vs. reactive threat responding is associated with differential c-Fos expression in specific regions of amygdala and prefrontal cortex. *Learn Mem, 20*(8), 446-452.
McCarthy, M. M., Arnold, A. P., Ball, G. F., Blaustein, J. D., & De Vries, G. J. (2012). Sex differences in the brain: the not so inconvenient truth. *J Neurosci, 32*(7), 2241-2247.
McDonald, A. J. (1987). Organization of amygdaloid projections to the mediodorsal thalamus and prefrontal cortex: a fluorescence retrograde transport study in the rat. *J Comp Neurol, 262*(1), 46-58.

McDonald, A. J. (1991). Organization of amygdaloid projections to the prefrontal cortex and associated striatum in the rat. *Neuroscience, 44*(1), 1-14.
McDonald, A. J. (1992). Projection neurons of the basolateral amygdala: a correlative Golgi and retrograde tract tracing study. *Brain Res Bull, 28*(2), 179-185.
McDonald, A. J. (1998). Cortical pathways to the mammalian amygdala. *Progress in Neurobiology, 55*(3), 257-332.
McDonald, A. J., Mascagni, F., & Guo, L. (1996). Projections of the medial and lateral prefrontal cortices to the amygdala: a Phaseolus vulgaris leucoagglutinin study in the rat. *Neuroscience, 71*(1), 55-75.
McDonald, A. J., Shammah-Lagnado, S. J., Shi, C., & Davis, M. (1999). Cortical afferents to the extended amygdala. *Ann N Y Acad Sci, 877*, 309-338.
McLean, C. P., & Anderson, E. R. (2009). Brave men and timid women? A review of the gender differences in fear and anxiety. *Clin Psychol Rev, 29*(6), 496-505.
Meister, B. (2007). Neurotransmitters in key neurons of the hypothalamus that regulate feeding behavior and body weight. *Physiol Behav, 92*(1-2), 263-271.
Mena, J. D., Sadeghian, K., & Baldo, B. A. (2011). Induction of hyperphagia and carbohydrate intake by mu-opioid receptor stimulation in circumscribed regions of frontal cortex. *J Neurosci, 31*(9), 3249-3260.
Mena, J. D., Selleck, R. A., & Baldo, B. A. (2013). Mu-opioid stimulation in rat prefrontal cortex engages hypothalamic orexin/hypocretin-containing neurons, and reveals dissociable roles of nucleus accumbens and hypothalamus in cortically driven feeding. *J Neurosci, 33*(47), 18540-18552.
Mendoza, J., Sanio, C., & Chaudhri, N. (2014). Inactivating the infralimbic but not prelimbic medial prefrontal cortex facilitates the extinction of appetitive Pavlovian conditioning in Long-Evans rats. *Neurobiol Learn Mem*.
Morgan, J. I., & Curran, T. (1991). Stimulus-transcription coupling in the nervous system: involvement of the inducible proto-oncogenes fos and jun. *Annu Rev Neurosci, 14*, 421-451.
Moscarello, J. M., Ben-Shahar, O., & Ettenberg, A. (2009). Effects of food deprivation on goal-directed behavior, spontaneous locomotion, and c-Fos immunoreactivity in the amygdala. *Behav Brain Res, 197*(1), 9-15.
Moscarello, J. M., & LeDoux, J. E. (2013). Active avoidance learning requires prefrontal suppression of amygdala-mediated defensive reactions. *J Neurosci, 33*(9), 3815-3823.
Muller, J. F., Mascagni, F., & McDonald, A. J. (2006). Pyramidal cells of the rat basolateral amygdala: synaptology and innervation by parvalbumin-immunoreactive interneurons. *J Comp Neurol, 494*(4), 635-650.
Nahon, J. L., Presse, F., Bittencourt, J. C., Sawchenko, P. E., & Vale, W. (1989). The rat melanin-concentrating hormone messenger ribonucleic acid encodes multiple putative neuropeptides coexpressed in the dorsolateral hypothalamus. *Endocrinology, 125*(4), 2056-2065.
Nair, S. G., Golden, S. A., & Shaham, Y. (2008). Differential effects of the hypocretin 1 receptor antagonist SB 334867 on high-fat food self-administration and reinstatement of food seeking in rats. *Br J Pharmacol, 154*(2), 406-416.

Nair, S. G., Navarre, B. M., Cifani, C., Pickens, C. L., Bossert, J. M., & Shaham, Y. (2011). Role of dorsal medial prefrontal cortex dopamine D1-family receptors in relapse to high-fat food seeking induced by the anxiogenic drug yohimbine. *Neuropsychopharmacology, 36*(2), 497-510.

Nakamura, S., Tsumori, T., Yokota, S., Oka, T., & Yasui, Y. (2009). Amygdaloid axons innervate melanin-concentrating hormone- and orexin-containing neurons in the mouse lateral hypothalamus. *Brain Res, 1278*, 66-74.

Namburi, P., Beyeler, A., Yorozu, S., Calhoon, G. G., Halbert, S. A., Wichmann, R., et al. (2015). A circuit mechanism for differentiating positive and negative associations. *Nature, 520*(7549), 675-678.

Niu, J. G., Yokota, S., Tsumori, T., Oka, T., & Yasui, Y. (2012). Projections from the anterior basomedial and anterior cortical amygdaloid nuclei to melanin-concentrating hormone-containing neurons in the lateral hypothalamus of the rat. *Brain Res, 1479*, 31-43.

Nugent, B. M., & McCarthy, M. M. (2011). Epigenetic underpinnings of developmental sex differences in the brain. *Neuroendocrinology, 93*(3), 150-158.

Ono, T., Luiten, P. G. M., Nishijo, H., Fukuda, M., & Nishino, H. (1985). Topographic organization of projections from the amygdala to the hypothalamus of the rat. *Neuroscience Research, 2*(4), 221-238.

Pare, D., & Duvarci, S. (2012). Amygdala microcircuits mediating fear expression and extinction. *Curr Opin Neurobiol, 22*(4), 717-723.

Pare, D., Quirk, G. J., & Ledoux, J. E. (2004). New vistas on amygdala networks in conditioned fear. *J Neurophysiol, 92*(1), 1-9.

Park, T. H., & Carr, K. D. (1998). Neuroanatomical patterns of fos-like immunoreactivity induced by a palatable meal and meal-paired environment in saline- and naltrexone-treated rats. *Brain Res, 805*(1-2), 169-180.

Perez-Jaranay, J. M., & Vives, F. (1991). Electrophysiological study of the response of medial prefrontal cortex neurons to stimulation of the basolateral nucleus of the amygdala in the rat. *Brain Res, 564*(1), 97-101.

Petrovich, G. D. (2013). Forebrain networks and the control of feeding by environmental learned cues. *Physiol Behav, 121*, 10-18.

Petrovich, G. D., Canteras, N. S., & Swanson, L. W. (2001). Combinatorial amygdalar inputs to hippocampal domains and hypothalamic behavior systems. *Brain Res Rev, 38*(1-2), 247-289.

Petrovich, G. D., Hobin, M. P., & Reppucci, C. J. (2012). Selective Fos induction in hypothalamic orexin/hypocretin, but not melanin-concentrating hormone neurons, by a learned food-cue that stimulates feeding in sated rats. *Neuroscience, 224*, 70-80.

Petrovich, G. D., Holland, P. C., & Gallagher, M. (2005). Amygdalar and prefrontal pathways to the lateral hypothalamus are activated by a learned cue that stimulates eating. *J Neurosci, 25*(36), 8295-8302.

Petrovich, G. D., & Lougee, M. A. (2011). Sex differences in fear-induced feeding cessation: prolonged effect in female rats. *Physiol Behav, 104*(5), 996-1001.

Petrovich, G. D., Risold, P. Y., & Swanson, L. W. (1996). Organization of projections from the basomedial nucleus of the amygdala: a PHAL study in the rat. *J Comp Neurol, 374*(3), 387-420.

Petrovich, G. D., Ross, C. A., Gallagher, M., & Holland, P. C. (2007). Learned contextual cue potentiates eating in rats. *Physiol Behav, 90*(2-3), 362-367.

Petrovich, G. D., Ross, C. A., Holland, P. C., & Gallagher, M. (2007). Medial prefrontal cortex is necessary for an appetitive contextual conditioned stimulus to promote eating in sated rats. *J Neurosci, 27*(24), 6436-6441.

Petrovich, G. D., Ross, C. A., Holland, P. C., & Gallagher, M. Central but not basolateral amygdala is critical for control of feeding by aversive, conditioned cues. Program No. 373.7. 2006 Neuroscience Meeting Planner. Atlanta, GA: Society for Neuroscience, 2006. Online.

Petrovich, G. D., Ross, C. A., Mody, P., Holland, P. C., & Gallagher, M. (2009). Central, but not basolateral, amygdala is critical for control of feeding by aversive learned cues. *J Neurosci, 29*(48), 15205-15212.

Petrovich, G. D., Setlow, B., Holland, P. C., & Gallagher, M. (2002). Amygdalo-hypothalamic circuit allows learned cues to override satiety and promote eating. *J Neurosci, 22*(19), 8748-8753.

Petrovich, G. D., & Swanson, L. W. (1997). Projections from the lateral part of the central amygdalar nucleus to the postulated fear conditioning circuit. *Brain Res, 763*(2), 247-254.

Pezzone, M. A., Lee, W. S., Hoffman, G. E., & Rabin, B. S. (1992). Induction of c-Fos immunoreactivity in the rat forebrain by conditioned and unconditioned aversive stimuli. *Brain Res, 597*(1), 41-50.

Pitkänen, A., Savander, V., & LeDoux, J. E. (1997). Organization of intra-amygdaloid circuitries in the rat: an emerging framework for understanding functions of the amygdala. *Trends Neurosci, 20*(11), 517-523.

Pitkänen, A., Stefanacci, L., Farb, C. R., Go, G. G., LeDoux, J. E., & Amaral, D. G. (1995). Intrinsic connections of the rat amygdaloid complex: projections originating in the lateral nucleus. *J Comp Neurol, 356*(2), 288-310.

Poulin, A. M., & Timofeeva, E. (2008). The dynamics of neuronal activation during food anticipation and feeding in the brain of food-entrained rats. *Brain Res, 1227*, 128-141.

Pryce, C. R., Lehmann, J., & Feldon, J. (1999). Effect of sex on fear conditioning is similar for context and discrete CS in Wistar, Lewis and Fischer rat strains. *Pharmacology Biochemistry and Behavior, 64*(4), 753-759.

Quirk, G. J., Likhtik, E., Pelletier, J. G., & Pare, D. (2003). Stimulation of medial prefrontal cortex decreases the responsiveness of central amygdala output neurons. *J Neurosci, 23*(25), 8800-8807.

Reppucci, C. J., Kuthyar, M., & Petrovich, G. D. (2013). Contextual fear cues inhibit eating in food-deprived male and female rats. *Appetite, 69*, 186-195.

Reppucci, C. J., & Petrovich, G. D. (2012). Learned food-cue stimulates persistent feeding in sated rats. *Appetite, 59*(2), 437-447.

Reppucci, C.J. & Petrovich, G.D. Suppressed Fos induction within the central nucleus of the amygdala corresponds with inhibited feeding in the presence of a fear-cue in male and female rats. Program No. 256.10. 2014 Neuroscience Meeting Planner. Washington, DC: Society for Neuroscience, 2014.

Risold, P. Y., & Swanson, L. W. (1996). Structural evidence for functional domains in the rat hippocampus. *Science, 272*(5267), 1484-1486.

Ritter, S., & Dinh, T. T. (1994). 2-Mercaptoacetate and 2-deoxy-D-glucose induce Fos-like immunoreactivity in rat brain. *Brain Res, 641*(1), 111-120.

Roberts, G. W., Woodhams, P. L., Polak, J. M., & Crow, T. J. (1982). Distribution of neuropeptides in the limbic system of the rat: the amygdaloid complex. *Neuroscience, 7*(1), 99-131.

Rodgers, R. J., Halford, J. C., Nunes de Souza, R. L., Canto de Souza, A. L., Piper, D. C., Arch, J. R., et al. (2000). Dose-response effects of orexin-A on food intake and the behavioural satiety sequence in rats. *Regul Pept, 96*(1-2), 71-84.

Rosen, J. B., Fanselow, M. S., Young, S. L., Sitcoske, M., & Maren, S. (1998). Immediate-early gene expression in the amygdala following footshock stress and contextual fear conditioning. *Brain Res, 796*(1-2), 132-142.

Rosenkranz, J. A., & Grace, A. A. (2001). Dopamine attenuates prefrontal cortical suppression of sensory inputs to the basolateral amygdala of rats. *J Neurosci, 21*(11), 4090-4103.

Rosenkranz, J. A., & Grace, A. A. (2002). Cellular mechanisms of infralimbic and prelimbic prefrontal cortical inhibition and dopaminergic modulation of basolateral amygdala neurons in vivo. *J Neurosci, 22*(1), 324-337.

Sakurai, T., Amemiya, A., Ishii, M., Matsuzaki, I., Chemelli, R. M., Tanaka, H., et al. (1998). Orexins and orexin receptors: a family of hypothalamic neuropeptides and G protein-coupled receptors that regulate feeding behavior. *Cell, 92*(4), 573-585.

Saper, C. B. (1985). Organization of cerebral cortical afferent systems in the rat. II. Hypothalamocortical projections. *J Comp Neurol, 237*(1), 21-46.

Saper, C. B. (2000). Hypothalamic connections with the cerebral cortex. *Prog Brain Res, 126*, 39-48.

Saper, C. B., Swanson, L. W., & Cowan, W. M. (1979). An autoradiographic study of the efferent connections of the lateral hypothalamic area in the rat. *J Comp Neurol, 183*(4), 689-706.

Savander, V., Go, C. G., LeDoux, J. E., & Pitkänen, A. (1995). Intrinsic connections of the rat amygdaloid complex: projections originating in the basal nucleus. *J Comp Neurol, 361*(2), 345-368.

Savander, V., Go, C. G., Ledoux, J. E., & Pitkänen, A. (1996). Intrinsic connections of the rat amygdaloid complex: projections originating in the accessory basal nucleus. *J Comp Neurol, 374*(2), 291-313.

Schiltz, C. A., Bremer, Q. Z., Landry, C. F., & Kelley, A. E. (2007). Food-associated cues alter forebrain functional connectivity as assessed with immediate early gene and proenkephalin expression. *BMC Biol, 5*, 16.

Schmitt, O., Usunoff, K. G., Lazarov, N. E., Itzev, D. E., Eipert, P., Rolfs, A., et al. (2012). Orexinergic innervation of the extended amygdala and basal ganglia in the rat. *Brain Struct Funct, 217*(2), 233-256.

Schone, C., & Burdakov, D. (2012). Glutamate and GABA as rapid effectors of hypothalamic "peptidergic" neurons. *Front Behav Neurosci, 6*, 81.

Scicli, A. P., Petrovich, G. D., Swanson, L. W., & Thompson, R. F. (2004). Contextual fear conditioning is associated with lateralized expression of the immediate early gene c-fos in the central and basolateral amygdalar nuclei. *Behav Neurosci, 118*(1), 5-14.

Senn, V., Wolff, S. B., Herry, C., Grenier, F., Ehrlich, I., Grundemann, J., et al. (2014). Long-range connectivity defines behavioral specificity of amygdala neurons. *Neuron, 81*(2), 428-437.

Sesack, S. R., Deutch, A. Y., Roth, R. H., & Bunney, B. S. (1989). Topographical organization of the efferent projections of the medial prefrontal cortex in the rat: an anterograde tract-tracing study with Phaseolus vulgaris leucoagglutinin. *J Comp Neurol, 290*(2), 213-242.

Seymour, B., & Dolan, R. (2008). Emotion, decision making, and the amygdala. *Neuron, 58*(5), 662-671.

Sherwood, A., Holland, P. C., Adamantidis, A., & Johnson, A. W. (2015). Deletion of Melanin Concentrating Hormone Receptor-1 disrupts overeating in the presence of food cues. *Physiol Behav, in press*.

Sierra-Mercado, D., Padilla-Coreano, N., & Quirk, G. J. (2011). Dissociable roles of prelimbic and infralimbic cortices, ventral hippocampus, and basolateral amygdala in the expression and extinction of conditioned fear. *Neuropsychopharmacology, 36*(2), 529-538.

Sigurdsson, T., Doyere, V., Cain, C. K., & LeDoux, J. E. (2007). Long-term potentiation in the amygdala: a cellular mechanism of fear learning and memory. *Neuropharmacology, 52*(1), 215-227.

Simerly, R. B. (2002). Wired for reproduction: organization and development of sexually dimorphic circuits in the mammalian forebrain. *Annu Rev Neurosci, 25*, 507-536.

Simmons, D. M., & Swanson, L. W. (1993) The Nissl stain. Neuroscience Protocols. 050-12-01-07.

Sotres-Bayon, F., & Quirk, G. J. (2010). Prefrontal control of fear: more than just extinction. *Curr Opin Neurobiol, 20*(2), 231-235.

Sotres-Bayon, F., Sierra-Mercado, D., Pardilla-Delgado, E., & Quirk, G. J. (2012). Gating of fear in prelimbic cortex by hippocampal and amygdala inputs. *Neuron, 76*(4), 804-812.

Stanley, B. G., Urstadt, K. R., Charles, J. R., & Kee, T. (2011). Glutamate and GABA in lateral hypothalamic mechanisms controlling food intake. *Physiol Behav, 104*(1), 40-46.

Stefanik, M. T., & Kalivas, P. W. (2013). Optogenetic dissection of basolateral amygdala projections during cue-induced reinstatement of cocaine seeking. *Front Behav Neurosci, 7*, 213.

Steinglass, J. E., Sysko, R., Mayer, L., Berner, L. A., Schebendach, J., Wang, Y., et al. (2010). Pre-meal anxiety and food intake in anorexia nervosa. *Appetite, 55*(2), 214-218.

Stowe, Z. N., & Nemeroff, C. B. (1991). The electrophysiological actions of neurotensin in the central nervous system. *Life Sci, 49*(14), 987-1002.

Strober, M. (2004). Pathologic fear conditioning and anorexia nervosa: on the search for novel paradigms. *Int J Eat Disord, 35*(4), 504-508.

Swanson, L. W. (2000). Cerebral hemisphere regulation of motivated behavior. *Brain Res, 886*(1-2), 113-164.

Swanson, L. W. (2004). *Brain maps III: Structure of the rat brain. An atlas with printed and electronic templates for data, models, and schematics* (3rd rev. ed.). Amsterdam: Elsevier, Academic Press.

Swanson, L. W. (2005). Anatomy of the soul as reflected in the cerebral hemispheres: neural circuits underlying voluntary control of basic motivated behaviors. *J Comp Neurol, 493*(1), 122-131.

Swanson, L. W., & Petrovich, G. D. (1998). What is the amygdala? *Trends Neurosci, 21*(8), 323-331.

Swanson, L. W., Sanchez-Watts, G., & Watts, A. G. (2005). Comparison of melanin-concentrating hormone and hypocretin/orexin mRNA expression patterns in a new parceling scheme of the lateral hypothalamic zone. *Neurosci Lett, 387*(2), 80-84.

Takagishi, M., & Chiba, T. (1991). Efferent projections of the infralimbic (area 25) region of the medial prefrontal cortex in the rat: an anterograde tracer PHA-L study. *Brain Research, 566*(1-2), 26-39.

Toth, M., Fuzesi, T., Halasz, J., Tulogdi, A., & Haller, J. (2010). Neural inputs of the hypothalamic "aggression area" in the rat. *Behav Brain Res, 215*(1), 7-20.

Tsujino, N., & Sakurai, T. (2009). Orexin/hypocretin: a neuropeptide at the interface of sleep, energy homeostasis, and reward system. *Pharmacol Rev, 61*(2), 162-176.

Uher, R., Murphy, T., Brammer, M. J., Dalgleish, T., Phillips, M. L., Ng, V. W., et al. (2004). Medial prefrontal cortex activity associated with symptom provocation in eating disorders. *Am J Psychiatry, 161*(7), 1238-1246.

Veening, J. G. (1978). Subcortical afferents of the amygdaloid complex in the rat: an HRP study. *Neurosci Lett, 8*(3), 197-202.

Verhagen, L. A., Luijendijk, M. C., de Groot, J. W., van Dommelen, L. P., Klimstra, A. G., Adan, R. A., et al. (2011). Anticipation of meals during restricted feeding increases activity in the hypothalamus in rats. *Eur J Neurosci, 34*(9), 1485-1491.

Vertes, R. P. (2004). Differential projections of the infralimbic and prelimbic cortex in the rat. *Synapse, 51*(1), 32-58.

Villalobos, J., & Ferssiwi, A. (1987). The differential ascending projections from the anterior, central and posterior regions of the lateral hypothalamic area: an autoradiographic study. *Neurosci Lett, 81*(1-2), 89-94.

Viviani, D., Haegler, P., Strasser, D. S., & Steiner, M. A. (2012). Sex comparison on long-lasting behavioral and physiological disturbances induced by single shock experience in rats. *Physiology & Behavior, 107*(2), 243-251.

Wakefield, C. (1979). The intrinsic connections of the basolateral amygdaloid nuclei as visualized with the HRP method. *Neurosci Lett, 12*(1), 17-21.
Watts, A. G., Salter, D. S., & Neuner, C. M. (2007). Neural network interactions and ingestive behavior control during anorexia. *Physiol Behav, 91*(4), 389-396.
Weingarten, H. P. (1983). Conditioned cues elicit feeding in sated rats: a role for learning in meal initiation. *Science, 220*(4595), 431-433.
Weingarten, H. P. (1984). Meal initiation controlled by learned cues: basic behavioral properties. *Appetite, 5*(2), 147-158.
Wheeler, D. S., Wan, S., Miller, A., Angeli, N., Adileh, B., Hu, W., et al. (2014). Role of lateral hypothalamus in two aspects of attention in associative learning. *Eur J Neurosci, 40*(2), 2359-2377.
Wise, R. A. (1974). Lateral hypothalamic electrical stimulation: does it make animals 'hungry'? *Brain Res, 67*(2), 187-209.
Wood, G. E., & Shors, T. J. (1998). Stress facilitates classical conditioning in males, but impairs classical conditioning in females through activational effects of ovarian hormones. *Proc Natl Acad Sci U S A, 95*(7), 4066-4071.
Wray, S., & Hoffman, G. E. (1983). Organization and interrelationship of neuropeptides in the central amygdaloid nucleus of the rat. *Peptides, 4*(4), 525-541.
Yoshida, K., McCormack, S., Espana, R. A., Crocker, A., & Scammell, T. E. (2006). Afferents to the orexin neurons of the rat brain. *J Comp Neurol, 494*(5), 845-861.
Zucker, I., & Beery, A. K. (2010). Males still dominate animal studies. *Nature, 465*(7299), 690.

VI. Appendix

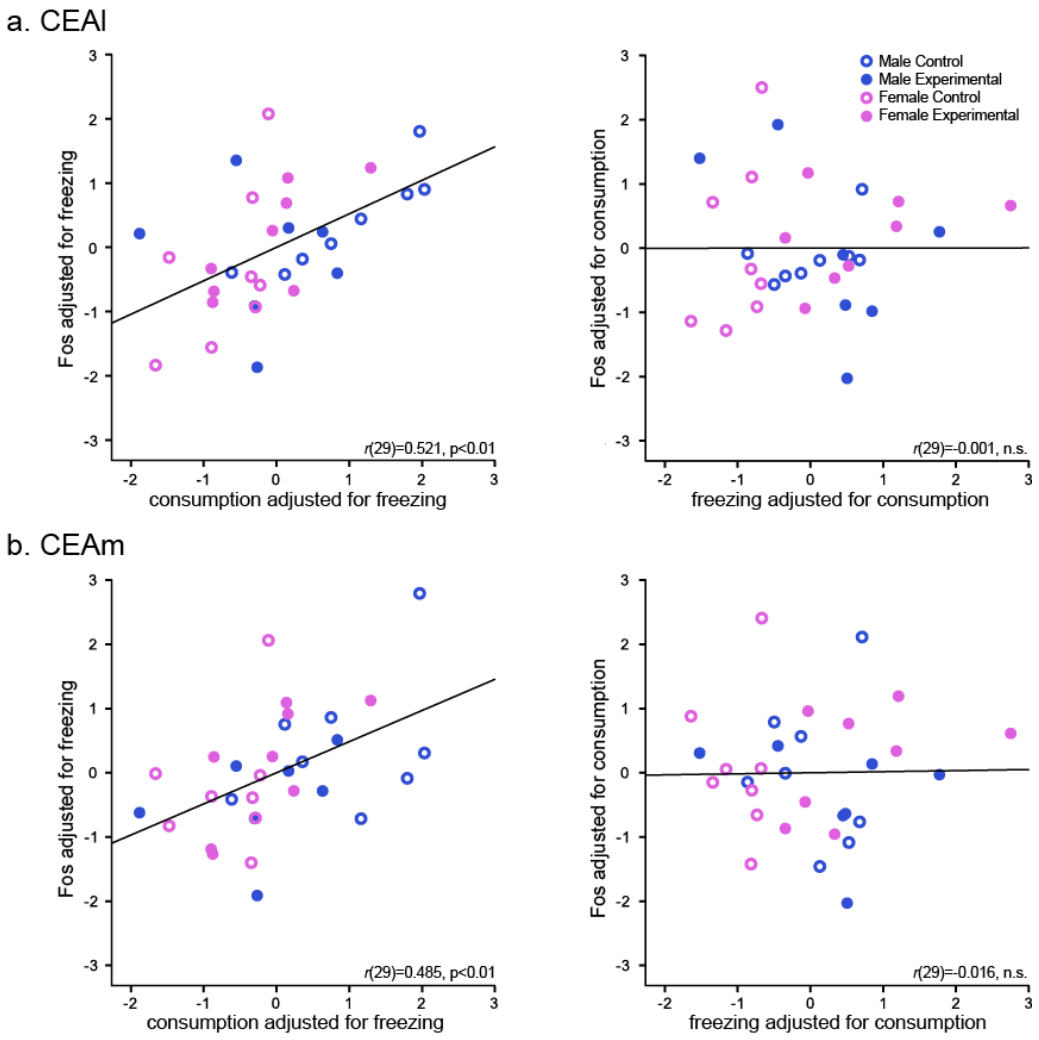

Fig. 6.1. Scatter plots depicting the partial correlation statistics from Study 2 for regions that showed effects of experimental or food access condition (completed for the food access groups and collapsed across the sexes, except for the mPFC where only females showed differential Fos induction across groups). Plots were created using the standardized residuals from linear regressions against the controlling variable. Statistics reported on the plots are the simple Pearson correlations between the resulting residuals, and are comparable to the results from the original partial correlations. (continued on following pages)

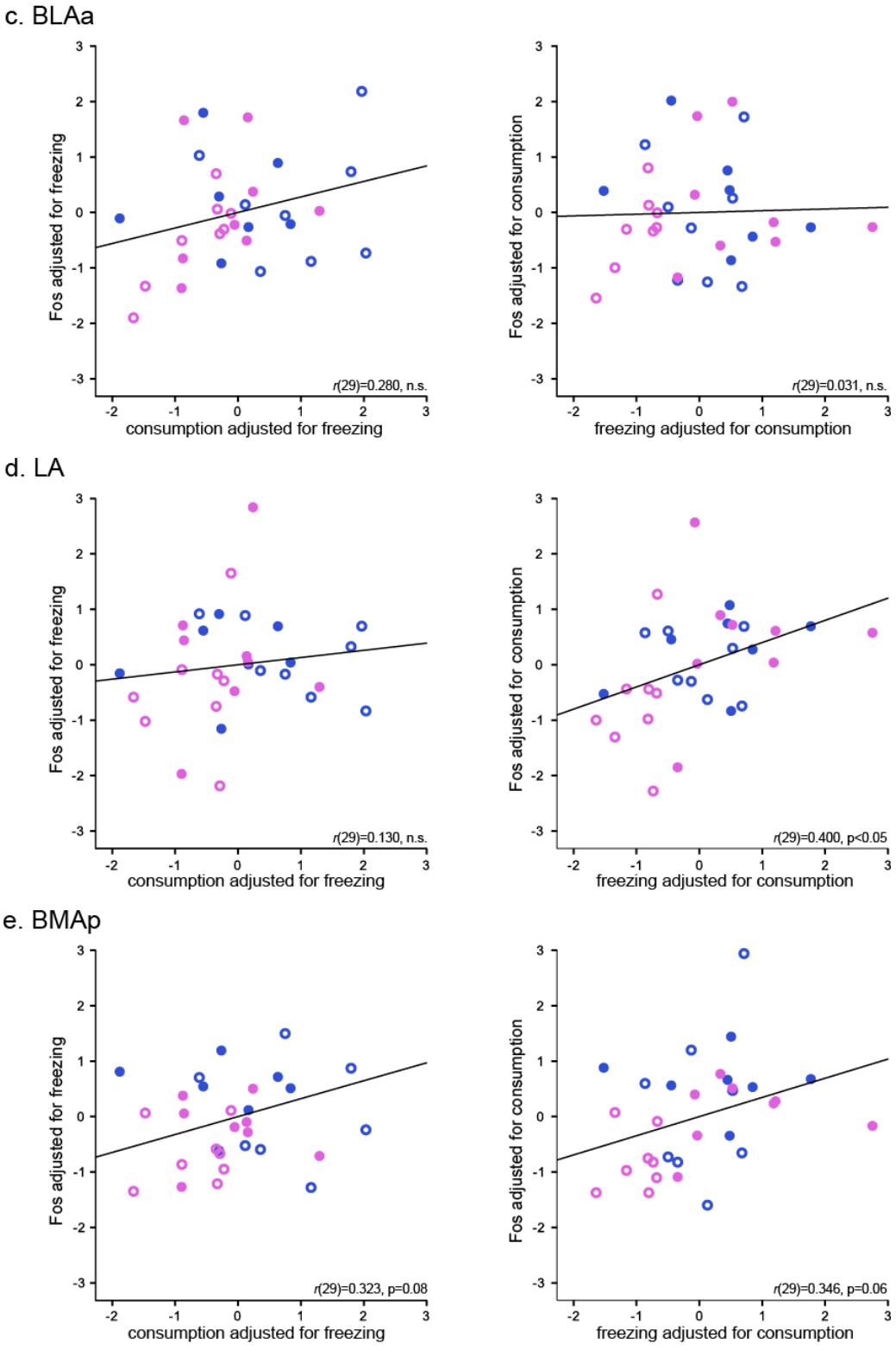

Fig. 6.1, continued

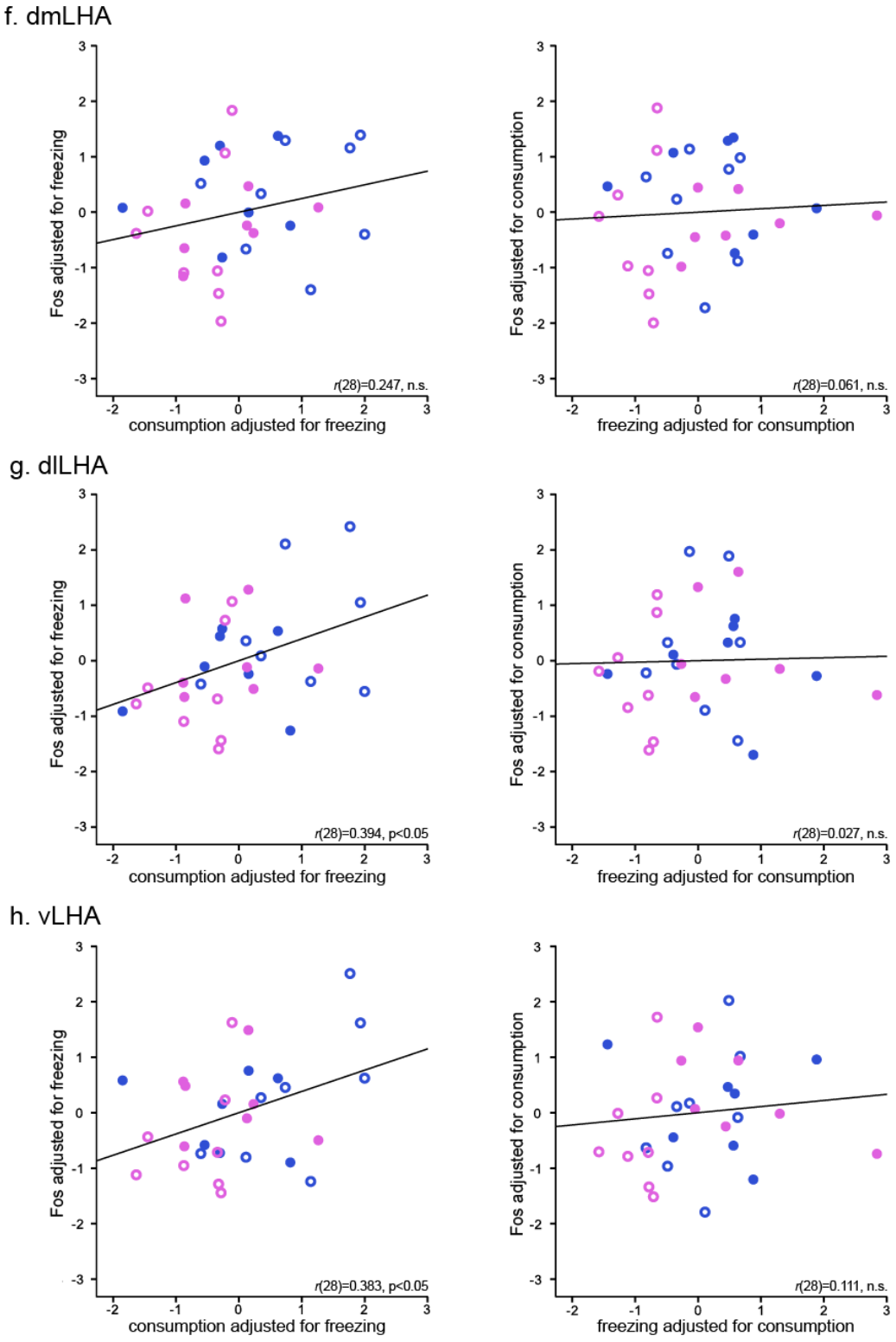

Fig. 6.1, continued

i. mPFC

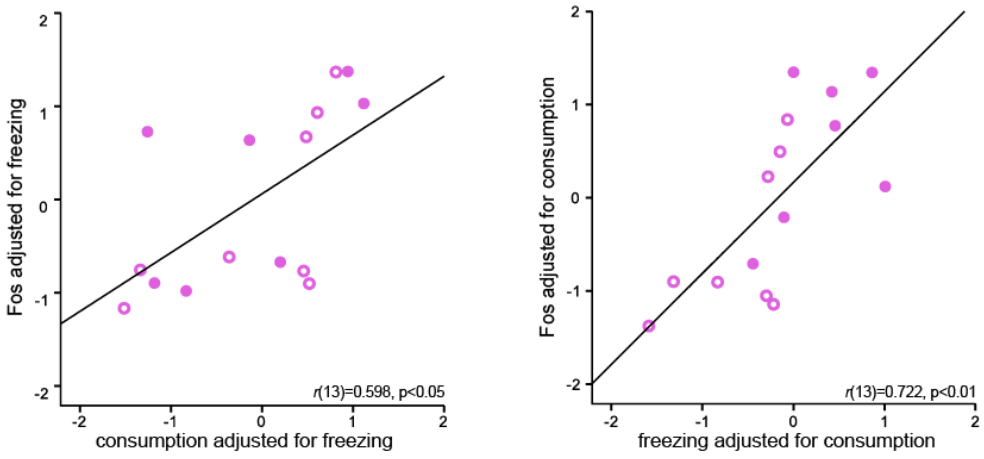

Fig. 6.1, continued